

SONOCHEMICAL DEGRADATION OF OCTYLBENZENE SULFONATE BY PULSED
ULTRASOUND AT 616, 205 and 69 kHz

DISSERTATION

Presented in Partial Fulfillment of the Requirements for Degree Master of Science in
the Graduate School of The Ohio State University

By

Dawn M. Deojay, M.S.

* * * * *

The Ohio State University
2008

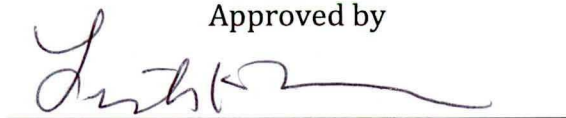
Dissertation Committee:

Professor Linda Weavers, Adviser

Professor Harold Walker

Professor John Lenhart

Approved by



Adviser

Environmental Science Graduate Program

Copyright by

Dawn Marie Deojay

2008

ABSTRACT

Comparative sonochemistry methods are a way to standardize sonochemical output based on the measurement of sonochemical energy input. In the current study and in a preliminary study by Yang et al. (2008), comparative sonochemistry was used to probe the mechanisms of degradation of a surface active compound, 4-octylbenzene sulfonate (OBS), under pulsed ultrasound relative to continuous mode ultrasound. Specifically, the rates of OBS degradation were compared to the formation rates of hydroxyterephthalic acid produced from terephthalic acid reaction with hydroxyl radical. In the current study, comparative rates were studied at the frequencies 616, 205 and 69 kHz.

The rate data of this study indicate that pulsed ultrasound statistically increases or decreases both the rate of degradation of OBS and the rate of formation of HTA. However, from this data it was apparent that not all pulsing conditions statistically change the rate of these sonochemical reactions compared to continuous wave ultrasound. Also, the effect of pulsed ultrasound on sonochemical rates depended on the frequency of sonolysis. Therefore, these results confirm that the experimental design used in the current study, was a useful technique to help understand the effect of pulsing on the sonochemical degradation of surface active solutes over a broad range of pulsing conditions.

Upon further analysis of the rate data starting at 616 kHz, there was a noticeable trend where under all pulsing conditions a pulsed enhancement of HTA formation occurred. Comparatively, OBS rate trends resulted in more negative or no pulsed enhancements. It was

therefore concluded that the comparative method chosen had limitations and restrictions in its ability to understand how OBS degrades under these ultrasound conditions. However, the trends do suggest that the role of transient and stable bubbles may be important in the relative difference between the rate of OBS degradation to that of HTA formation during both continuous and pulsed ultrasound modes at 616 kHz and 69 kHz. At a frequency of 205 kHz there were great variations in the pulsed enhanced data between sets, therefore this same hypothesis could not be made.

Over long sonication times, under continuous modes of sonication, surface active and/or volatile byproducts may accumulate in and/or around the cavitation bubble reducing the rate of OBS degradation at these longer sonication times. This observed decrease in the degradation rate under continuous ultrasound was minimal during extended sonication times operating under pulsed mode. The methods used in the comparative sonochemical analysis of the current study were valuable in making certain conclusions based on the observations. However, it is shown that there are limitations in comparing OBS degradation to HTA formation rates for understanding how pulsing and frequency affect acoustic cavitation, since the two processes may be affected differently by the sonochemically active bubble population. It is proposed that a method wherein the standard reaction (i.e., OBS degradation) is compared to a more suitable "test reaction" that minimizes independent variables, for example, comparison of the sonochemical degradation of OBS to that of a n-alkyl benzene sulfonate that has a shorter n-alkyl chain.

Dedicated to my mother

ACKNOWLEDGMENTS

During my time as a graduate student I have gained a great deal of experience and knowledge to broaden my abilities and understanding in the areas of scientific research. I could not have made it through successfully without the guidance from a number of people.

To my advisor, Dr. Linda Weavers, thank you for your assistance, and direction during my time with your group. Also thank you for the opportunity to do independent research in your laboratory as it was an extremely fruitful and rewarding.

Also, I would like to extend a very gracious thank you to Dr. Joe Sostaric, for the detailed and rewarding lectures, discussions and critiques in the science of surface chemistry and sonochemistry. Your availability and willingness to answer my many questions regarding equipment, theories and in general life's questions was extremely rewarding.

Much thanks to my committee members Dr. Harold Walker and Dr. John Lenhart for their valuable advice and suggestions throughout my time as a graduate student in the Weavers group and in their proof reading of my thesis.

I would also like to thank Dr. Karl Graff and Dr. James Rathman for help and assistance in the areas of understanding lab equipment operations and/or statistical programs.

Thank you to Jung-Ju Lee and Yu Sik Hwang for valuable and detailed explanations of chemical instrumentation and method protocols in the environmental engineering labs.

Also, to my group mates thank you for making my time in the environmental engineering chemistry labs that much more enjoyable.

I would also like to thank Tim Henthorne for his artistic abilities and the many hours that went into making the glass reactors for this project.

VITA

2003.....B.S. Environmental Science, North Carolina State University

2004.....B.A. Chemistry, North Carolina State University

1999 – 2004.....Technician

Department of Soil Science

North Carolina State University, Raleigh, NC

2005 – Present.....Graduate Teaching and Research Associate, ESGP

The Ohio State University

FIELDS OF STUDY

Major Field: Environmental Science

TABLE OF CONTENTS

	Page
Abstract.....	ii
Dedication.....	iv
Acknowledgements.....	v
Vita.....	vii
List of Tables.....	xii
List of Schemes.....	xii
List of Figures.....	xiii
Chapters:	
1. Introduction.....	1
1.1 Environmental implications of LAS use.....	1
1.2 Fate of LAS in environmental matrices.....	2
1.2.1 Fate of LAS in aquatic environments.....	2
1.2.2 Aerobic Bacterial Degradation.....	3
1.2.3 Fate of LAS from sludge application.....	3
1.3 Oxidative reactions involved in LAS degradation.....	5
1.4 Enhanced degradation of LAS compounds through advanced oxidation technologies.....	6
1.5 Ultrasound as an advanced oxidation technology.....	7
1.5.1 The bubble.....	8

1.5.2	Bubble nucleation to hot spot formation.....	9
1.5.3	Temperature of the hot spot.....	13
1.5.4	Radical generation via the homolysis of water molecules.....	14
1.5.5	Growth via rectified diffusion.....	16
1.5.6	Types of bubbles that are formed.....	17
1.5.7	Preferential surfactant degradation via ultrasound.....	18
1.5.7.1	Initial surfactant concentration effects.....	19
1.5.7.2	Coalescence prevention and declustering via surfactant adsorption.....	19
1.5.7.3	Decreased surface tension as a result of surfactant addition.....	20
1.5.7.4	Adsorption of surfactant to the air/water interface.....	21
1.5.8	Degradation of various surfactant compounds with ultrasound.....	22
1.5.9	Comparative Sonochemistry.....	24
1.5.9.1	History of comparative studies.....	24
1.5.9.2	Comparative studies using HTA formation.....	26
1.5.10	Pulsed ultrasound.....	28
1.5.11	Research objectives.....	30
2.	Experimental.....	32
2.1	Materials.....	32
2.2	Ultrasound apparatus.....	32

2.3	Ultrasonic calorimetric power.....	34
2.4	Surface tension measurements.....	35
2.5	HPLC analysis of OBS degradation.....	36
2.6	Fluorescence detection of HTA formation.....	37
3.	Results.....	46
3.1	Effect of ultrasound intensity on sonochemical yield.....	46
3.2	Effect of OBS and TA initial concentrations on sonochemical rates.....	48
3.3	Effect of sonolysis time on sonochemical rate of reaction.....	50
3.4	OBS and HTA kinetic experiments.....	52
4.	Discussion.....	66
4.1	HTA and OBS pulsed enhancements.....	67
4.2	OBS degradation at extended sonolysis times.....	79
5.	Conclusions.....	91
	List of References.....	95

APPENDICES

A.	616 kHz OBS and HTA kinetic rate plots.....	101
B.	205 kHz OBS and HTA kinetic rate plots.....	128
C.	69 kHz OBS kinetic rate plots.....	155
D.	Impedance graphs.....	169

LIST OF TABLES

Table

3.1	616 kHz OBS and HTA k_{weighted} values at each pulsed setting.....	63
3.2	205 kHz OBS and HTA k_{weighted} values at each pulsed setting.....	64
3.3	69 kHz OBS and HTA k_{weighted} values at each pulsed setting.....	65
4.1.	Description of possible comparative data sets, following the definitions of Yang et al. (2008) for Sets 1(a), 2 and 3. Additional sets shown are described for the first time in the current work. "+" refers to a pulse enhancement. "-" indicates a negative pulse enhancement value (i.e., data points that lie below the 0% line in Figures 4.1 and 4.2. "0" indicates that no pulse enhancement was observed.....	82

LIST OF SCHEMES

Scheme

1.1	Dominant chemical reactions generating radicals resulting from water homolysis.....	15
-----	---	----

LIST OF FIGURES

Figure

1.1	Pictorial representation of the ultrasound wave as it affects the growth of the cavitation bubble. This is followed by the sudden growth and adiabatic collapse of the bubble to create the hot spot.....	10
1.2	Pictorial representation of the Hot Spot. Notice the radicals that are formed as a result of thermolysis degradation of the surfactant and water molecules.....	12
1.3	Schematic representation of the mechanism in which TA reacts with OH radicals to form fluorescent and stable HTA ions.....	27
2.1.	The ultrasonic reactor and transducer(s) housing.....	39
2.2	Calorimetric power determinations at 616 kHz.....	40
2.3	Calorimetric power determinations at 205 kHz.....	41
2.4	Calorimetric power determinations at 69 kHz.....	42
2.5	OBS concentration effects on equilibrium surface tension.....	43
2.6	(a) HPLC calibration peaks of known concentration. (b) Typical HPLC / OBS calibration curve.....	44
2.7	(a) Fluorometer calibration peaks of known concentration (b) Typical HTA, RF Spectrofluorophotometer calibration curve.....	45
3.1	(a) OBS degradation rate constant and (b) HTA formation rate as a function of electrical power at 616 kHz.....	55
3.2	(a) OBS degradation rate constant and (b) HTA formation rate as a function of electrical power at 205 kHz.....	56
3.3	HTA formation rate as a function of TA concentration. Rates of reaction were determined in aqueous solutions (1mM, 300mL) exposed to continuous ultrasound (f = 616 kHz).....	57

3.4	HTA formation rate as a function of TA concentration. Rates of reaction were determined in aqueous solutions (1mM, 300mL) exposed to continuous ultrasound (f = 205 kHz).....	57
3.5	OBS first order degradation rates were determined in aqueous solutions (1mM, 300mL) exposed to continuous ultrasound (f = 616 kHz).....	58
3.6	OBS first order degradation rates were determined in aqueous solutions (1mM, 300mL) exposed to continuous ultrasound (f = 205 kHz).....	58
3.7	OBS first order degradation rates were determined in aqueous solutions (1mM, 300mL) exposed to continuous ultrasound (f = 69 kHz).....	59
3.8	HTA formation as a function of sonolysis time was determined in aqueous solutions (1mM, 300mL) exposed to continuous ultrasound (f = 616 kHz).....	60
3.9	HTA formation as a function of sonolysis time was determined in aqueous solutions (1mM, 300mL) exposed to continuous ultrasound (f = 205 kHz).....	60
3.10	First order ultrasonic degradation of OBS in aqueous solution (1mM, 300ml) exposed to continuous ultrasound (f = 205 kHz).....	61
3.11	First order ultrasonic degradation of OBS in aqueous solution (1mM, 300ml) exposed to pulsed wave (100ms lengths and 100ms intervals) ultrasound (f = 205 kHz).....	61
3.12	Zero order ultrasonic formation of HTA in aqueous solution (1mM, 300mL) exposed to continuous ultrasound (f = 205 kHz).....	62
3.13	Zero order ultrasonic formation of HTA in aqueous solution (1mM, 300ml) exposed to pulsed wave (100ms lengths and 100ms intervals) ultrasound (f = 205 kHz).....	62
4.1	Pulsed enhancement values for, degradation of OBS (a) and formation of HTA (b) under various pulsed ultrasound (f= 616 kHz, P= 27W) conditions (data points), relative to continuous wave ultrasound (i.e., the dashed line).....	83
4.2	Pulsed enhancement values for degradation of OBS (a) and formation of HTA (b) under various pulsed ultrasound (f= 205 kHz, P= 27W) conditions (data points), relative to continuous wave ultrasound (i.e.,the dashed line).....	84
4.3	Pulsed enhancement values for degradation of OBS under various pulsed ultrasound (f=69 kHz; P = 27W) conditions (data points), relative to continuous wave ultrasound (i.e., the dashed line).....	85
4.4	OBS first order degradation rates were determined in aqueous solutions (1mM, 300mL) exposed to continuous ultrasound (f = 616 kHz).....	86

4.5	First order ultrasonic degradation of OBS in aqueous solution (1mM, 300ml) exposed to pulsed wave (length = 100ms; interval = 100ms) ultrasound (f = 616 kHz).....	86
4.6	First order ultrasonic degradation of OBS in aqueous solution (1mM, 300ml) exposed to pulsed wave (length = 60ms; interval = 320ms) ultrasound (f = 616 kHz).....	87
4.7	First order degradation of OBS in aqueous solutions (1mM, 300mL) exposed to continuous ultrasound (f = 205 kHz, 20±°C).....	88
4.8	First order ultrasonic degradation of OBS in aqueous solution (1mM, 300ml) exposed to pulsed wave (length = 100ms; interval = 100ms) ultrasound (f = 205 kHz).....	88
4.9	First order degradation of OBS in aqueous solutions (1mM, 300mL) exposed to continuous ultrasound (f = 69 kHz, 20±°C).....	89
4.10	First order ultrasonic degradation of OBS in aqueous solution (1mM, 300ml) exposed to pulsed wave (length = 60ms; interval = 30ms) ultrasound (f = 69 kHz).....	89
4.11	First order ultrasonic degradation of OBS in aqueous solution (1mM, 300ml) exposed to pulsed wave (length = 60ms; interval = 60ms) ultrasound (f = 69 kHz).....	90
A1.1	First order ultrasonic degradation of OBS in aqueous solution (1mM, 300ml) exposed to continuous ultrasound (f = 616 kHz).....	102
A1.2	First order ultrasonic degradation of OBS in aqueous solution (1mM, 300ml) exposed to pulsed wave (30ms lengths and 30ms intervals) ultrasound (f = 616 kHz).....	102
A1.3	First order ultrasonic degradation of OBS in aqueous solution (1mM, 300ml) exposed to pulsed wave (30ms lengths and 60ms intervals) ultrasound (f = 616 kHz).....	103
A1.4	First order ultrasonic degradation of OBS in aqueous solution (1mM, 300ml) exposed to pulsed wave (30ms lengths and 100ms intervals) ultrasound (f = 616 kHz).....	103
A1.5	First order ultrasonic degradation of OBS in aqueous solution (1mM, 300ml) exposed to pulsed wave (30ms lengths and 160ms intervals) ultrasound (f = 616 kHz).....	104
A1.6	First order ultrasonic degradation of OBS in aqueous solution (1mM, 300ml) exposed to pulsed wave (30ms lengths and 320ms intervals) ultrasound (f = 616 kHz).....	104
A1.7	First order ultrasonic degradation of OBS in aqueous solution (1mM, 300ml) exposed to pulsed wave (60ms lengths and 30ms intervals) ultrasound (f = 616 kHz).....	105
A1.8	First order ultrasonic degradation of OBS in aqueous solution (1mM, 300ml) exposed to pulsed wave (60ms lengths and 60ms intervals) ultrasound (f = 616 kHz).....	105
A1.9	First order ultrasonic degradation of OBS in aqueous solution (1mM, 300ml) exposed to pulsed wave (60ms lengths and 100ms intervals) ultrasound (f = 616 kHz).....	106

A1.10	First order ultrasonic degradation of OBS in aqueous solution (1mM, 300ml) exposed to pulsed wave (60ms lengths and 160ms intervals) ultrasound (f = 616 kHz).....	106
A1.11	First order ultrasonic degradation of OBS in aqueous solution (1mM, 300ml) exposed to pulsed wave (60ms lengths and 320ms intervals) ultrasound (f = 616 kHz).....	107
A1.12	First order ultrasonic degradation of OBS in aqueous solution (1mM, 300ml) exposed to pulsed wave (100ms lengths and 30ms intervals) ultrasound (f = 616 kHz).....	107
A1.13	First order ultrasonic degradation of OBS in aqueous solution (1mM, 300ml) exposed to pulsed wave (100ms lengths and 60ms intervals) ultrasound (f = 616 kHz).....	108
A1.14	First order ultrasonic degradation of OBS in aqueous solution (1mM, 300ml) exposed to pulsed wave (100ms lengths and 100ms intervals) ultrasound (f = 616 kHz).....	108
A1.15	First order ultrasonic degradation of OBS in aqueous solution (1mM, 300ml) exposed to pulsed wave (100ms lengths and 160ms intervals) ultrasound (f = 616 kHz).....	109
A1.16	First order ultrasonic degradation of OBS in aqueous solution (1mM, 300ml) exposed to pulsed wave (100ms lengths and 320ms intervals) ultrasound (f = 616 kHz).....	109
A1.17	First order ultrasonic degradation of OBS in aqueous solution (1mM, 300ml) exposed to pulsed wave (160ms lengths and 30ms intervals) ultrasound (f = 616 kHz).....	110
A1.18	First order ultrasonic degradation of OBS in aqueous solution (1mM, 300ml) exposed to pulsed wave (160ms lengths and 60ms intervals) ultrasound (f = 616 kHz).....	110
A1.19	First order ultrasonic degradation of OBS in aqueous solution (1mM, 300ml) exposed to pulsed wave (160ms lengths and 100ms intervals) ultrasound (f = 616 kHz).....	111
A1.20	First order ultrasonic degradation of OBS in aqueous solution (1mM, 300ml) exposed to pulsed wave (160ms lengths and 160ms intervals) ultrasound (f = 616 kHz).....	111
A1.21	First order ultrasonic degradation of OBS in aqueous solution (1mM, 300ml) exposed to pulsed wave (160ms lengths and 320ms intervals) ultrasound (f = 616 kHz).....	112
A1.22	First order ultrasonic degradation of OBS in aqueous solution (1mM, 300ml) exposed to pulsed wave (320ms lengths and 30ms intervals) ultrasound (f = 616 kHz).....	112
A1.23	First order ultrasonic degradation of OBS in aqueous solution (1mM, 300ml) exposed to pulsed wave (320ms lengths and 60ms intervals) ultrasound (f = 616 kHz).....	113
A1.24	First order ultrasonic degradation of OBS in aqueous solution (1mM, 300ml) exposed to pulsed wave (320ms lengths and 100ms intervals) ultrasound (f = 616 kHz).....	113
A1.25	First order ultrasonic degradation of OBS in aqueous solution (1mM, 300ml) exposed to pulsed wave (320ms lengths and 160ms intervals) ultrasound (f = 616 kHz).....	114

A1.26	First order ultrasonic degradation of OBS in aqueous solution (1mM, 300ml) exposed to pulsed wave (320ms lengths and 320ms intervals) ultrasound (f = 616 kHz).....	114
A2.1	Zero order ultrasonic HTA formation reactions of in aqueous solution (1mM, 300ml) exposed to continuous ultrasound (f = 616 kHz).....	115
A2.2	Zero order ultrasonic HTA formation reactions of in aqueous solution (1mM, 300ml) exposed to pulsed wave (30ms lengths and 30ms intervals) ultrasound (f = 616 kHz).....	115
A2.3	Zero order ultrasonic HTA formation reactions of in aqueous solution (1mM, 300ml) exposed to pulsed wave (30ms lengths and 60ms intervals) ultrasound (f = 616 kHz).....	116
A2.4	Zero order ultrasonic HTA formation reactions of in aqueous solution (1mM, 300ml) exposed to pulsed wave (30ms lengths and 100ms intervals) ultrasound (f = 616 kHz).....	116
A2.5	Zero order ultrasonic HTA formation reactions of in aqueous solution (1mM, 300ml) exposed to pulsed wave (30ms lengths and 160ms intervals) ultrasound (f = 616 kHz).....	117
A2.6	Zero order ultrasonic HTA formation reactions of in aqueous solution (1mM, 300ml) exposed to pulsed wave (30ms lengths and 320ms intervals) ultrasound (f = 616 kHz).....	117
A2.7	Zero order ultrasonic HTA formation reactions of in aqueous solution (1mM, 300ml) exposed to pulsed wave (60ms lengths and 30ms intervals) ultrasound (f = 616 kHz).....	118
A2.8	Zero order ultrasonic HTA formation reactions of in aqueous solution (1mM, 300ml) exposed to pulsed wave (60ms lengths and 60ms intervals) ultrasound (f = 616 kHz).....	118
A2.9	Zero order ultrasonic HTA formation reactions of in aqueous solution (1mM, 300ml) exposed to pulsed wave (60ms lengths and 100ms intervals) ultrasound (f = 616 kHz).....	119
A2.10	Zero order ultrasonic HTA formation reactions of in aqueous solution (1mM, 300ml) exposed to pulsed wave (60ms lengths and 160ms intervals) ultrasound (f = 616 kHz).....	119
A2.11	Zero order ultrasonic HTA formation reactions of in aqueous solution (1mM, 300ml) exposed to pulsed wave (60ms lengths and 320ms intervals) ultrasound (f = 616 kHz).....	120
A2.12	Zero order ultrasonic HTA formation reactions of in aqueous solution (1mM, 300ml) exposed to pulsed wave (100ms lengths and 30ms intervals) ultrasound (f = 616 kHz).....	120
A2.13	Zero order ultrasonic HTA formation reactions of in aqueous solution (1mM, 300ml) exposed to pulsed wave (100ms lengths and 60ms intervals) ultrasound (f = 616 kHz).....	121
A2.14	Zero order ultrasonic HTA formation reactions of in aqueous solution (1mM, 300ml) exposed to pulsed wave (100ms lengths and 100ms intervals) ultrasound (f = 616 kHz)....	121
A2.15	Zero order ultrasonic HTA formation reactions of in aqueous solution (1mM, 300ml) exposed to pulsed wave (100ms lengths and 160ms intervals) ultrasound (f = 616 kHz)...	122

A2.16	Zero order ultrasonic HTA formation reactions of in aqueous solution (1mM, 300ml) exposed to pulsed wave (100ms lengths and 320ms intervals) ultrasound (f = 616 kHz)...	122
A2.17	Zero order ultrasonic HTA formation reactions of in aqueous solution (1mM, 300ml) exposed to pulsed wave (160ms lengths and 30ms intervals) ultrasound (f = 616 kHz).....	123
A2.18	Zero order ultrasonic HTA formation reactions of in aqueous solution (1mM, 300ml) exposed to pulsed wave (160ms lengths and 60ms intervals) ultrasound (f = 616 kHz).....	123
A2.19	Zero order ultrasonic HTA formation reactions of in aqueous solution (1mM, 300ml) exposed to pulsed wave (160ms lengths and 100ms intervals) ultrasound (f = 616 kHz)...	124
A2.20	Zero order ultrasonic HTA formation reactions of in aqueous solution (1mM, 300ml) exposed to pulsed wave (160ms lengths and 160ms intervals) ultrasound (f = 616 kHz)...	124
A2.21	Zero order ultrasonic HTA formation reactions of in aqueous solution (1mM, 300ml) exposed to pulsed wave (160ms lengths and 320ms intervals) ultrasound (f = 616 kHz)...	125
A2.22	Zero order ultrasonic HTA formation reactions of in aqueous solution (1mM, 300ml) exposed to pulsed wave (320ms lengths and 30ms intervals) ultrasound (f = 616 kHz).....	125
A2.23	Zero order ultrasonic HTA formation reactions of in aqueous solution (1mM, 300ml) exposed to pulsed wave (320ms lengths and 60ms intervals) ultrasound (f = 616 kHz).....	126
A2.24	Zero order ultrasonic HTA formation reactions of in aqueous solution (1mM, 300ml) exposed to pulsed wave (320ms lengths and 100ms intervals) ultrasound (f = 616 kHz)...	126
A2.25	Zero order ultrasonic HTA formation reactions of in aqueous solution (1mM, 300ml) exposed to pulsed wave (320ms lengths and 160ms intervals) ultrasound (f = 616 kHz)...	127
A2.26	Zero order ultrasonic HTA formation reactions of in aqueous solution (1mM, 300ml) exposed to pulsed wave (320ms lengths and 320ms intervals) ultrasound (f = 616 kHz)...	127
B1.1	First order ultrasonic degradation of OBS in aqueous solution (1mM, 300ml) exposed to continuous ultrasound (f = 205 kHz).....	129
B1.2	First order ultrasonic degradation of OBS in aqueous solution (1mM, 300ml) exposed to pulsed wave (30ms lengths and 30ms intervals) ultrasound (f = 205 kHz).....	129
B1.3	First order ultrasonic degradation of OBS in aqueous solution (1mM, 300ml) exposed to pulsed wave (30ms lengths and 60ms intervals) ultrasound (f = 205 kHz).....	130
B1.4	First order ultrasonic degradation of OBS in aqueous solution (1mM, 300ml) exposed to pulsed wave (30ms lengths and 100ms intervals) ultrasound (f = 205 kHz).....	130
B1.5	First order ultrasonic degradation of OBS in aqueous solution (1mM, 300ml) exposed to pulsed wave (30ms lengths and 160ms intervals) ultrasound (f = 205 kHz).....	131

B1.6	First order ultrasonic degradation of OBS in aqueous solution (1mM, 300ml) exposed to pulsed wave (30ms lengths and 320ms intervals) ultrasound (f = 205 kHz).....	131
B1.7	First order ultrasonic degradation of OBS in aqueous solution (1mM, 300ml) exposed to pulsed wave (60ms lengths and 30ms intervals) ultrasound (f = 205 kHz).....	132
B1.8	First order ultrasonic degradation of OBS in aqueous solution (1mM, 300ml) exposed to pulsed wave (60ms lengths and 60ms intervals) ultrasound (f = 205 kHz).....	132
B1.9	First order ultrasonic degradation of OBS in aqueous solution (1mM, 300ml) exposed to pulsed wave (60ms lengths and 100ms intervals) ultrasound (f = 205 kHz).....	133
B1.10	First order ultrasonic degradation of OBS in aqueous solution (1mM, 300ml) exposed to pulsed wave (60ms lengths and 160ms intervals) ultrasound (f = 205 kHz).....	133
B1.11	First order ultrasonic degradation of OBS in aqueous solution (1mM, 300ml) exposed to pulsed wave (60ms lengths and 320ms intervals) ultrasound (f = 205 kHz).....	134
B1.12	First order ultrasonic degradation of OBS in aqueous solution (1mM, 300ml) exposed to pulsed wave (100ms lengths and 30ms intervals) ultrasound (f = 205 kHz).....	134
B1.13	First order ultrasonic degradation of OBS in aqueous solution (1mM, 300ml) exposed to pulsed wave (100ms lengths and 60ms intervals) ultrasound (f = 205 kHz).....	135
B1.14	First order ultrasonic degradation of OBS in aqueous solution (1mM, 300ml) exposed to pulsed wave (100ms lengths and 100ms intervals) ultrasound (f = 205 kHz).....	135
B1.15	First order ultrasonic degradation of OBS in aqueous solution (1mM, 300ml) exposed to pulsed wave (100ms lengths and 160ms intervals) ultrasound (f = 205 kHz).....	136
B1.16	First order ultrasonic degradation of OBS in aqueous solution (1mM, 300ml) exposed to pulsed wave (100ms lengths and 320ms intervals) ultrasound (f = 205 kHz).....	136
B1.17	First order ultrasonic degradation of OBS in aqueous solution (1mM, 300ml) exposed to pulsed wave (160ms lengths and 30ms intervals) ultrasound (f = 205 kHz).....	137
B1.18	First order ultrasonic degradation of OBS in aqueous solution (1mM, 300ml) exposed to pulsed wave (160ms lengths and 60ms intervals) ultrasound (f = 205 kHz).....	137
B1.19	First order ultrasonic degradation of OBS in aqueous solution (1mM, 300ml) exposed to pulsed wave (160ms lengths and 100ms intervals) ultrasound (f = 205 kHz).....	138
B1.20	First order ultrasonic degradation of OBS in aqueous solution (1mM, 300ml) exposed to pulsed wave (160ms lengths and 160ms intervals) ultrasound (f = 205 kHz).....	138
B1.21	First order ultrasonic degradation of OBS in aqueous solution (1mM, 300ml) exposed to pulsed wave (160ms lengths and 320ms intervals) ultrasound (f = 205 kHz)	139

B1.22	First order ultrasonic degradation of OBS in aqueous solution (1mM, 300ml) exposed to pulsed wave (320ms lengths and 30ms intervals) ultrasound (f = 205 kHz).....	139
B1.23	First order ultrasonic degradation of OBS in aqueous solution (1mM, 300ml) exposed to pulsed wave (320ms lengths and 60ms intervals) ultrasound (f = 205 kHz).....	140
B1.24	First order ultrasonic degradation of OBS in aqueous solution (1mM, 300ml) exposed to pulsed wave (320ms lengths and 100ms intervals) ultrasound (f = 205 kHz).....	140
B1.25	First order ultrasonic degradation of OBS in aqueous solution (1mM, 300ml) exposed to pulsed wave (320ms lengths and 160ms intervals) ultrasound (f = 205 kHz).....	141
B1.26	First order ultrasonic degradation of OBS in aqueous solution (1mM, 300ml) exposed to pulsed wave (320ms lengths and 320ms intervals) ultrasound (f = 205 kHz).....	141
B2.1	Zero order ultrasonic HTA formation reactions of in aqueous solution (1mM, 300ml) exposed to continuous ultrasound (f = 205 kHz).....	142
B2.2	Zero order ultrasonic HTA formation reactions of in aqueous solution (1mM, 300ml) exposed to pulsed wave (30ms lengths and 30ms intervals) ultrasound (f = 205 kHz).....	142
B2.3	Zero order ultrasonic HTA formation reactions of in aqueous solution (1mM, 300ml) exposed to pulsed wave (30ms lengths and 60ms intervals) ultrasound (f = 205 kHz).....	143
B2.4	Zero order ultrasonic HTA formation reactions of in aqueous solution (1mM, 300ml) exposed to pulsed wave (30ms lengths and 100ms intervals) ultrasound (f = 205 kHz).....	143
B2.5	Zero order ultrasonic HTA formation reactions of in aqueous solution (1mM, 300ml) exposed to pulsed wave (30ms lengths and 160ms intervals) ultrasound (f = 205 kHz).....	144
B2.6	Zero order ultrasonic HTA formation reactions of in aqueous solution (1mM, 300ml) exposed to pulsed wave (30ms lengths and 320ms intervals) ultrasound (f = 205 kHz).....	144
B2.7	Zero order ultrasonic HTA formation reactions of in aqueous solution (1mM, 300ml) exposed to pulsed wave (60ms lengths and 30ms intervals) ultrasound (f = 205 kHz).....	145
B2.8	Zero order ultrasonic HTA formation reactions of in aqueous solution (1mM, 300ml) exposed to pulsed wave (60ms lengths and 60ms intervals) ultrasound (f = 205 kHz).....	145
B2.9	Zero order ultrasonic HTA formation reactions of in aqueous solution (1mM, 300ml) exposed to pulsed wave (60ms lengths and 100ms intervals) ultrasound (f = 205 kHz).....	146
B2.10	Zero order ultrasonic HTA formation reactions of in aqueous solution (1mM, 300ml) exposed to pulsed wave (60ms lengths and 160ms intervals) ultrasound (f = 205 kHz).....	146
B2.11	Zero order ultrasonic HTA formation reactions of in aqueous solution (1mM, 300ml) exposed to pulsed wave (60ms lengths and 320ms intervals) ultrasound (f = 205 kHz)....	147

B2.12	Zero order ultrasonic HTA formation reactions of in aqueous solution (1mM, 300ml) exposed to pulsed wave (100ms lengths and 30ms intervals) ultrasound (f = 205 kHz)....	147
B2.13	Zero order ultrasonic HTA formation reactions of in aqueous solution (1mM, 300ml) exposed to pulsed wave (100ms lengths and 60ms intervals) ultrasound (f = 205 kHz).....	148
B2.14	Zero order ultrasonic HTA formation reactions of in aqueous solution (1mM, 300ml) exposed to pulsed wave (100ms lengths and 100ms intervals) ultrasound (f = 205 kHz)...	148
B2.15	Zero order ultrasonic HTA formation reactions of in aqueous solution (1mM, 300ml) exposed to pulsed wave (100ms lengths and 160ms intervals) ultrasound (f = 205 kHz)...	149
B2.16	Zero order ultrasonic HTA formation reactions of in aqueous solution (1mM, 300ml) exposed to pulsed wave (100ms lengths and 320ms intervals) ultrasound (f = 205 kHz)...	149
B2.17	Zero order ultrasonic HTA formation reactions of in aqueous solution (1mM, 300ml) exposed to pulsed wave (160ms lengths and 30ms intervals) ultrasound (f = 205 kHz).....	150
B2.18	Zero order ultrasonic HTA formation reactions of in aqueous solution (1mM, 300ml) exposed to pulsed wave (160ms lengths and 60ms intervals) ultrasound (f = 205 kHz).....	150
B2.19	Zero order ultrasonic HTA formation reactions of in aqueous solution (1mM, 300ml) exposed to pulsed wave (160ms lengths and 100ms intervals) ultrasound (f = 205 kHz)...	151
B2.20	Zero order ultrasonic HTA formation reactions of in aqueous solution (1mM, 300ml) exposed to pulsed wave (160ms lengths and 160ms intervals) ultrasound (f = 205 kHz)...	151
B2.21	Zero order ultrasonic HTA formation reactions of in aqueous solution (1mM, 300ml) exposed to pulsed wave (160ms lengths and 320ms intervals) ultrasound (f = 205 kHz)...	152
B2.22	Zero order ultrasonic HTA formation reactions of in aqueous solution (1mM, 300ml) exposed to pulsed wave (320ms lengths and 30ms intervals) ultrasound (f = 205 kHz).....	152
B2.23	Zero order ultrasonic HTA formation reactions of in aqueous solution (1mM, 300ml) exposed to pulsed wave (320ms lengths and 60ms intervals) ultrasound (f = 205 kHz).....	153
B2.24	Zero order ultrasonic HTA formation reactions of in aqueous solution (1mM, 300ml) exposed to pulsed wave (320ms lengths and 100ms intervals) ultrasound (f = 205 kHz)...	153
B2.25	Zero order ultrasonic HTA formation reactions of in aqueous solution (1mM, 300ml) exposed to pulsed wave (320ms lengths and 160ms intervals) ultrasound (f = 205 kHz)...	154
B2.26	Zero order ultrasonic HTA formation reactions of in aqueous solution (1mM, 300ml) exposed to pulsed wave (320ms lengths and 320ms intervals) ultrasound (f = 205 kHz)....	154
C1.1	First order ultrasonic degradation of OBS in aqueous solution (1mM, 300ml) exposed to continuous ultrasound (f = 69 kHz).....	156

C1.2	First order ultrasonic degradation of OBS in aqueous solution (1mM, 300ml) exposed to pulsed wave (30ms lengths and 30ms intervals) ultrasound (f = 69 kHz).....	156
C1.3	First order ultrasonic degradation of OBS in aqueous solution (1mM, 300ml) exposed to pulsed wave (30ms lengths and 60ms intervals) ultrasound (f = 69 kHz).....	157
C1.4	First order ultrasonic degradation of OBS in aqueous solution (1mM, 300ml) exposed to pulsed wave (30ms lengths and 100ms intervals) ultrasound (f = 69 kHz).....	157
C1.5	First order ultrasonic degradation of OBS in aqueous solution (1mM, 300ml) exposed to pulsed wave (30ms lengths and 160ms intervals) ultrasound (f = 69 kHz).....	158
C1.6	First order ultrasonic degradation of OBS in aqueous solution (1mM, 300ml) exposed to pulsed wave (30ms lengths and 320ms intervals) ultrasound (f = 69 kHz).....	158
C1.7	First order ultrasonic degradation of OBS in aqueous solution (1mM, 300ml) exposed to pulsed wave (60ms lengths and 30ms intervals) ultrasound (f = 69 kHz).....	159
C1.8	First order ultrasonic degradation of OBS in aqueous solution (1mM, 300ml) exposed to pulsed wave (60ms lengths and 60ms intervals) ultrasound (f = 69 kHz).....	159
C1.9	First order ultrasonic degradation of OBS in aqueous solution (1mM, 300ml) exposed to pulsed wave (60ms lengths and 100ms intervals) ultrasound (f = 69 kHz).....	160
C1.10	First order ultrasonic degradation of OBS in aqueous solution (1mM, 300ml) exposed to pulsed wave (60ms lengths and 160ms intervals) ultrasound (f = 69 kHz).....	160
C1.11	First order ultrasonic degradation of OBS in aqueous solution (1mM, 300ml) exposed to pulsed wave (60ms lengths and 320ms intervals) ultrasound (f = 69 kHz).....	161
C1.12	First order ultrasonic degradation of OBS in aqueous solution (1mM, 300ml) exposed to pulsed wave (100ms lengths and 30ms intervals) ultrasound (f = 69 kHz).....	161
C1.13	First order ultrasonic degradation of OBS in aqueous solution (1mM, 300ml) exposed to pulsed wave (100ms lengths and 60ms intervals) ultrasound (f = 69 kHz).....	162
C1.14	First order ultrasonic degradation of OBS in aqueous solution (1mM, 300ml) exposed to pulsed wave (100ms lengths and 100ms intervals) ultrasound (f = 69 kHz).....	162
C1.15	First order ultrasonic degradation of OBS in aqueous solution (1mM, 300ml) exposed to pulsed wave (100ms lengths and 160ms intervals) ultrasound (f = 69 kHz).....	163
C1.16	First order ultrasonic degradation of OBS in aqueous solution (1mM, 300ml) exposed to pulsed wave (100ms lengths and 320ms intervals) ultrasound (f = 69 kHz).....	163
C1.17	First order ultrasonic degradation of OBS in aqueous solution (1mM, 300ml) exposed to pulsed wave (160ms lengths and 30ms intervals) ultrasound (f = 69 kHz).....	164

C1.18	First order ultrasonic degradation of OBS in aqueous solution (1mM, 300ml) exposed to pulsed wave (160ms lengths and 60ms intervals) ultrasound (f = 69 kHz).....	164
C1.19	First order ultrasonic degradation of OBS in aqueous solution (1mM, 300ml) exposed to pulsed wave (160ms lengths and 100ms intervals) ultrasound (f = 69 kHz).....	165
C1.20	First order ultrasonic degradation of OBS in aqueous solution (1mM, 300ml) exposed to pulsed wave (160ms lengths and 160ms intervals) ultrasound (f = 69 kHz).....	165
C1.21	First order ultrasonic degradation of OBS in aqueous solution (1mM, 300ml) exposed to pulsed wave (160ms lengths and 320ms intervals) ultrasound (f = 69 kHz).....	166
C1.22	First order ultrasonic degradation of OBS in aqueous solution (1mM, 300ml) exposed to pulsed wave (320ms lengths and 30ms intervals) ultrasound (f = 69 kHz).....	166
C1.23	First order ultrasonic degradation of OBS in aqueous solution (1mM, 300ml) exposed to pulsed wave (320ms lengths and 60ms intervals) ultrasound (f = 69 kHz).....	167
C1.24	First order ultrasonic degradation of OBS in aqueous solution (1mM, 300ml) exposed to pulsed wave (320ms lengths and 100ms intervals) ultrasound (f = 69 kHz).....	167
C1.25	First order ultrasonic degradation of OBS in aqueous solution (1mM, 300ml) exposed to pulsed wave (320ms lengths and 160ms intervals) ultrasound (f = 69 kHz).....	168
C1.26	First order ultrasonic degradation of OBS in aqueous solution (1mM, 300ml) exposed to pulsed wave (320ms lengths and 320ms intervals) ultrasound (f = 69 kHz).....	168
D.1	Impedance test output of the 70 kHz transducer.....	170
D.2	Impedance test output of the 205 kHz transducer.....	171
D.3	Impedance test output of the 620 kHz transducer.....	172
D.4	Impedance test output of the 806 kHz transducer.....	173
D.5	Impedance test output of the 279 kHz transducer.....	174
D.6	Impedance test output of the 1054 kHz transducer.....	175
D.7	Impedance test output of the 354 kHz transducer.....	176
D.8	Comparative Impedance test output of a standard 20 kHz transducer.....	177

CHAPTER 1

INTRODUCTION

1.1 ENVIRONMENTAL IMPLICATIONS OF LAS USE

For over 30 years linear alkyl benzene sulfonate (LAS) has been the most globally used anionic surfactant (Ying et al., 2006). The yearly global consumption of LAS is approximately 2 million tons. It constitutes around 40% of all products leading to a large amount of LAS in wastewater from domestic and industrial applications (Bakirel et al., 2005). One problem associated with high volumes of LAS in wastewater influent is that it has a high chemical oxygen demand (COD). It has been suggested that the pollution associated with surfactants may be further reduced by lowering the quantity used in all domestic and industrial cleaning applications (Venhuis et al., 2004). However, this is a difficult task to regulate and enforce.

1.2 FATE OF LAS IN ENVIRONMENTAL MATRICES

Because so much LAS is used, and it has been found to be harmful and toxic at certain levels, it has become important to understand how to effectively treat LAS in wastewater before it is released as effluent or as wastewater sludge to be applied to agricultural land. Once released into the environment, it is imperative to understand how LAS will partition and decay within various environmental matrices (Ying et al., 2006; Sharvelle et al., 2007).

1.2.1 FATE OF LAS IN AQUATIC ENVIRONMENTS

In river water LAS is quickly degraded with a half-life of 3 days due to the higher levels of natural micro fauna and dissolved oxygen. In marine waters with lower levels of microbes and in groundwater with lower levels of dissolved oxygen only a small percentage of LAS is degraded (Ying et al., 2006).

LAS compounds have surface active properties and therefore tend to partition to biological membranes (Shavelle et al., 2007; Bakirel et al., 2005). Fish are sensitive to LAS in aquatic environments. The gills which are very thin and have a great amount of surface area, have been found to be a site for higher concentrations (Alvarez-Munoz et al., 2007). Due to their extreme sensitivity to surfactants, fish will avoid contaminated waters containing LAS concentrations as low as 0.001 mg/L. However at higher levels around 0.1 mg/L fish have been found to lose their ability to sense the presence of the surfactant (Bakirel et al, 2005). Not only does the concentration of LAS in an aqueous environment have a negative effect on fish, but as the length of the n-alkyl chain of LAS increases the K_{ow} and as a result the bioavailability to fish also increases (i.e., through the gills) (Ying et al., 2006). Below toxic levels, the effects on fish include decreased growth, hindered swimming abilities, and pathologically altered gills (Holmstrump and Krogh, 2001). Above toxic levels LAS can

denature proteins and disrupt membranes (Holmstrump and Krogh, 2001). Fish are a part of the food chain. Therefore, if LAS has bioconcentrated in fish, as the fish is consumed it can be bioconcentrated by those successive species up the food chain and potentially cause harm to them as well (Alvarez-Munoz et al., 2007).

1.2.2 AEROBIC BACTERIAL DEGRADATION

LAS is quickly degraded by aerobic microbial processes of wastewater treatment plants. For example, it has been reported that 99% of LAS in the aqueous portion of waste water is removed during treatment before it is released into the environment (Venhuis et al., 2004). In addition, even at very low concentrations in soil (lower than 50 ng/g soil) the aerobic community in a variety of geographically diverse soils was found to be effective in mineralizing LAS (Knaebel et al., 1990). In aerobic soil conditions, the half-life of LAS ranges from 7-33 days. When LAS-contaminated sludge is applied to soil, the degradation rate depends on the aerobic bacteria present. The type of soil, vegetation, and soil conditions had little to no effect on the degradation compared to the effects from the aerobic bacteria that were present (Ying et al., 2006).

1.2.3 FATE OF LAS FROM SLUDGE APPLICATION

Of the sewage sludge that was land applied for agricultural purposes it was found that on average, concentrations of 530 mg of LAS per kg of dry sludge were observed in one Danish study (Torslov et al. 1997). In that same study the highest concentration of LAS in dry sludge was on the order of 16000 mg/kg dry weight. Venhuis et al. (2004) documented that 0-488 mg/kg of the dry

weight portion of sewage sludge was made up of LAS compounds. The reason for such high levels of LAS in sludge is that much of the LAS is recalcitrant. The reason for this is that it can strongly adsorb to the sludge particles, and it is not degraded by the secondary anaerobic destructive processes of waste water treatment plants (Holmstrump and Krogh, 2001; Ying et al., 2006; McAvoy et al., 2002). A most recent study however, did find that when in the presence of the correct types of sulfur reducing and methanogenic anaerobic bacteria environments, the LAS compounds in sludge could be degraded upon being applied to anoxic marine sediments, with an average half-life of 90 days (Lara-Martin et al., 2007).

When sewage sludge containing pollutants such as LAS is applied as a soil improving agent there can be reason for concern (Morgensen et al., 2002). By increasing the amount of surfactant in sludge the mobility of other potential toxins in sludge may be increased (Geilsberg et al. 2001). There are a few studies on the toxic effects of varying amounts of LAS in soil and sludge. In one study on the effects of sludge amended soil Holstrump et al. (2001) observed that the, half maximal effective concentration (EC 50) for LAS occurred at concentrations in the sludge between 934 to 1269 mg/kg. However in another study the EC 50 was much lower and was found to be between 8 and 14 mg/kg dry sludge amended soil. This difference was found potentially to be the result of other toxins present in the sludge that were increasingly mobilized with the lower concentrations of LAS in the sludge. This comparison was made by Geilsberg et al. (2001) who also did a similar study and found toxicity levels to be comparable to those found by Holstrump et al. (2001).

There are few studies on the effects of LAS on soil biota and invertebrates that may be affected by sludge applications. Holstrump et al. (2001) also studied the effects of various concentrations of LAS contaminated sludge on soil invertebrates. They found toxic effects to occur at levels slightly above 40 to 60 mg/kg dry sludge on average in invertebrates that are typically found in soil, including earthworms, enchytraeids, springtails and mites.

There are even fewer studies on the effects of LAS bioavailability in plants such as those that could be used as phytoremediators of such compounds or those grown in agricultural soil where sludge is applied. However in one study it was found that a bioconcentration factor (BCF), which is used to correlate the amount of the contaminant concentrated in the organism to that in surrounding aqueous fractions of the environment, was observed to range between 2 and 7 for grass, bean, radish and potato species of plants being grown in soils that were spiked with 16 and 27 mg/kg of LAS (Ying et al., 2006). When testing the preliminary effects of LAS concentrations on willow trees to be used as potential phytoremediators, Yu et al. (2006) found that at the levels of LAS found in the environment, this compound would not be toxic.

1.3 OXIDATIVE REACTIONS INVOLVED IN LAS DEGRADATION

There are two main pathways involved in the anaerobic degradation of LAS. First the tail methyl group is oxidized (ω -oxidation) which includes the substitution of the methyl group with a carboxylic acid; this is then followed by successive slicing of the alkyl chain (β -oxidation). As the LAS compound is degraded its polarity is increased. Concurrently as the LAS, BCF is decreased, it loses its ability to be retained on membranes (Alvarez-Munoz, 2007). The byproducts of LAS during oxidative degradation include mono and dicarboxylic, sulfophenyl acids (SPCs) of chain lengths 4 to 13 carbons (Alvarez-Munoz et al., 2007). After the carbon chain is oxidized in this way the sulfonate group is desulfonated during the second pathway of degradation which then involves the cleavage of the benzene ring. Much of this process requires oxygen, and therefore little evidence has been shown that LAS compounds degrade under anaerobic conditions (Ying et al., 2006). The complete oxidative degradation of LAS results in the production of CO₂, water, inorganic salts and biomass (Di Corcia et al., 1999).

1.4 ENHANCED DEGRADATION OF LAS COMPOUNDS THROUGH ADVANCED OXIDATION TECHNOLOGIES

One option in remediation of LAS classified surfactants which are completely synthetic, is to replace them with the more environmentally friendly versions that are made from natural chemicals that are not as robust. If this is not an option, a remediation technology is needed that can degrade LAS before it is released into the environment. Ultrasound as an advanced oxidative technology could be a possible treatment technology for these surfactants. However, it may be too energy intensive to degrade the complete compound via ultrasound. It has been thought that bioremediation could be combined with another type of treatment technology such as ultrasound to enhance the degradation of LAS, especially the slower degradation processes during the second phase of desulfonation and attack of the benzene ring (Mantzavinos et al., 2001) when byproducts that have formed are more difficult to degrade and desorb from sediment (McAvoy et al., 1992).

For example, when oxidative degradation of LAS was performed in the presence of H_2O_2 and UV light, only 5 minutes of exposure was required to degrade the initial compound. In the presence of UV light alone, the degradation of LAS was much slower. It took 5 hours to degrade to just 80% of the initial compound (Venhuis et al., 2004). Exposure of LAS to UV light in the presence of H_2O_2 may be an efficient process however such applications have been found to be costly (Swisher et al. 1987).

Another approach is the use of Fenton oxidative technology. This technology employs $FeSO_4$ and H_2O_2 to generate OH radicals which oxidize and degrade the surfactant compounds. It has been shown that OH radicals are strong oxidants (Lin et al., 1999). The oxidative potential for OH radicals is 2.8 V, while ozone holds a potential of 2.07 V indicating that OH radicals are much more powerful oxidants (Lin et al., 1999). The use of iron sulfate in place of other oxidative technologies such as ozone, has also been found to be cheaper. In addition, the removal efficiency of LAS was found to be over 95% (Lin, et al., 1999). The resulting dissolved Fe concentrations in the wastewater are effectively removed by subsequent chemical coagulation (Lin et al., 1999).

Foam fractionation offers an interesting method of decontaminating a system of surface active compounds. During this method air is simply sparged into solution creating bubbles in solution which collect the surface active compounds at the air/water interface as the bubbles rise and float out of solution. It was observed that 90% of the surfactant could be removed effectively in this manner (Venhuis et al., 2004).

1.5 ULTRASOUND AS AN ADVANCED OXIDATION TECHNOLOGY

Ultrasound has been proposed as another potential advanced oxidation technology to degrade contaminants such as LAS and other surface active compounds in water (Abu-Hassan et al., 2006; Weavers et al., 2005).

When a solution is exposed to high intensity ultrasound, tiny bubbles are formed. Some of these bubbles will be affected by the ultrasonic wave in such a way that they become micro-reactors. (Leighton, 1994). Depending on the physical properties of the pollutant (i.e., volatility or hydrophobicity) the pollutant will be degraded in different reaction sites either in and/or around these bubbles. The resulting chemistry formed by the effects of sound waves has understandably been termed sonochemistry. To have a better understanding, a brief background in bubble dynamics follows.

1.5.1 THE BUBBLE

Bubbles that are present in a liquid are inherently unstable. They either float out of solution due to buoyancy or dissolve away due to an excess pressure acting outward. There are a number of variables that come into play in determining whether bubbles will grow or shrink in size (Epstein and Plesset, 1950). The pressure acting on the outside of a bubble in solution is due to the sum of the external pressure (P_o) and a surface tension pressure (P_γ). The pressure inside the bubble (P_{in}) is due the pressure of the gas (P_g) and the vapor pressure of the liquid (P_v). However, because of the curvature of the bubble, there is an excess pressure on the inside of the bubble, known as the Laplace pressure, which would have to be balanced by the external surface tension pressure (P_γ) for the bubble to be stable in solution. Therefore, the overall pressure inside a static bubble (P_i) can be equated, as shown in Equation 1.1 (Leighton, 1994):

$$P_{out} + P_\gamma = P_g + P_v \quad (1.1)$$

If the two sides of the equation are equal, the bubble will remain static and stable in the liquid. In this case, the excess Laplace pressure is balanced by the surface tension pressure (i.e., $P_\gamma = 2\gamma/R$). However, for relatively small bubbles with a large surface curvature, the excess Laplace pressure forces gas out of the bubble and causes it to dissolve away. In the presence of ultrasound, however, bubbles can absorb energy from the pressure wave and either pulsate for many acoustic cycles or grow in size, as described below.

1.5.2 BUBBLE NUCLEATION TO HOT SPOT FORMATION

Ultrasound passed through a liquid acts as a longitudinal pressure wave (Mason and Lorimer, 1988). When introduced into a liquid, the pressure in the liquid will oscillate between low and high pressure as compared to the ambient pressure as a function of time. Any impurities that hold trapped pockets of gas and/or bubbles present in this solution will be affected by the pressure wave. In any liquid, even the most filtered container of water, trapped pockets of gas exist within the liquid, on the sides of containers, and on tiny particles that are not completely removed from the liquid (Suslick, 1988). As the negative pressure cycle of the wave is passed through a trapped gas pocket, the gas pocket will expand. The gas molecules in this impurity move further apart; if the pressure is low enough, the gas pocket will expand to the point where it detaches from the liquid. This is how bubble nucleation occurs (Suslick, 1988). Bubbles that are present in a liquid adsorb energy from the wave and are stabilized from floating out of or dissolving into the liquid. These bubbles grow and shrink with the subsequent rarefaction and compression phases of the ultrasound wave. A representation of the ultrasound pressure wave is shown in Figure 1.1.

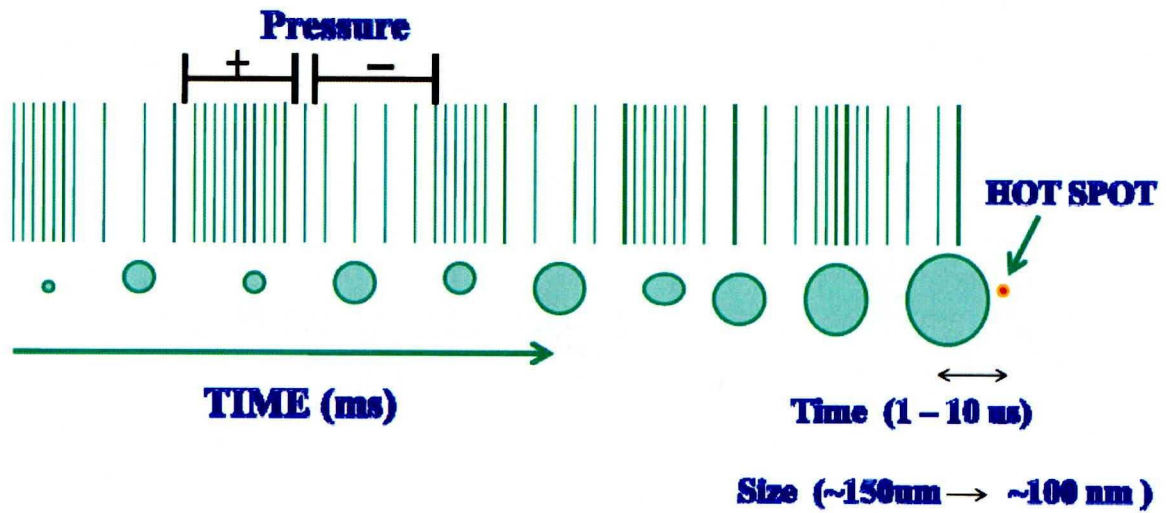


Figure 1.1 Pictorial representation of the ultrasound wave as it affects the growth of the cavitation bubble. This is followed by the sudden growth and adiabatic collapse of the bubble to create the hot spot.

The bubble can absorb energy from the wave and expand and contract under the influence of the alternating rarefaction and compression cycle of the wave. However, due to phenomena such as bubble-bubble coalescence and a process called rectified diffusion, the bubble can grow in size over a number of acoustic cycles (Leighton, 1994).

Bubbles that create sonochemistry will eventually reach resonance with the wave whether it is through many acoustic cycles as during rectified diffusion (these bubbles are known as stable bubbles) or over the course of just a few cycles as for purely transient bubbles. Once a bubble has reached resonance with the wave, it can then adsorb energy most effectively from the wave. When a negative pressure cycle passes through, the bubble expands so rapidly that it continues to expand out of phase with the wave. Once the bubble reaches a size where its radius is at a maximum (R_{max}) it is so large that it is extremely unstable. The overall pressure acting on the outside of the bubble causes the bubble to rapidly collapse until it reaches R_{min} . This collapse time is so fast that there is no time for vapor or gas to diffuse out of the bubble resulting in little mass and heat transfer to the bubble surroundings (Suslick, 1991). This is essentially an adiabatic compression. Therefore, this rapid compression not only results in a massive build up of pressure but also a massive build up of temperature in the hot spot as shown in Figure 1.2.

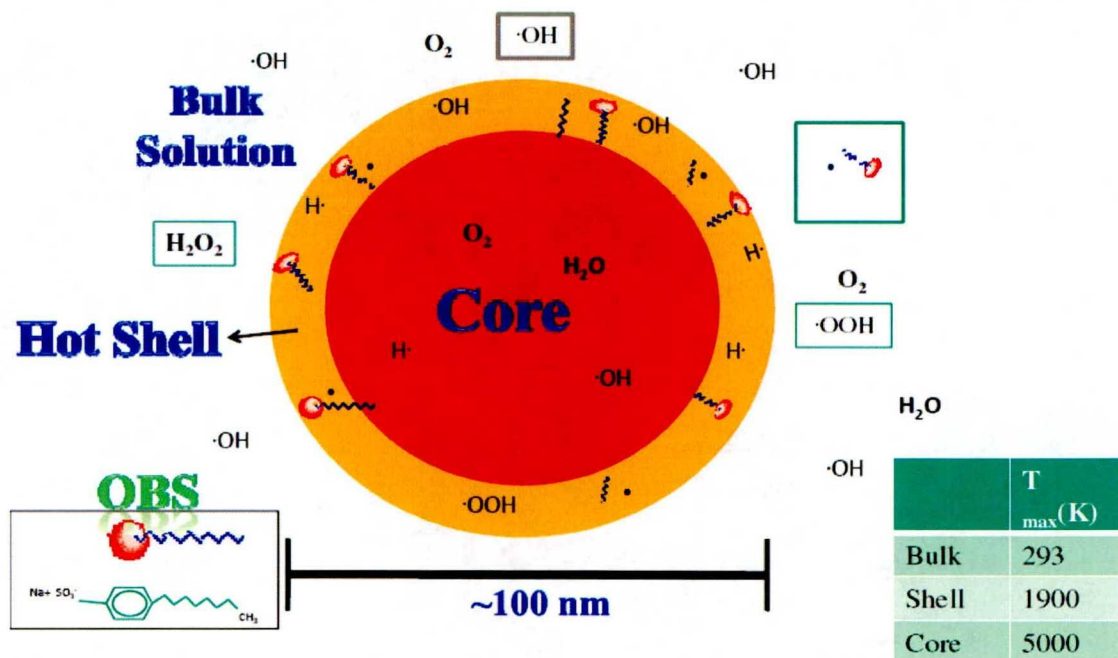


Figure 1.2 Pictorial representation of the Hot Spot. Notice the radicals that are formed as a result of thermolysis degradation of the surfactant and water molecules.

1.5.3 TEMPERATURE OF THE HOT SPOT

Suslick determined that temperatures generated in the localized cavitation bubble environments are as high as ~5000 K (Suslick, 1991). Theoretical modeling of a collapse suggested a maximum collapse core temperature of around 20,000 K (Ashokkumar et al., 2005). The maximum temperature attained at collapse is estimated using the following equation:

$$T_{max} = T_0 P_a \left(\left(\frac{c_p}{c_v} \right) - 1 \right) / P_v \quad (1.2)$$

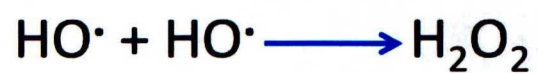
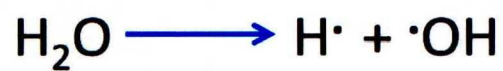
Where T_{max} is the maximum temperature generated upon collapse of the bubble, P_v is the pressure inside of the bubble and P_a is the external pressure acting on the bubble at collapse, T_0 is the temperature in the bulk of the solution and $\frac{c_p}{c_v}$ is the ratio of the specific heat of the gas (Noltingk and Neppiras, 1950; Flynn et al., 1964; Neppiras et al., 1980) all as cited by (Mason and Lorimer, 1988). It is known that the thermal conductivity of the gas also affects the bubble temperature upon collapse. As the thermal conductivity increases the atomic weight decreases, therefore of the noble gases helium has the least ability to hold the temperature within the bubble core (Grieser et al., 2001; Grieser et al., 2004). As a result of rectified diffusion, the temperature of collapse can also be appreciably decreased. Rectified diffusion can cause a buildup of vapor in the bubble (i.e., P_v will increase) and the overall T_{max} will decrease (i.e Eq. 1.2). The reason for this decrease in temperature is that the molecules of the vapor will absorb some of the energy in the form of endothermic chemical reactions taking away from the absolute temperatures formed upon collapse (Vinodgopal et al., 2001).

The temperatures generated upon the formation of the hot spot are concentrated in the core of the hot spot. Therefore volatile compounds are thermally degraded inside collapsing cavitation

bubbles. However, in sonochemistry, it has been observed that nonvolatile surfactants are also thermally degraded. During the collapse of cavitation bubbles, the liquid immediately surrounding the bubble is heated to extremely high temperatures. Therefore, any nonvolatile organic molecules that have partitioned to the outside of the bubble will also be thermally degraded upon collapse (Vinodgopal et al., 2001)

1.5.4 RADICAL GENERATION VIA THE HOMOLYSIS OF WATER MOLECULES

When cavitation bubbles are generated in water not only are high temperatures and pressures created as a result of the collapse of the bubbles (Leighton, 1994) but highly reactive radical species are also created. During ultrasound exposure, radical species such as H atoms and OH radicals are formed that react with target organic pollutants. These radicals result from the degradation of water vapor molecules that have diffused into the bubble prior to collapse (Pertrier et al., 1994). In the presence of oxygen, H atoms react with oxygen to form hydroperoxyl radicals ($HO_2\cdot$). The four main reactions depicting the formation and combination of these radicals is shown in Scheme 1.1. These oxidative radicals act to degrade volatile compounds that have diffused into the bubble during its lifetime. The radicals also react with pollutants that have adsorbed to the surface of the bubble. Therefore upon collapse of the cavitation bubble an environment has been created where the target pollutant may potentially degrade via high temperatures as well as via reaction with the created radicals (Leighton, 1994). Although hydroxyl radicals ($OH\cdot$) are highly reactive, they can diffuse from the bubble into the bulk solution to a certain degree. Therefore, the amount of $OH\cdot$ created in solution may be measured; the quantity measured gives an estimate of the system's overall chemical reactivity (Price et al., 1993).



Scheme 1.1 Dominant chemical reactions generating radicals resulting from water homolysis.

1.5.5 GROWTH VIA RECTIFIED DIFFUSION

Rectified diffusion is a process of bubble growth through ultrasound. This growth via rectified diffusion occurs in two parts. The first is called the area effect. When the surface area of the bubble is smaller than the bubble radius at equilibrium size, (R_0), the concentration of the gas inside the bubble is under more pressure than the concentration in the bulk phase. When this occurs gas will diffuse out of the bubble. On the other hand, when the surface area of the bubble is greater than equilibrium size, the pressure of the gas inside the bubble is lower than that in the bulk phase and gas from the bulk will diffuse into the bubble. Because the surface area of the bubble is lower when gas diffuses outward compared to when gas diffuses inward, there is a greater amount of gas coming into the bubble over time. Therefore, the bubble will grow, allowing it to eventually reach its resonance radius (Leighton, 1994).

The second process influencing rectified diffusion is called the shell effect. Around the surface of the bubble there is a layer called the air/liquid interface or the bubble shell. This shell becomes thickened as the bubble shrinks and is thinner as the bubble grows. The influence of the gas concentration in the shell and the shell thickness help to set in place the same types of concentration gradients observed due to the area effect. When the bubble expands the concentration of the gas in the shell is lower than in the bulk and the shell thickness is thinner; therefore, the barrier for gas to diffuse toward the bubble is smaller, enhancing the ability of the gas to diffuse into the bubble. Upon contraction, the shell of the bubble thickens and the concentration of gas in the shell increases due to less surface area. The resulting concentration gradient is lower than when the bubble is expanded. In addition, the thickness of the shell is enhanced creating a greater barrier to diffusion outward than when the bubble is expanded (Leighton, 1994).

1.5.6 TYPES OF BUBBLES THAT ARE FORMED

The types of bubbles that are formed at varying frequencies and the resulting effects of these types of bubbles on the overall system is quite complicated. At higher frequencies, “stable” cavitation bubbles tend to form which grow via a process of rectified diffusion. There are two classifications of stable bubbles. One type are the high energy stable bubbles (HES). These bubbles, upon rectified diffusion and subsequent bubble growth and collapse, will create chemistry and sonoluminescence (Beckett and Hua, 2001). However as a result of decreased amplitude associated with the bubble radius, the adiabatic collapse at the end of the bubble lifetime may not be great enough to create high enough temperatures and pressures to increase the chemical and physical reactivity of the system in comparison to that of lower frequency transient bubbles (Thompson and Doraiswamy, 1999).

The second type of stable bubble existing at high frequency are low energy stable bubbles (LES). These bubbles are stabilized by the wave but never reach resonance with the wave and therefore will never create a hot spot. From a sonochemical standpoint, it is the HES bubble population of stable bubbles that are important (Leighton, 1994).

At lower frequencies transient bubbles are predominant in aqueous systems. These bubbles can reach resonance with the wave more quickly and the collapse compression ratio R_{\max}/R_{\min} is much greater than at lower frequencies. Therefore, the bubbles can collapse more rapidly and with a greater volume decrease, resulting in higher temperatures. However, the number of bubbles in a solution will be lower when transient bubbles are predominant. Also the bubble size, buoyancy and irradiative pressures can act on the bubble to distort the sphericity of the bubble to create a less spherical collapse and therefore decreased chemical reactivity. However, as a result of this distorted collapse of the bubble, fragmentation can occur which can lead to additional nucleation sites for more bubbles to form and lead to more sonochemistry (Beckett and Hua, 2001).

The two types of cavitation bubbles that are created have been categorized conceptually as well as mathematically. Flynn defined a transient bubble as the ratio of maximum bubble radius, R_{\max} , to equilibrium bubble radius, R_0 , being greater than or equal to 2.0. Noltingk and Neppiras calculated a slightly larger bubble size ratio of 2.3 based on a supersonic adiabatic bubble collapse, as cited by (Leighton, 1994). Alternately, stable bubbles by either model have a radius ratio less than either of the ratios calculated by these models (Leighton, 1994).

1.5.7 PREFERENTIAL SURFACTANT DEGRADATION VIA ULTRASOUND

Upon collapse of a bubble in a surfactant contaminated solution, the degradation of surfactant is expected to occur primarily at the hot shell area of the collapsing bubble. Additionally degradation may occur via the oxidative radicals that have formed as a result of vapor dissociation reactions and thermal decomposition. It has been shown that most of the radicals will concentrate at the hot shell of the hot spot. A small amount of OH radicals will reach the bulk of the solution to interact with surfactant monomers that have not adsorbed at the interface; therefore, chemical reactions with surfactant molecules will most likely happen at that hot shell area upon collapse of a bubble as a result of thermal decomposition of water vapor (Vinodgopal et al., 2001).

Since surfactant molecules adsorb at the bubble surfaces it is imperative that an understanding of the effect of surfactants on bubble dynamics be understood when implementing ultrasound as a potential treatment technology. The influence of the structure of the surfactant combined with the bubble lifetime and concentration of the surfactant will constitute the ability of the surfactant to be degraded upon hot spot formation (Sunartio et al., 2006).

1.5.7.1 INITIAL SURFACTANT CONCENTRATION EFFECTS

The concentration of a surfactant can affect its own initial decomposition rate in the presence of ultrasound. Vinodgopal et al. (2001) observed that as a concentration of surfactant increased up to the CMC the initial degradation rate also increased. However, at the CMC and above the degradation rate reached a plateau. This they said illustrated the point that the individual surfactant monomers had a main effect on the ability of the surfactant to degrade but after a certain concentration where micelles were being created, additional monomers added to solution would not aid in the degradation of the surfactant. (Vinodgopal et al., 2001).

1.5.7.2 COALESCENCE PREVENTION AND DECLUSTERING VIA SURFACTANT ADSORPTION

As bubbles form in a cavitating aqueous system they will cluster when in high enough concentrations as a result of Bjerknes forces. Bjerknes forces enhance clustering by forcing bubbles of similar sizes into regions in the ultrasonic field known as nodes and antinodes (Lee et al., 2005). There are negative impacts as a result of this clustering effect. The cluster formations act as barriers for the ultrasound wave from influencing the bubbles at the interior of the clusters. Also, as bubbles contact and coalesce, larger bubbles are created that may be too buoyant and large to be affected by ultrasonic wave. Therefore, bubbles become inactive as a result of being in the center of a cluster or as a result of floating out of solution (Sunartio et al., 2006). In effect coalescence and clustering decrease the overall sonochemical yield of a system. However, when surfactants are present, they can act to inhibit the negative effects of bubble coalescence and or clustering (Sunartio et al., 2006; Brotchie et al., 2006).

When an anionic surfactant such as LAS adsorbs to the interface of the bubble the exterior of the bubble it will possess an overall negative charge. As a result long range electrostatic repulsions

between bubbles act to separate the cavitation bubbles, resulting in the declustering of bubble clusters and prevention of bubble coalescence. These effects are in addition to short range steric repulsions which are present when noncharged surfactant molecules are adsorbed to the bubble surface. However, short range steric repulsions only prevent the coalescence of bubbles but have little effect on bubble declustering (Ashokkumar et al., 2007). As a result of surfactant addition, the bubble distribution within the solution will be more uniform and the ultrasound adsorption by bubbles will be more efficient due to the declustering (Ashokkumar et al., 2007).

1.5.7.3 DECREASED SURFACE TENSION AS A RESULT OF SURFACTANT ADDITION

The Laplace pressure (P_L) or the pressure acting on the bubble is directly correlated to the surface tension and the bubble curvature, and is inversely proportional to the bubble radius. The Laplace pressure is calculated via the following equation (Crum, 1999):

$$P_L = \frac{2\gamma}{R} \quad (1.3)$$

The surface tension (γ) can be measured in a bubble of radius R that has reached equilibrium with the surfactant. As the concentration of surfactant in solution is increased the surface tension of the interface will decrease, resulting in a decrease in the Laplace pressure (eq. 1.3). This may decrease the amount of bubbles that are lost to dissolution (i.e. it will increase the lifetime of the bubbles) or even coalescence (i.e., the surface tension is increased enough to relieve some of the Laplace pressure that bubbles can become too large and float out of solution).

From the surface tension of the gas/solution interface, it is possible to calculate a parameter known as the Gibbs surface excess Γ_{eq} which is the measure of the amount of surfactant adsorbed to the gas/solution interface as a result of equilibrium adsorption (Adamson and Gast, 1997).

$$\Gamma_{eq} = -\frac{1}{2}RT\left[\frac{d\gamma_{eq}}{dLn C_{eq}}\right] \quad (1.4)$$

At equilibrium, the amount of surfactant C_{eq} and the surface tension γ_{eq} at the air/water interface is constant. The ability of a surfactant to reach equilibrium may be severely affected in an ultrasonic system where the bubbles exist for finite time periods. If the surfactant does not reach equilibrium the ability for the surfactant to affect the surface activity of a cavitation bubble becomes dynamic in nature. It is known that as the chain length on a surfactant within a homologous series increases, the ability of that surfactant to reach equilibrium concentrations is diminished (Sostaric and Reisz 2001; 2002).

1.5.7.4 ADSORPTION OF SURFACTANT TO THE AIR / LIQUID INTERFACE

As the n-alkyl chain of the surfactant becomes longer its ability to reduce the surface tension is stronger under equilibrium conditions. However, cavitation systems are not at equilibrium; in fact the surface activity is not correlated to the hydrophobicity of the compound. Sostaric et al, 2001 reported that in a cavitation system, both the equilibrium and dynamic surface tension of the surfactants being studied need to be considered. They found that, even though longer chain surfactants are more surface active over the short lifetime of a cavitation bubble they may not be able

to reach this equilibrium as fast as a shorter chain surfactant in the same homologous series. This was explained by dynamics and the time it takes for a surfactant to orient itself at the bubble. It takes a longer time for the longer chain surfactant to properly orient its tail and head along the air water interface compared to a shorter chain molecule. As the surfactant approaches the interface, it will encounter other surfactants and it will need to shift to the next vacant area. The shorter chain surfactant can do this with more ease. In the end shorter chain surfactants are more dynamic than longer chain surfactants. Due to the short life time of the bubble, the dynamic surface tension is then very important.

1.5.8 DEGRADATION OF VARIOUS SURFACTANT COMPOUNDS WITH ULTRASOUND

It was concluded by Weavers et al. (2005), as well as Pee et al. (2005) and Yang et al. (2007) that as the concentration of the surfactant increases in the presence of ultrasound the amount of surfactant degradation actually increases. They also concluded that ultrasound is more appropriate to use on surfactant degradation than non surface-active compounds. There are a number of surface active compounds that are reported to be harmful to the environment. Ultrasound has proven to be a method for removing these compounds before their release into the environment.

One surfactant that is widely used in commercial products are the nonionic Alkyl ethoxylates (APEs). The byproducts of these compounds have been found to be estrogenic and toxic in nature. (Ying, 2006). The sonochemical degradation of APE was found to be enhanced at a frequency of approximately 360 kHz (Destailats et al., 2000; Venhuis et al., 2004). The pathways of degradation for this surface active molecule was also said to be through thermal and oxidative radical reactivity. Being a surfactant the degradation of this molecule was found to be dependent on initial concentration. However above the CMC, the initial degradation of this surfactant was no longer

effected specifically by varying concentration but by the physical hindrance of the ultrasound wave to reach the cavitation bubbles effectively due to barriers in the form of micelles (Venhuis et al., 2004; Destailats et al., 2000).

Another type of surfactant that has gotten much attention as a potentially harmful and toxic pollutant that are also highly persistent and bioaccumulative are the perfluorinated class of surfactants. The effect of ultrasound on these compounds was first investigated by Dreese, (2005). More recently Moriwaki et al. (2005) showed that upon sonolysis of perfluorinated sulfonate (PFOS) and perfluorooctanoic acid (PFOA) the surfactant chain could be shortened which has been shown to reduce the toxicity of the perfluorinated surfactants. Further, Vecitis et al. (2008) found that PFOS and PFOA could be completely mineralized upon using ultrasound as a remediation technology. This was an important finding seeing that these two compounds have been found to be recalcitrant and can actually accumulate to higher levels upon typical treatment practices found in water treatment plants (Shultz et al. 2006; 2006).

Abu-Hassan et al. 2006 investigated the degradation of LAS with ultrasound at low frequencies. LAS also being surface active will preferentially distribute to the interface of the bubble. At lower frequency purely transient bubbles are present thus a more adiabatic collapse of cavitation bubbles can be achieved creating higher localized temperatures at the lower frequencies. However, the bubbles have a shorter life time so there is less time for the surfactant to accumulate to that interface of the cavitation bubble prior to collapse. Since the LAS compounds will mostly degrade at the interface, the use of lower frequencies may limit the amount of surfactant degradation due to this reason. They also found that as the power emitted into the system increased so did the degradation rate of the LAS compound. This allows the transient bubbles to grow to larger sizes in the same amount of time to R_{max} right before collapse and therefore create an even higher temperature and pressure upon final adiabatic collapse. They did not observe complete mineralization of the SDBS as the byproducts of LAS were recalcitrant and resistant to total degradation.

1.5.9 COMPARATIVE SONOCHEMISTRY

There is a fundamental complication of studying ultrasound to degrade chemical pollutants.

Essentially cavitation bubbles act as tiny microreactors (Leighton, 1994). However, in an acoustic cavitation system, when one parameter such as frequency is varied, other parameters are also adjusted such as bubble population, size and dynamics of microreactors in the system. The linked parameters make it difficult to truly compare the effect of one variable in ultrasonic systems.

(Petrier et al., 1991). Comparative sonochemistry is a method that attempts to reduce the effect of multiple parameters changing by normalizing a result (i.e., degradation) to another parameter (i.e., OH \cdot formation).

1.5.9.1 HISTORY OF COMPARATIVE STUDIES

In the early 1990s Petrier first used comparative sonochemistry (Petrier et al., 1991). He developed a method to correlate the energy input to the sonochemical output of the cavitation bubbles in a system (Petrier et al., 1994; Petrier et al., 1991). In this comparative study, he explored the effect of changing frequency from 20 kHz probe to a 487 kHz bath on the degradation of phenol to radical formation at the same acoustical power. He found an increase in sonochemical yield in the form of H₂O₂ formation of both chemical systems at the higher frequency. The identification of OH radical induced intermediates revealed a degradation pathway for phenol relative to carbon tetrachloride.

It was the first time that a frequency effect was observed for pollutant degradation and showed that it was necessary to optimize the frequency of a system to reduce the energy needed for maximum destruction during treatment (Petrier and Francony, 1997). Jacques Reisse criticized Petrier's comparative study. Particularly he stated that one cannot compare sonochemical reactions

occurring in two different set-ups due to differences in heat generated from the transducers. Dekerckheer and Reisse (1997) further critique Petrier's comparative study because different compounds degrade in different regions of a cavitation bubble due to differing chemical characteristics such as hydrophobicity, surface activity, and volatility. Thus, the rates of reaction between two different types of compounds cannot be compared since they degrade by different mechanisms.

Drivers et al. (1999) further developed comparative sonochemistry to explore the role of diffusion in degradation by comparing the reaction rates of compounds differing only by a halogen. They concluded that the ultimate degradation of the compounds was correlated to the Henry's Law coefficient of the compounds not the diffusion coefficients (Drivers et al., 1999).

To explore surface excess in cavitation systems Sostaric et al. (2001, 2002) compared two surfactants within the same homologous series. They found that by changing the frequency and comparing relative rates of radical production dynamic adsorption of surfactants controlled the surfactant's surface activity. Furthermore, as the intensity of ultrasound increases, the sonochemical yield ratio for one less surface active compound relative to another more surface active compound was the same within a given frequency. However as the frequency changed the ratio of the sonochemical yield changed. They apportioned this change to the understanding that as the frequency is increased there is more time for the less dynamic and more surface active compound to reach the bubble. They could make this conclusion based on the knowledge that these compounds were both going to degrade at the interface region of the bubble and they both had similar chemical and physical properties. The only difference between the surfactants was their surface activity.

Yang et al. (2007) studied the effect of pulsed ultrasound on the degradation of two surface active compounds. Based on the work of Sostaric et al. (2001, 2002) the power conversions within a frequency were also assumed to be the same between their changing pulsing conditions within a frequency. Follow-on work in 2008 compared the degradation of OBS to HTA formation again

assuming power differences within a frequency did not affect relative results (Yang et al., 2008). Under this assumption, the effects from different pulsing conditions (the dependent variable) within a frequency were studied but direct comparisons between frequencies were not made. The objective in most comparative studies is to eliminate or at least reduce the effect from most variables and draw conclusions on a specific targeted effect based on the system involved. Using hydroxyl terephthalic acid (HTA) formation studies to understand the chemical effects of ultrasound and relating it to the energy conversion to produce these effects is an established sensitive method for understanding the sonochemical reactivity of a system (Price et al., 1993). Therefore using this comparative method changing reactivity under different pulsing conditions was separated from changing surfactants adsorption on cavitation bubble surfaces. This work found that under a pulsing condition of 100 ms interval and a 100 ms length, an increased degradation rate was observed compared to that of a continuous wave with the same amount of ultrasound energy input.

1.5.9.2 COMPARATIVE STUDIES USING HTA FORMATION

The production of $OH\cdot$ can be measured via its reaction with Terephthalic acid (TA) to form the very stable and fluorescent ion hydroxyterephthalic acid (HTA) (Price et. al. 1993).

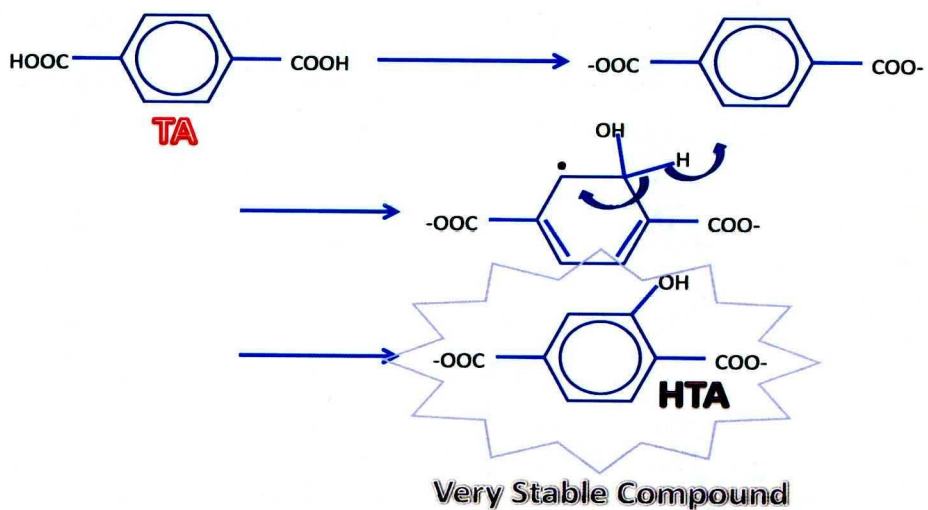


Figure 1.3 Schematic representation of the mechanism in which TA reacts with OH radicals to form fluorescent and stable HTA ions.

The rate of formation for this reaction follows a zero-order trend as it is not dependent upon the concentration of the TA in solution over the course of the experiment, and only upon the ability of the OH· that are formed via thermolysis of the water vapor inside the hot spots to diffuse and combine with TA to form HTA. This method is very sensitive and it has been used by other sonochemists to determine the chemical reactivity of sonochemical systems (Mason et al., 1994). When the comparison of reaction rates from one chemical to another are made, the reaction rates of HTA and the target pollutant ideally vary in relation to one another regardless of the dependent variable that is chosen (i.e. frequency, pulsing condition, reactor design, etc) (Mason et al., 1994).

1.5.10 PULSED ULTRASOUND

Pulsed ultrasound involved turning on (pulsed length) and turning off (pulsed interval) the ultrasound wave for short times. This effect can increase the bubble life time and therefore the amount of surface active compound that can preferentially adsorb to the bubble during to the extended bubble lifetime.

Henglein et al., (1995) found that depending on the pulse length, the ability to produce and grow chemically active bubbles changes. This amount of time required to grow at least a small population of cavitation bubbles over many pulsing sets is called the activation time. The pulse interval time will then affect the ability to keep a stable population of bubbles or optimize that population to create the greatest amount of sonochemical reactivity. As the interval time is increased the number of those active bubbles and nuclei present will start to diminish. If the interval time is long enough that population of bubbles will dissolve and/or float out of solution. The time required for this to happen is called the “deactivation time” (Henglein, 1989).

Atchley et al., (1988) found that at a pulse length of longer than 4 μ s the threshold for cavitation was not a concern. Also, they found that at a frequency greater than 5 MHz this threshold was not a factor. They state that their findings are comparable to what Flynn (1982) had found. These studies were not conducted with surface active compounds, if they were, one could potentially hypothesize that the threshold for cavitation could be decreased due to the resulting decreased surface tension on the bubbles.

When ultrasound is emitted into solution under continuous wave there may be clustering of bubbles created. This will create a shielding effect where the population of bubbles at the front of the ultrasound wave could be too dense and inhibit the ability of the wave to reach those cavitation bubbles deeper within the bubble cloud. By decreasing the bubble density through the overall effect of pulsed ultrasound the ability of the ultrasound wave to reach the resulting cavitation bubble population in the field may be increased. This would then lead to a better transfer of energy to the active population of bubbles, and may in effect enhance the sonochemical reactions happening in the solution (Francescutto et al., 1999). Ciaravino et al. (1981) saw an increase in sonochemical activity with pulsed wave ultrasound in comparison to continuous wave ultrasound when studying the release of iodine upon sonication of 131 labeled sodium iodine solutions under intensities similar to that used in the following research.

It has been determined that pulsing the ultrasound wave may be a method to increase the overall efficiency of sonochemical processes of pollutant degradation. In determining the pulsing conditions the length to interval ratio of the pulsed wave of ultrasound is a critical parameter in design characteristics that needs to be optimized to efficiently degrade each target compound within a target frequency. For example, Lee et al. 2005 found that this optimized condition at 515 kHz was 4 ms interval with a 4 ms width for their system. Yang et al, (2005) found that at a frequency of 354 kHz a pulsed length and width of 100ms each, enhanced degradation of alkylbenzene sulfonate surfactants was observed.

When making comparisons of continuous wave experiments to pulsed experiments or between pulsed experiments of varying pulsed interval/width settings the amount of ultrasound emission into the system during the course of each experiment needs to be the same. Therefore equation 1.5 was developed to keep the total pulse length time of ultrasound the same between experiments (Henglein, 1989).

$$T_{EXP} = T_{SON} \left(1 + \frac{T_{OFF}}{T_{ON}} \right) \quad (1.5)$$

Where T_{EXP} is the total experimental time and T_{SON} is the total sonolysis time. T_{OFF} is the pulsed interval time and T_{ON} is the pulsed length time.

1.5.11 RESEARCH OBJECTIVES

It is of interest to gain insight into the cavitation induced degradation of a target pollutant through pulsed degradation over a very detailed range of pulsing conditions. However, there is no standard of measurement of sonochemical output in terms of the energy input. This complication is due to the understanding that cavitation bubbles create sonochemistry, and the energy or power transfer to these bubbles is not consistent as the parameters of the experimental conditions change. The target compound, OBS, is known to degrade directly via physical degradation by the high temperatures and pressures formed during hot spot formation as well as via radical attack. If the chemical reactivity enhancements in terms of radical production are known and it is then compared to how the compound degrades as we change a single parameter of the system. Mechanisms of

degradation can be theorized from the understanding that surfactant that have adsorbed to the air/water interface of the bubble can either degrade by chemical reactivity and/or thermolysis reactions.

Yang et. al. (2008) determined that pulsing ultrasound will enhance the degradation of OBS compared to continuous wave ultrasound. One of the settings where greatest pulsed enhancement was achieved at different frequencies was that of 100 ms length and 100 ms interval. They attributed this to the ability of the surfactant to preferentially adsorb more as a result of increased bubble life time as well as allowing some of the bubbles to dissolve during the pulse interval to increase the ability of the wave to reach the bubbles without the interference from clustering or the resulting coalescence from clustering.

To better elucidate the true mechanism of OBS degradation via pulsed enhancement, this study aimed to empirically model what is happening in and around a multibubble system similar to the Yang et al. 2008 study. Therefore, pulsed lengths and intervals chosen for this study were 30 ms, 60 ms, 100 ms, 160 ms and 320 ms. In the current study, the LAS homologue, octyl benzene sulfonate (OBS), was chosen as a model compound that represents surface active pollutants, mainly LAS compounds. My goals were to gain a clearer depiction of how this compound degrades via ultrasound over detailed pulsing conditions by using HTA formation as a comparative system to link changes in OBS degradation to increased adsorption on collapsing cavitation bubbles.

CHAPTER 2

EXPERIMENTAL

2.1. MATERIALS

The sodium salt of 4-octylbenzene sulfonate (OBS; 97%) was obtained from Sigma-Aldrich Corp. Terephthalic acid (TA; 99+%) was obtained from Acros Chemicals. TA buffering solution was made with 7 mM potassium phosphate monobasic, (certified ACS), as well as 4.4 mM sodium phosphate, dibasic anhydrous, (Certified ACS), and 5mM sodium hydroxide, (NF/FCC). All three were obtained from Fisher Scientific. Purified water was obtained from a Milli-Q filtered water system ($R = 18.2 \text{ m}\Omega \text{ cm}^{-1}$). An HPLC eluent of 33% acetonitrile (Fisher Scientific, HPLC Grade) and 67% phosphate buffer was used. The phosphate buffer was made up to a pH of 2.2 with 50 mM sodium phosphate, monobasic anhydrous and 52 mM o-phosphoric acid both were also obtained from Fisher Scientific.

2.2 ULTRASOUND APPARATUS

Flat plate transducers (Types: USW 51-106, USW 51-051) operating at a tuned frequency of 69, 205, or 616 kHz (ELAC-Nautik, L-3 Communication, GmbH, Kiel, Germany) emitted ultrasound through a round stainless steel plate ($A = 23.4 \text{ cm}^2$). A custom cylindrical glass reactor (approx.

volume was 320 mL), that was open at the bottom and clamped to the top of the housing of the flat plate transducers. This reactor also had two ports at the top for obtaining samples and dispensing contents, is shown in Figure 2.1. To maintain the sample solution temperature at $20 \pm 1^\circ\text{C}$ the glass reactor had an outer water jacket attached to a water cooling system (Isotemp 1006S, Fisher Scientific). 300 mL of sample solution was poured into the glass ultrasonic reactor and exposed to ultrasound while in direct contact with the stainless steel flat plate. After each experiment the reactor was rinsed three times with Milli-Q water. The reactor was never separated from the transducer housing between experiments under the same frequency thereby, reducing potential changes to the ultrasonic field, which could result in alterations in the populations of bubbles and subsequent changes in the overall calorimetric power values and sonochemical yields (Price et al., 1992).

Power was supplied to this ultrasound system by a function/pulse generator, (SM-1020; Signametrics Corp., Seattle, WA). Signals in the form of continuous waves as well as pulse lengths/intervals of 30 ms, 60 ms, 100 ms, 160 ms and 320 ms were generated for the experiments. There were 25 different pulse combinations, i.e. pulse lengths (ON times) and pulsed intervals (OFF times) at each of the ultrasound frequencies studied. The total sonication times were the same for continuous and pulsed ultrasound in order to make comparisons between experiments. A linear amplifier (AG 1021; T&C Power Conversion, Inc., Rochester, NY) magnified the generated electrical signal. This signal was sent to the transducer, which converted the electrical signal in the form of ultrasound intensity. An oscilloscope (model number: 54501, 100 MHz Digitizing Oscilloscope, supplied by Hewlett Packard) was used to verify the wave properties of the pulse experiments.

Tuning, impedance tests and pressure tests were conducted on all transducers to check the functionality before beginning this research. First, impedance tests were done to test for the operating resonance frequencies of each transducer available in our lab. Appendix D shows the output from the impedance tests. Next the transducers were connected to the amplifier and

generator. The reflected intensity at each frequency was then observed under continuous ultrasound exposure. The reflected power indicates a mismatch between the transducer and the medium being exposed to ultrasound. Therefore, if the reflective ultrasound intensity is high, then the ultrasound intensity being applied to the medium will be low. This second step was repeated three times to check the reproducibility of the reflected and incident ultrasound intensity and to test for the lowest possible reflected ultrasound intensity to be obtained within each transducer. The transducers used in this study were used in part because their reflected power was less than 10 percent of the total power. Standard pressure tests were also conducted on each transducer to check for leaking. No pressure drops were observed through the stainless steel frequency plates of the transducer housing, indicating that there were no leaks.

2.3 ULTRASONIC CALORIMETRIC POWER

In sonochemistry, it is typical to report the ultrasound energy supplied to the solution in terms of a calorimetric power determined by the temperature rise in the solution during sonolysis. The power input into a solution for both continuous and pulsed ultrasonic modes was 27 W, as measured by calorimetry (Kimura et al., 1996) indicating that an equivalent amount of acoustical energy was used in each experiment. The temperature rise of 300 mL of water was determined during 3 minutes of sonolysis. Temperature measurements were performed using a thermocouple (Omega Corporation, Stamford, CT), which was connected to a Fluke industrial scope meter (model 123, Supplied by Everett, WA). The measurements were taken at 20 second intervals with the first measurement at 20 seconds. The 20 second delay in temperature readings was used to reduce the physical interference resulting from the cavitation bubbles on the thermocouple readings, especially

at the lower 69 kHz frequency. Over a short time period, the correlation between heating and time is a linear correlation (Kimura et al. 1996). The calorimetric power was calculated using equation 2.1.

$$P_{calorimetric} = \frac{dT}{dt} C_p M \quad (2.1)$$

where T is the temperature of the bulk solution, t is the time of sampling, C_p is the heat capacity of water ($4.179 \text{ J g}^{-1} \text{ K}^{-1}$) and M is the mass of water used. For each frequency used, this correlation was set to generate a calorimetric power of $27 \pm 1.5 \text{ W}$. Throughout experiments at each frequency the calorimetric power was monitored periodically to check the system functionality. Examples of calorimetric results at all frequencies, 616, 205, and 69 kHz are shown in Figures 2.2, 2.3 and 2.4, respectively.

2.4 SURFACE TENSION MEASUREMENTS

The surface tension of aqueous OBS solutions (0 to 10 mM) was measured by the expanding bubble technique (Hunter, 2002) with a Sensadyne surface tensiometer, (Model PC 500, Chem-Dyne Research Corp., Mesa, AZ). The results are shown in Figure 2.5. An average of approximately 100 readings of surface tension at each concentration was used to determine each data point shown in Figure 2.5 within an error of $\pm 1 \text{ dyne/cm}$.

2.5 HPLC ANALYSIS OF OBS DEGRADATION

Solutions of OBS (1mM, 300mL) were prepared for each experiment by mixing 150 mL of the stock solution with 150 mL of the Milli-Q water. This 300 mL solution was then transferred to the ultrasonic reactor for sonolysis. 2 mM stock solutions were prepared in pure Milli-Q filtered water ($R = 18.2 \text{ mV cm}^{-1}$) for calibration curve concentrations of 0 to 1.25 mM. A Hewlett-Packard 1100 high pressure liquid chromatograph (HPLC) with a 100×2.1 mm C18 ODS Hypersil column (Thermo Electron Corp., Bellefonte, PA) was used to measure the OBS concentration following sonolysis of aqueous OBS solutions (300 mL) at an initial concentration of 1mM. Sample volumes (200 μL) were collected a total of 11 times over the course of an ultrasound experiment. (Experiments ranged from 15 minutes to 11.5 hours, depending on the ultrasound pulsing condition). Samples were taken using a 1000 μL glass syringe (Gastight 1001, Hamilton Corp., Reno, NV). The samples were stored in 350 μL glass, flat bottom insert vials (RESTEK Corp.) that were then placed in 2 mL crimp top amber glass HPLC vials (Agilent Technologies, New Castle, DE), and stored under refrigeration up to three days prior to HPLC analysis. Less than 1% of the reactor volume was taken during the course of this analysis. The HPLC retention time of 5 minutes was observed for OBS as shown in Figure 2.6 (a). This figure is showing the HPLC peaks from a typical calibration curve. The areas under the peak and the known concentrations correlating to each peak were used to generate the calibration curve in Figure 2.6 (b).

2.6 FLUORESCENCE DETECTION OF HTA FORMATION

A buffered stock TA solution (2 mM; 6 L) was prepared for each batch of 26 experiments (one full set of continuous and pulsing settings at a given frequency) following Mason et al. (1994). Solutions of TA (1 mM, 300 mL) for sonolysis were prepared for each experiment by mixing 150 mL of the stock solution in 150 mL of the Milli-Q water. For calibration purposes HTA, was synthesized according to Mason et al., (1994) and Field et al. (1970). Calibration curve concentrations for HTA ranged from 0 to 0.2 mM. The OH radical yield was calculated from a standard fluorescence curve for aqueous HTA solutions and on the assumption that TA reacts with OH radicals in a 1:1 molar ratio. Hydroxyl radical formation during sonolysis of aqueous TA (1 mM) solutions was determined by the detection of HTA (Fang, 1996) using a Shimadzu RF-5301 PC spectrofluorophotometer. (Columbia, MD). Experimental time depended on the pulsed setting and ranged anywhere from between 10 minutes to approximately 6 hours for each experiment. Approximately six samples, 3 mL each were taken over the course of each experiment. Therefore, not more than 6% of the original volume was used throughout the course of the TA experiments.

Samples were directly placed in a quartz cell with a 10 mm-path-length for insertion into the spectrofluorophotometer for fluorescence measurements. The following parameters were used in this analysis: excitation and emission beam slit width 1.5 nm, sampling interval 0.2 nm, excitation wavelength 315 nm, and emission wavelength 428 nm. Concentrations ranging from 0 to 0.2 mM were used for the HTA calibration curve. The fluorometer output from calibration standards is shown in Figure 2.7 (a). The peak maximum was determined to occur at a wavelength of 428 nm. For each fluorescent measurement the intensity was then determined at this wavelength. The increasing intensities and known concentrations associated with each peak were used to generate the calibration curve in Figure 2.7 (b).

Volume changes affect sonochemical yield. During sonication at 69 kHz the amount of volume being removed as a result of sampling caused a loss in linearity between fluorescent emission intensity and sonolysis time. This effect arose due to a standing wave. A standing wave occurs

when the incident wave is reflected from the air/water interface of the sample (Leighton, 1994). The nature of the standing wave will affect bubble dynamics and, therefore, the sonochemical yield. The height of the liquid above the transducer will affect the phase of the reflected wave in relation to the incident wave, thereby changing the overall ultrasound intensity in the sample solution (Leighton, 1994). To alleviate this problem, each 3 mL sample was returned back into the reactor after fluorescence analysis (total time outside of the vessel was less than 30 seconds for each sample). This protocol improved the accuracy of the 69 kHz experiments.

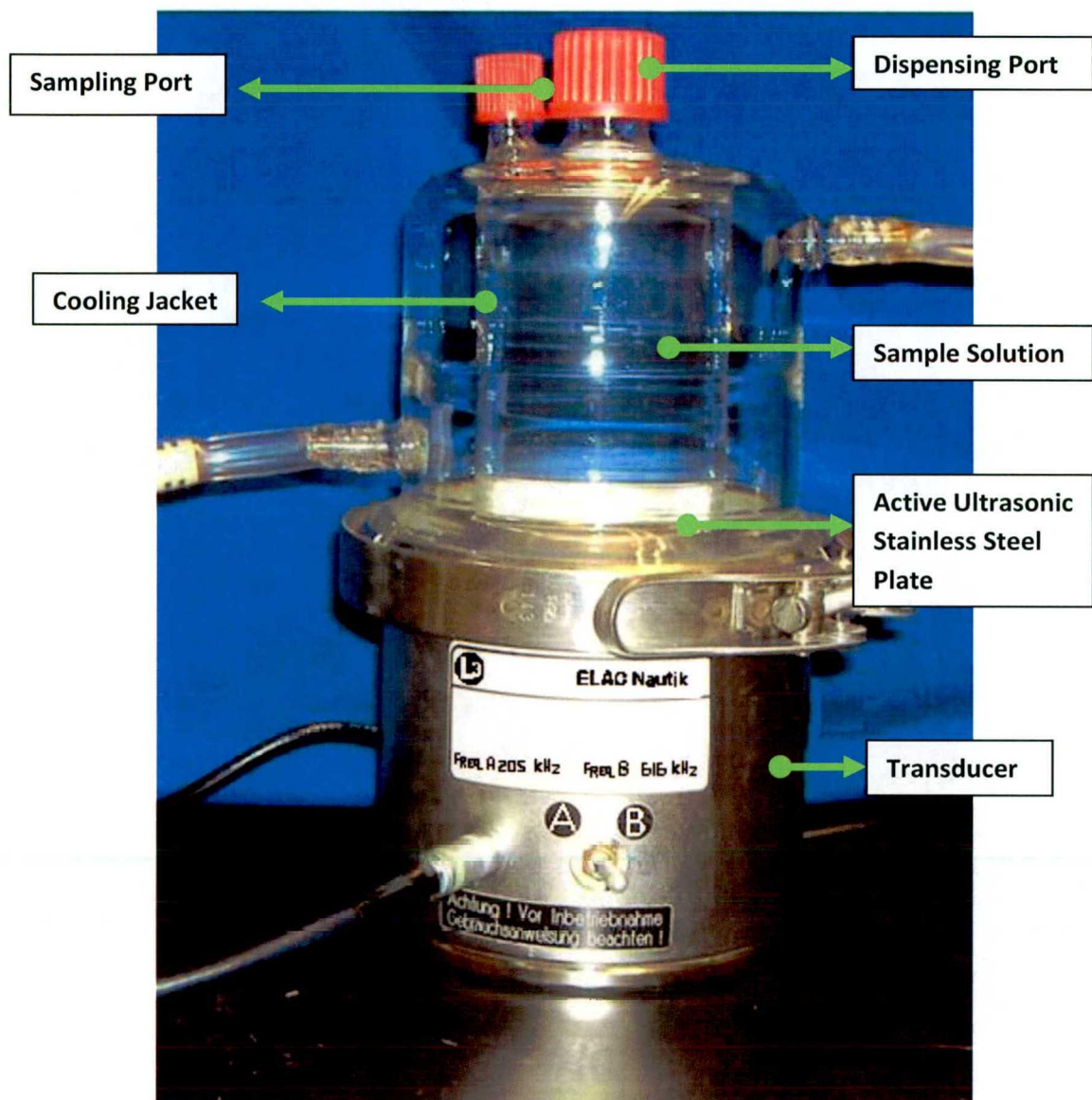


Figure 2.1. The ultrasonic reactor and transducer(s) housing.

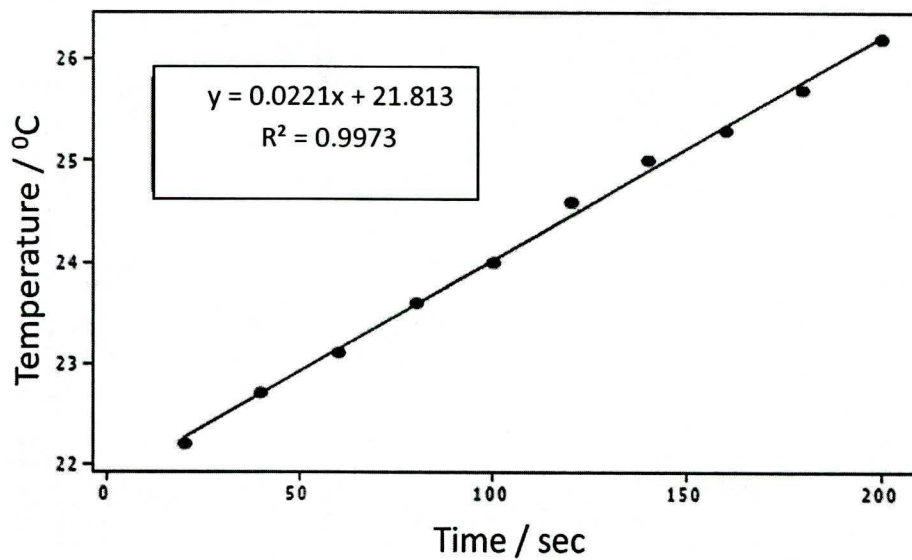


Figure 2.2 At an electrical power of 34 W, the temperature rise in Milli-Q water as a function of time at 616 kHz is shown above. At a reactor volume of 300 mL, this correlates to a calorimetric power of 27.6 W.

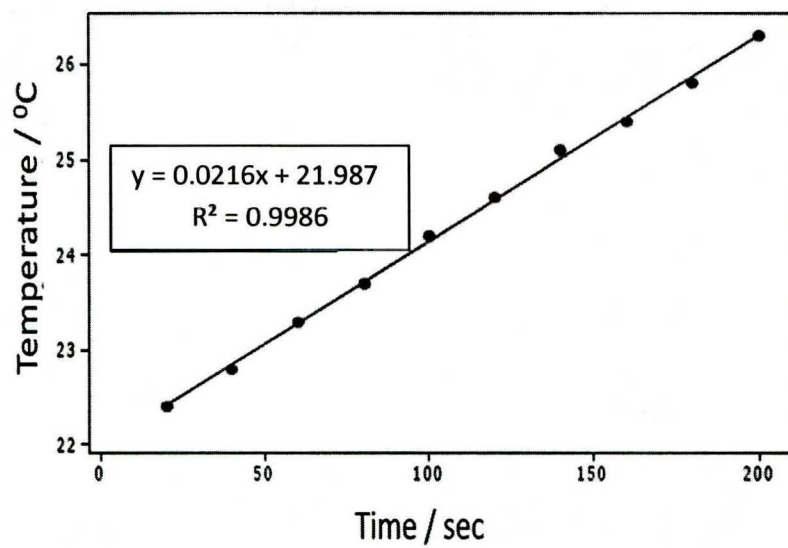


Figure 2.3 At an electrical power of 29.6 W, the temperature rise in Milli-Q water as a function of time at 205 kHz is shown above. At a reactor volume of 300 mL, this correlates to a calorimetric power of 26.99 W.

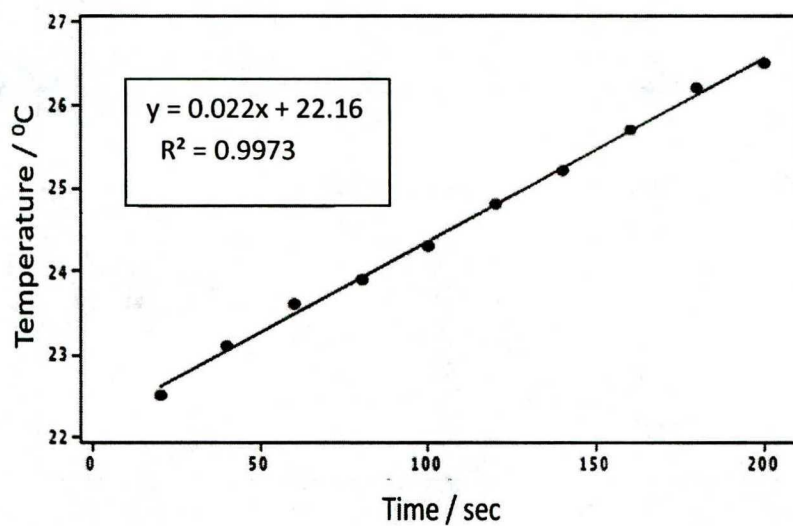


Figure 2.4 At an electrical power of 42.5 W, the temperature rise in Milli-Q water as a function of time at the 69 kHz is shown above. At a reactor volume of 300 mL, this correlates to a calorimetric power of 27.5 W.

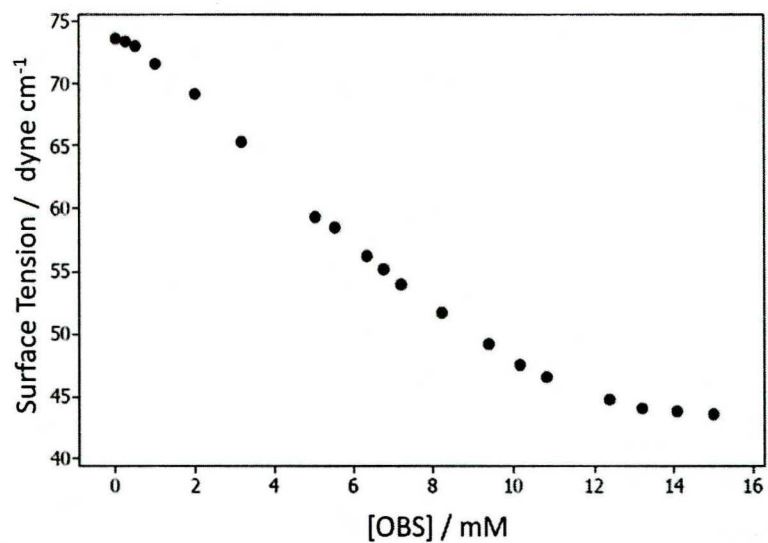
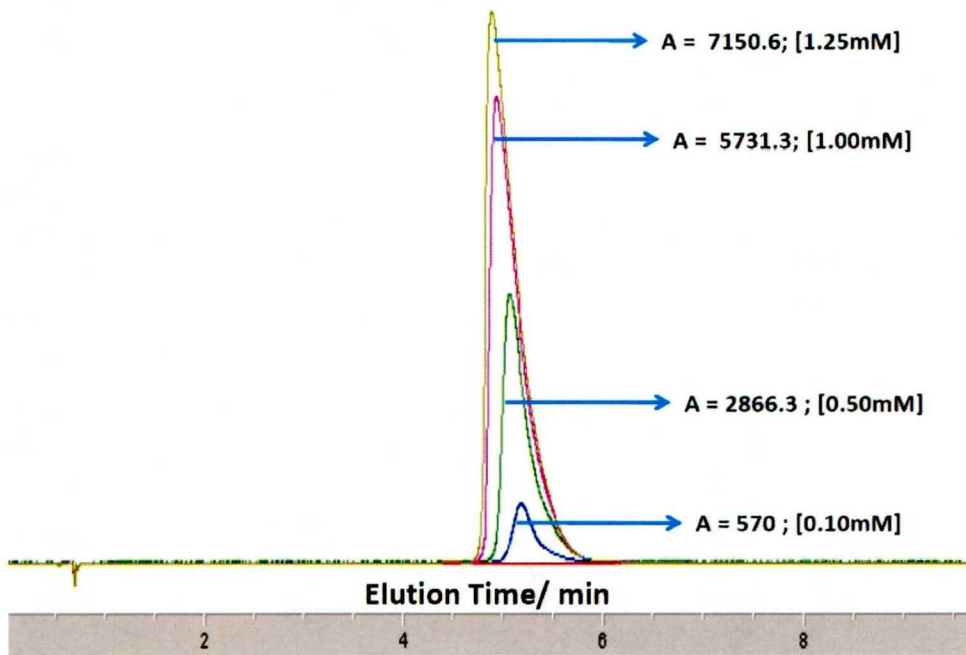
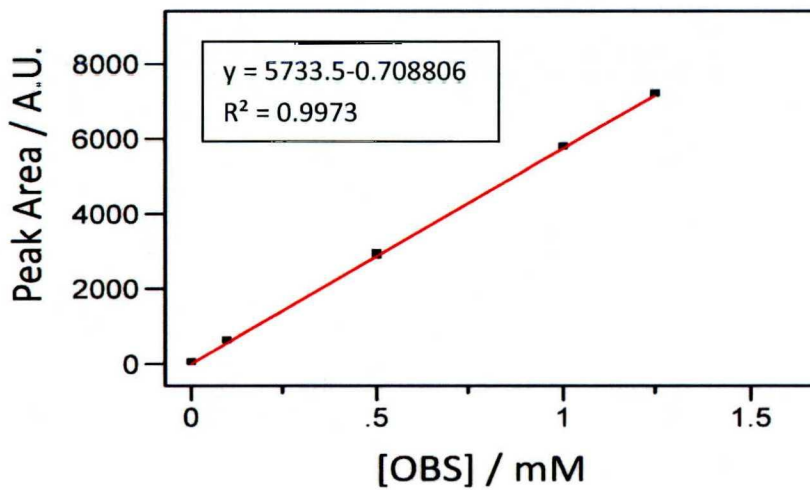


Figure 2.5 OBS concentration effects on equilibrium surface tension. Concentration batches were made up of 5 mM, 10 mM and 15 mM from a 15 mM stock solution. With each successive dilution from each concentration, the surface tension was measured. An average of approximately 100 readings of surface tension at each concentration was used to determine the value.



(a)



(b)

Figure 2.6 (a) HPLC calibration peaks of known concentration showing a 5 min elution time. **(b)** Typical HPLC / OBS calibration curve. The high linearity and the range below and above all concentrations observed decreases any error associated with the OBS data.

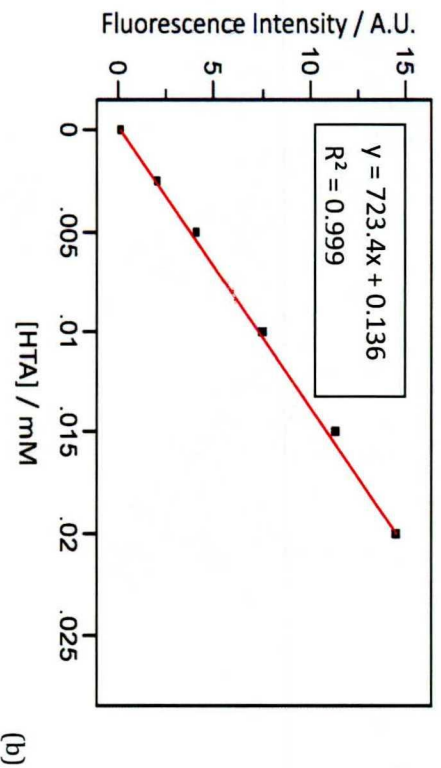
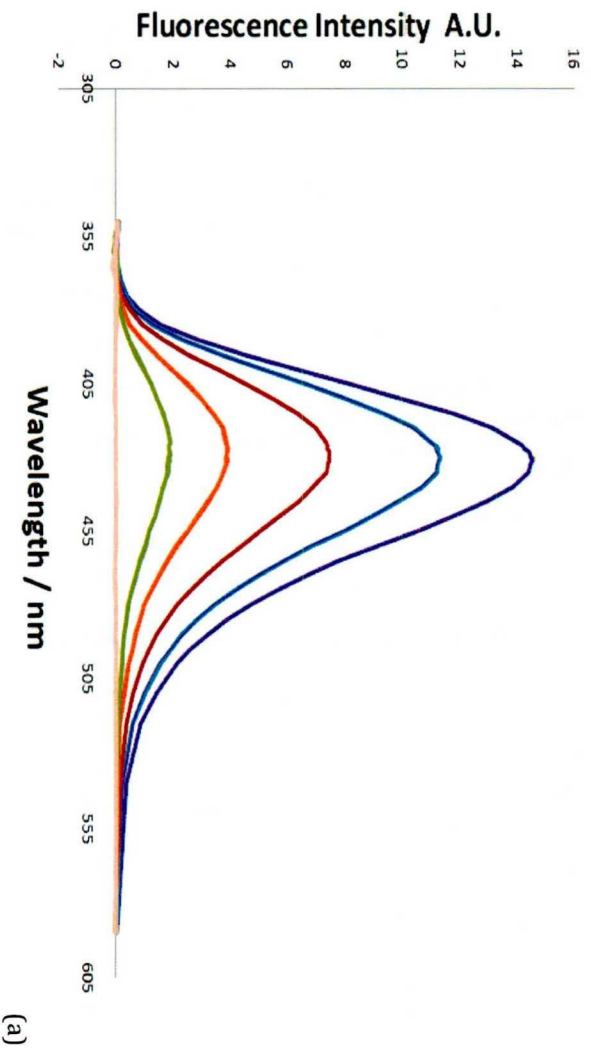


Figure 2.7 (a) Fluorometer calibration peaks of known concentration showing a 428nm optimum wavelength. (b) Typical HTA, RF Spectrofluorophotometer calibration curve. The high linearity and the range below and above all concentrations observed decreases the error associated with the HTA fluorescence data.

CHAPTER 3

RESULTS

3.1. EFFECT OF ULTRASOUND INTENSITY ON SONOCHEMICAL YIELD

As the intensity of the ultrasound wave is increased, the sonochemical yield of a reaction in aqueous solution also increases due to increased OH radical production and temperature from cavitation bubble collapses (Sostaric et al., 2002; Price et al., 1993; Henglein et al., 1994). However, at relatively high ultrasonic intensities, the sonochemical yield plateaus and at even higher intensities, there is a continual and substantial decrease in sonochemical yield (Price et. al. 1993; Kanthale et al., 2007).

This decreased sonochemical yield at high intensities has been attributed to a number of factors, including the formation of a large population of bubbles in the liquid. Many bubbles will increase the rate of collisions between the bubbles creating what is called coalescence (Sunartio et. al., 2007). Therefore, bubbles simply grow too large and float out of solution, rather than undergoing inertial collapse (Sunartio et. al., 2007). In addition, a high density of bubbles near the surface of the transducer results in attenuation and reflection of the ultrasound wave (Ashokkumar et. al., 2007),

(Lee, 2005). Both effects act to lower the overall effect of ultrasound intensity resulting in a decrease in sonochemical yield.

Also, different compounds may have an effect on the properties and interactions of cavitation bubbles; therefore, it is necessary to study the effect of each compound while changing another variable such as power. The ultrasonic intensity for all experiments was chosen within the range where there was a linear relation between ultrasound intensity and sonochemical yield. Working within this linear region allowed for, quantitative comparisons between experimental runs under different ultrasound conditions could be made. A calorimetric power of 27 W was chosen for all experiments, which correlates to 42.5, 29.6 and 34 W electrical power, respectively, for 69, 205 and 616 kHz. Figure 3.1a demonstrates that at a frequency of 616 kHz the calorimetric power of 27 W falls within the range where there is a linear relationship between ultrasonic intensity and the degradation rate constant for OBS. Each OBS degradation experiment was run for a total sonication time of 15 minutes which was determined to get the best fit for all experiments regardless of intensity.

In Figure 3.1b at 616 kHz the calorimetric power of 27 W also falls within the range where there is a linear relationship between ultrasonic intensity and the formation rate constant for HTA. Each data point represents an individual HTA formation experiment that was run for a total sonication time of 10 minutes. The experimental times for all reactions in Figure 3.1b were also determined in the same way as those in Figure 3.1a. Similar experiments were conducted at a frequency of 205 kHz, as shown in Figure 3.2. As shown, 27 W calorimetric power is again within the ranges where there is a linear relationship between ultrasound intensity and sonochemical yield, before the yield plateaus.

3.2 EFFECT OF OBS AND TA INITIAL CONCENTRATIONS ON SONOCHEMICAL RATES

In sonochemical systems it is important to determine the effect of solute concentration on sonochemical reaction rates. The number of OH radicals that can react with a hydrophilic solute in the bulk of solution will depend on the concentration of solute. For example, in solutions of TA the formation of HTA will depend on the number of OH radicals that can react with TA if the initial concentration of TA is too low. In addition the surface active solute can adsorb to the interface of bubbles leading to changes in the bubble activity. Both of these effects depend on the solute concentration.

In an ultrasound system that contains a surfactant, the effects of its concentration on final sonochemical activity needs to be considered and understood carefully because frequency, power, reactor design etc. will effect and potentially change the population of cavitation bubbles that are created. The surfactant will partition to the interface of the cavitation bubbles with the charged or hydrophilic end facing toward the bulk solution if the surfactant has a formal charge, such as anionic or cationic surfactants. This creates an overall charge on the surface of cavitation bubbles (Sostaric thesis, 1999), (Ashokkumar et. al., 2007). These similarly charged bubbles repel one another if the interfacial potential between the bubble surface and bulk solution is high enough and if the Debye length is long enough (Sostaric thesis, 1999). Because coalescence is hindered by the presence of the surface charge, fewer bubbles will be lost due to the creation of larger bubbles that will be forced to the nodes by primary bejerknes forces (Leighton, 1990) or result in floating out of solution due to buoyancy forces (Sunartio et al., 2007).

Also, as a result of the electrostatic repulsive forces between the bubbles they will be more spread out within the solution with charged surfactants present, resulting in the declustering of bubble clusters. Therefore the efficiency at which the ultrasound wave can reach each of these bubbles will be greater (Sostaric thesis, 1999) allowing bubbles at the center of bubble clusters to adsorb energy as efficiently as those that were outside of the cluster. Overall the prevention of

coalescence and the effect of declustering can increase the sonochemical activity in the system by increasing the population of chemically active cavitation bubbles.

At concentrations where micelle formation occurs (i.e., the CMC), the sonochemical yield has been observed to increase or decrease. Ashokkumar et al. (1997) found that the formation of micelles hindered the rates of sonochemical yield. They attributed their findings to the hypothesis that the micelles create a barrier between the ultrasound wave and the bubbles or nucleation sites in the solution. Similarly, Destailats et al. (2000) and later Sostaric et al. (2001) also found that the onset of micelle formation resulted in a decrease in the observed sonochemical yield. However, Pee et al. (2004) found that the sonochemical yield increased upon micelle formation attributing their findings to additional nucleation sites within the center of the micelles. The equilibrium surface tension values of OBS, over a wide concentration range were determined as shown in Figure 2.5. This graph indicates that the CMC of OBS is approximately 14mM. To avoid any potential complications due to the formation of micelles, all experiments in the current study were conducted at a concentration of OBS of 1mM in aqueous solution, in order to be at a concentration where micelles will not form.

The effect of the initial TA concentration on HTA formation is shown in Figure 3.3. This figure shows the rate constants as determined under a frequency of 616 kHz with total sonolysis times of 10 minutes (this same sonolysis time was used for all TA kinetic studies). The rate of HTA formation for individual reactions (data points) over varying initial concentrations of TA is shown. Note that as the TA concentration increases the rate constant of HTA formation plateaus (Price et al., 1993). This occurs as a result of excess TA in the bulk solution available to scavenge all of the OH radicals that diffuse to the bulk solution during the time of sonolysis (Mason et. al., 1994). As a result any possible error associated with TA initial concentrations are removed since small variations in initial TA concentrations will not affect the formation of HTA at the plateau concentrations. Additionally, choosing a TA concentration within the plateau (Figure 3.3) region ensures that other

experimental parameters such as pulsing and frequency will not affect the ability for the TA to efficiently react with all available OH radicals, hence the number of OH radicals that diffuses into the bulk solution depends on the frequency and pulsing conditions. For this reason 1 mM TA (circled in figure 3.3) would be a reasonable choice for all experiments run under 616 kHz. Figure 3.4 shows the similar effects of TA concentration on the rate constants of HTA formation at 205 kHz. The chosen TA concentration of 1 mM for this set also falls within the plateau region.

3.3 EFFECT OF SONOLYSIS TIME ON SONOCHEMICAL RATE OF REACTION

Similarly to the effect of the initial concentration of solutes in a sonochemical system, the length of time at which a solution is exposed to ultrasound (at constant solution temperatures) can also affect the sonochemical rate of reaction. Figure 3.5 shows a pseudo first order degradation for OBS (1 mM, 300 mL) in aqueous solution exposed to continuous wave ultrasound, at a frequency of 616 kHz and in the first 20 minutes of degradation. This is supported by the linear correlation coefficient (R^2_{ADJ}) of 0.997 for this section of time. After 20 minutes the rate of degradation decreases.

It is a general rule that most thermolysis reactions follow at least a first-order trend (De Visscher et al., 1996). Also, in sonochemical systems where surfactants are present, there seems to be a change in the kinetics of the first-order degradation as the time of sonolysis reactions progress when initial concentrations of the surfactant are below the CMC (DeVisscher et al., 1996). Abu-Hassan et. al. 2006 shows an initial period of degradation that is controlled by a certain set of mechanisms of degradation. This initial period seems to be followed by a time period controlled by additional mechanisms. This change in kinetics has been speculated to be the result of byproduct formation (Tronson et al., 2003).

These byproducts compete with the parent compound for reactive species, temperature, and space at the interface whereupon collapse there is less accumulation of the parent compound to the interface of the bubble to be degraded by thermolysis or chemical reactivity. If byproducts are volatile they can diffuse into the bubble and react with oxidative radicals before the radicals reach the hot shell to react with the parent surfactant. Also, these byproducts can act to adsorb energy from the collapsing bubble and lower the specific heat of the bubble, in effect lowering the overall temperatures, pressures, and possibly chemical reactivity. This will affect the ability of the initial compound to degrade in comparison to a system with no byproducts present (Vinodgopal et al., 2001). Therefore, to compare the effect of changing dependent variables (i.e. the effect of changing pulsing condition), it is necessary that the comparison be made where the degradation rate constant is the result of similar mechanisms (Sostaric and Riesz, 2002). The total sonication times for all experiments were chosen to be within the initial time of degradation where additional mechanism of degradation did not influence the initial pseudo first order degradation of the parent compound. There is nothing that can be gained by conducting the OBS degradation experiments for longer sonolysis times at 616 kHz, as far as comparison of the 1st order degradation rates of reaction are concerned.

Similar observations as those made for sonolysis of aqueous OBS (1 mM, 300 mL) solutions described at 616 kHz were also made following sonolysis of the same solutions under continuous wave ultrasound at frequencies of 205 kHz (Figure 3.6) and 69 kHz (Figure 3.7). However, unlike the results observed at 616 kHz, where a pseudo first-order degradation rate was observed in the first 20 minutes of sonolysis, pseudo first-order degradation of OBS was observed for only 16 minutes (205 kHz; Figure 3.6), and up to 150 minutes at a frequency of 69 kHz (Figure 3.7). It is interesting to note that the amount of degradation at the point where the rate of reaction deviates from the pseudo first-order rate of reaction is similar at all ultrasound frequencies, (i.e. approximately 7 to 10 % degradation). As a result of these observations, the maximum sonolysis time for comparison of

first order degradation rates of OBS were chosen as 20, 15 and 60 minutes for sonolysis frequencies of 616, 205 and 69 kHz, respectively.

The total sonication time of TA experiments is also important for similar reasons as those described above for OBS degradation. Figure 3.8 illustrates the formation of HTA over extended sonolysis times. Note that the rate of formation of HTA is zero-order only in the first 30 minutes of sonolysis. It has been observed that after TA solutions have been exposed to ultrasound above a certain time, HTA that has formed in solution starts to sonochemically degrade (Fang, 1996). Therefore, an apparent decrease in the formation rate of HTA is observed. To generate an appropriate measure of the chemical reactivity in a system the total sonolysis time of all reactions for a given frequency needs to end before the HTA starts to degrade. In Figure 3.8 it is observed that the chosen sonolysis time for HTA formation experiments of 10 minutes would be well within this region of measurable chemical reactivity, which has a correlation coefficient of 0.991. Similarly, in Figure 3.9 there is a high correlation coefficient of 0.997 between the HTA formation and sonolysis time up to 35 minutes. Therefore, a sonolysis time of 10 minutes is appropriate at this frequency.

3.4 OBS AND HTA KINETIC EXPERIMENTS

After an appropriate sonolysis time was chosen at each frequency, the kinetic studies on the degradation of OBS and HTA at various pulsed settings within each frequency were conducted. Figure 3.10 shows the degradation of OBS under continuous wave conditions over 15 minutes of sonolysis time at 205 kHz. Experiments were typically run in duplicate unless otherwise stated in the figure captions. Upon analysis of the data set by the SAS statistical program, JMP, linear regression analysis through experimental blocking was used as a technique to attempt to alleviate nuisance variables (Ramsey and Schafer, 2001). Briefly this technique weights the correlation values

of each data point from the duplicate or triplicate experiments and calculates a slope, alternate to just averaging the slopes of each regression line. The resulting slope better represents the true rate constant. The weighted degradation rate constant ($k_{weighted}$) for the aqueous OBS solutions exposed to continuous wave ultrasound at 205 kHz was determined to be $5.5 \times 10^{-3} \text{ min}^{-1}$. The adjusted correlation coefficient R^2_{ADJ} was 0.992 indicating an excellent linear correlation. Figure 3.11 shows the degradation of OBS exposed to a pulsed ultrasound with a pulsed length and a pulsed interval of 100 ms. Again the total sonolysis time was 15 minutes, resulting in a total experimental time for this pulsed exposure as:

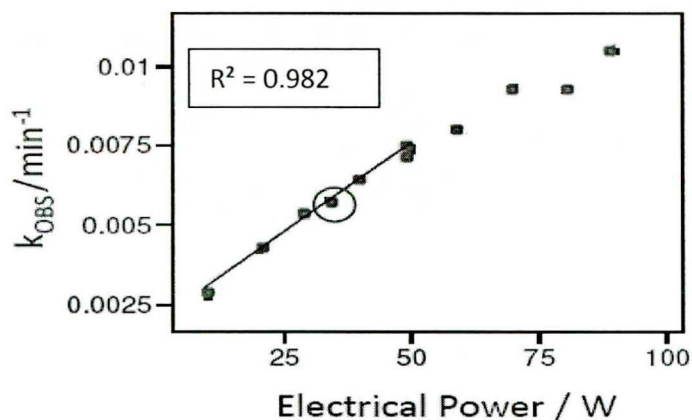
$$T_{experimental} = T_{sonolysis} \left(1 + \frac{T_{interval}}{T_{length}} \right) \quad (3.1)$$

Where $T_{experimental}$ is the total time of the experiment, $T_{sonolysis}$ is just the total time that the ultrasound is turned on over the course of one experiment. $T_{interval}$ is the off time of one pulsed condition, and the T_{length} is the on time of the pulsed condition. Using this equation, given a $T_{interval}$, and a T_{length} of 100 ms each, and a $T_{sonolysis}$ of 15 minutes, the $T_{experimental}$ was calculated to be 30 minutes. Under these pulsing conditions (Figure 3.11) $k_{weighted}$ value was calculated to be $7.2 \times 10^{-3} \text{ min}^{-1}$ with an R^2_{ADJ} of 0.984. For all kinetic plots of the sonochemical degradation rate of aqueous OBS solutions under all of the pulsing conditions in the current study, see Appendices A1, B1 and C1 respectively for 616 kHz, 205 kHz, and 69 kHz.

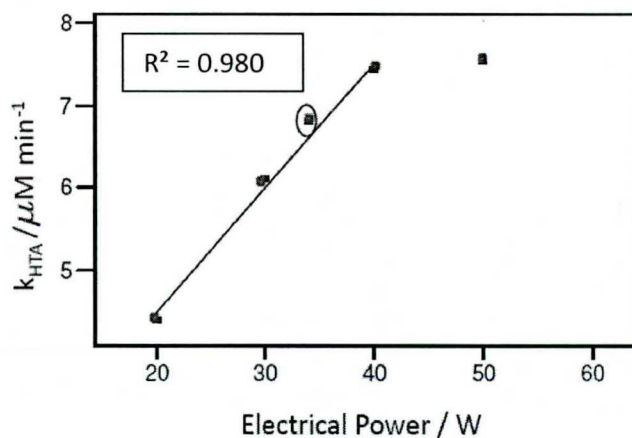
Similarly, Figures 3.12 and 3.13 show the sonochemical formation rate of HTA during exposure of aqueous TA solution to ultrasound at a frequency of 205 kHz. Figure 3.12 shows the sonochemical formation rate of HTA under continuous wave ultrasound. $k_{weighted}$ was calculated in the same way as it was calculated for the sonochemical degradation of OBS (Figure 3.10). Under a continuous ultrasound exposure of 10 minutes the $k_{weighted}$ was calculated to be $0.713 \text{ mM min}^{-1}$ with an R^2 value

of 0.9994. Figure 3.13 shows the zero- order formation rate of HTA under the pulsed condition with T_{interval} and T_{length} of 100ms each. Again the sonolysis time was 10 minutes, therefore using equation 3.1 the total experimental time was 20 minutes. k_{weighted} was calculated to be $0.686 \text{ mM min}^{-1}$ with an R^2_{ADJ} value of 0.9994. The correlation coefficients for the sonochemical formation rate of HTA under continuous and pulsed conditions represent the accuracy of this experimental technique. For all kinetic plots of the sonochemical formation rate of HTA in aqueous TA solutions under all of the pulsing conditions in the current study, see Appendices A2 and B2 respectively for 616 kHz and 205 kHz.

Under all conditions of sonolysis k_{weighted} for sonochemical degradation of aqueous OBS solutions and sonochemical formation of aqueous HTA, Table 3.1 was devised. The statistical method, Propagation of Errors was used to calculate the error on a 95% confidence interval for rate constants. These standard errors are also reported. Similarly, Tables 3.2 and 3.3 were constructed for the experiments conducted at 205 kHz and 69 kHz. Note how the degradation rate of OBS and as well the formation rate of HTA depends on the pulsing condition. From this complete data set it is possible to gain an understanding of how pulsing the ultrasound wave can affect the sonochemical degradation of OBS at different ultrasound frequencies, compared to the total sonochemical activity in a system determined from the sonochemical formation rate of HTA. In doing so I have gained information on the mechanism of any enhanced degradation rates of OBS as explained in the discussion section.

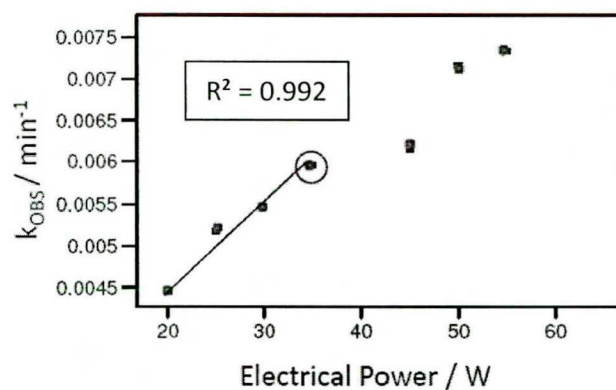


(a)

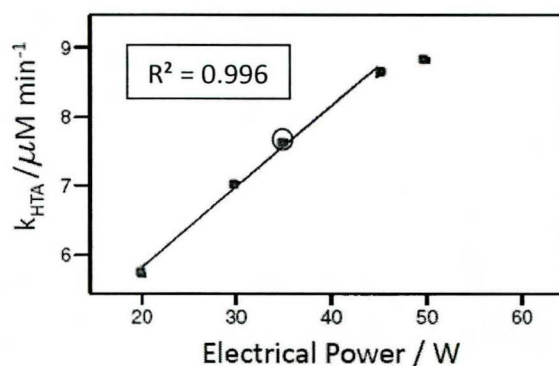


(b)

Figure 3.1 (a) OBS degradation rate constant and (b) HTA formation rate as a function of electrical power at 616 kHz. Rates of reaction were determined in aqueous solutions (1mM, 300mL) exposed to continuous ultrasound ($f = 616 \text{ kHz}$, $t_{\text{sonolysis}} = 15 \text{ min}$). The graph shows a circle around the experimental run at 34W electrical power. This electrical power is equivalent to a calorimetric power of 27W, and was therefore the power setting for all experiments run with the 616 kHz transducer.



(a)



(b)

Figure 3.2 (a) OBS degradation rate constant and **(b)** HTA formation rate as a function of electrical power at 205 kHz. Rates of reaction were determined in aqueous solutions (1mM, 300mL) exposed to continuous ultrasound ($f = 205 \text{ kHz}$, $t_{\text{sonolysis}} = 20 \text{ min}$). The graph shows a circle around the experimental run at 29.6 W electrical power. This electrical power is equivalent to a calorimetric power of 27W, and was therefore the power setting for all experiments run with the 205 kHz transducer.

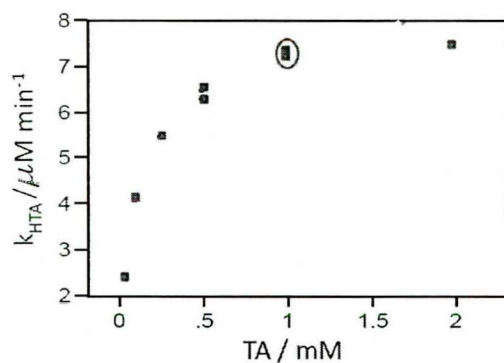


Figure 3.3 HTA formation rate as a function of TA concentration. Rates of reaction were determined in aqueous solutions (1mM, 300mL) exposed to continuous ultrasound ($f = 616 \text{ kHz}$, $t_{\text{sonolysis}} = 10 \text{ min}$). The graph shows a circle around the experimental run at TA concentration of 1mM. This concentration lies within the plateau region; therefore the TA concentration for all experiments was 1mM.

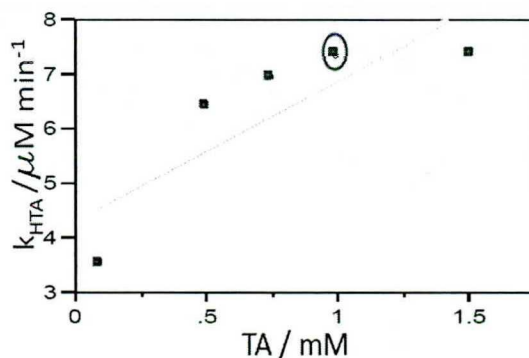


Figure 3.4 HTA formation rate as a function of TA concentration. Rates of reaction were determined in aqueous solutions (1mM, 300mL) exposed to continuous ultrasound ($f = 205 \text{ kHz}$, $t_{\text{sonolysis}} = 10 \text{ min}$). The graph shows a circle around the experimental run at TA concentration of 1mM. This concentration lies within the plateau region; therefore the TA concentration for all experiments was 1mM.

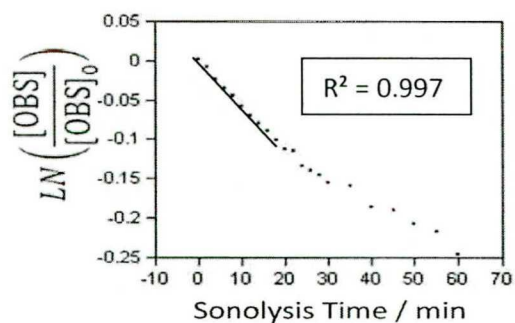


Figure 3.5 OBS first order degradation rates were determined in aqueous solutions (1mM, 300mL) exposed to continuous ultrasound ($f = 616$ kHz, $20 \pm ^\circ\text{C}$). Notice that the correlation between OBS degradation and sonolysis time is highly linear up to the sonolysis time of 20 minutes. After this time the rate of reaction slows and the correlation decreases. To investigate the initial degradation rate, a total sonolysis time of 20 minutes was chosen for all 616 kHz OBS degradation experiments.

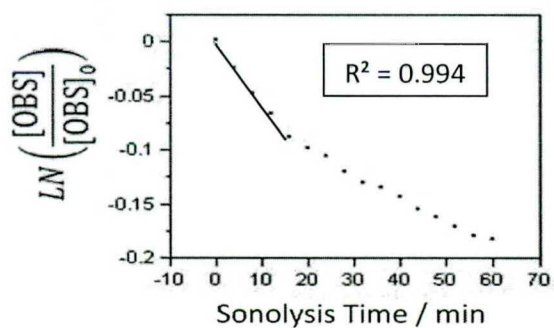


Figure 3.6 OBS first order degradation rates were determined in aqueous solutions (1mM, 300mL) exposed to continuous ultrasound ($f = 205$ kHz, $20 \pm ^\circ\text{C}$). Notice that the correlation between OBS degradation and sonolysis time is highly linear up to the sonolysis time of 15 minutes. After this time the rate of reaction slows and the correlation decreases. To investigate the initial degradation rate, a total sonolysis time of 15 minutes was chosen for all 205 kHz OBS degradation experiments.

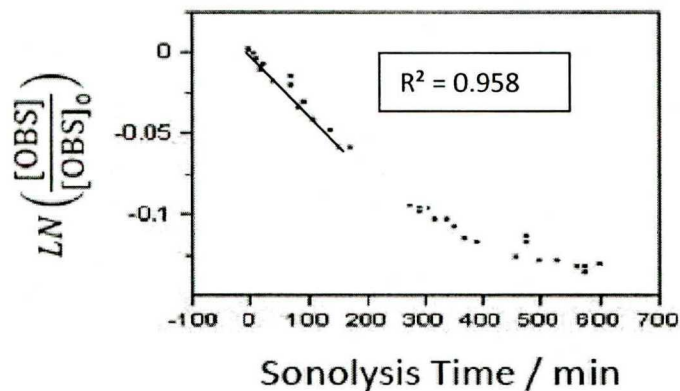


Figure 3.7 OBS first order degradation rates were determined in aqueous solutions (1mM, 300mL) exposed to continuous ultrasound ($f = 69 \text{ kHz}$, $20 \pm 1^\circ\text{C}$). Notice that the correlation between OBS degradation and sonolysis time is linear up to the sonolysis time of 150 minutes at least. After this time the rate of reaction slows and the correlation decreases. To investigate the initial degradation rate, a total sonolysis time of 60 minutes was chosen for all 69 kHz OBS experiments.

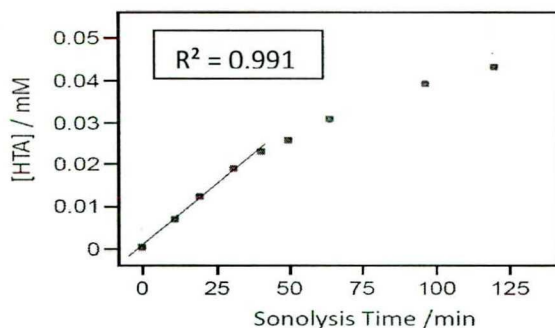


Figure 3.8 HTA formation as a function of sonolysis time was determined in aqueous solutions (1mM, 300mL) exposed to continuous ultrasound ($f = 616$ kHz, $20 \pm ^\circ\text{C}$). Notice that the correlation between HTA formation and sonolysis time is highly linear up to the sonolysis time of 30 minutes. After this time the rate of reaction slows and the correlation decreases. To investigate the initial degradation rate, a total sonolysis time of 10 minutes was chosen for all 616 kHz HTA experiments.

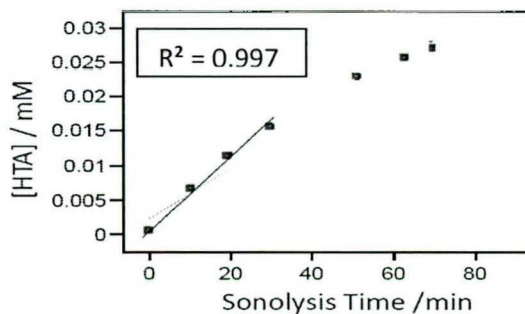


Figure 3.9 HTA formation as a function of sonolysis time was determined in aqueous solutions (1mM, 300mL) exposed to continuous ultrasound ($f = 205$ kHz, $20 \pm ^\circ\text{C}$). Notice that the correlation between HTA formation and sonolysis time is highly linear up to the sonolysis time of 35 minutes. After this time the rate of reaction slows and the correlation decreases. To investigate the initial degradation rate, a total sonolysis time of 10 minutes was chosen for all 205 kHz HTA experiments.

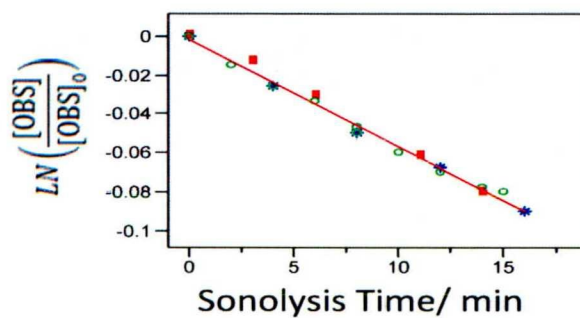


Figure 3.10 First order ultrasonic degradation of OBS (run in triplicate) in aqueous solution (1mM, 300ml) exposed to continuous ultrasound ($f = 205$ kHz; $P = 27W$; $t_{\text{sonolysis}} = 16$ min) The weighted degradation rate constant, $k_{\text{weighted}} = 5.5 \times 10^{-3} \text{ min}^{-1}$; adjusted correlation coefficient, $R^2_{\text{Adj}} = 0.992$; were determined using the JMP program for this set ($N_{\text{TOT}} = 20$).

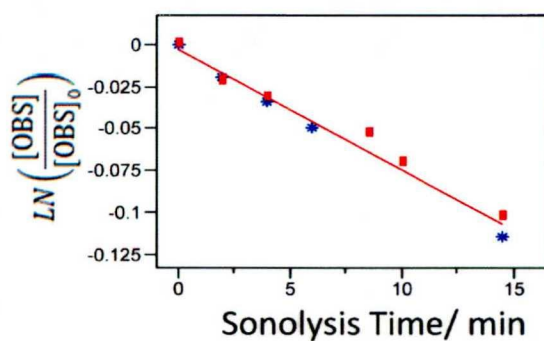


Figure 3.11 First order ultrasonic degradation of OBS (run in duplicate) in aqueous solution (1mM, 300ml) exposed to pulsed wave (100ms lengths and 100ms intervals) ultrasound ($f = 205$ kHz; $P = 27W$; $t_{\text{sonolysis}} = 15$ min) The weighted degradation rate constant, $k_{\text{weighted}} = 7.2 \times 10^{-3} \text{ min}^{-1}$; adjusted correlation coefficient $R^2_{\text{Adj}} = 0.984$; were determined using the JMP program for this set ($N_{\text{TOT}} = 11$).

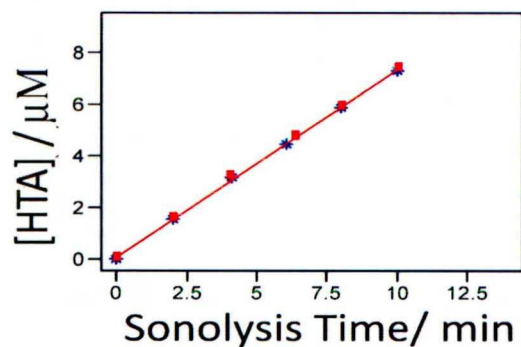


Figure 3.12 Zero order ultrasonic formation of HTA (run in duplicate) in aqueous solution (1mM, 300mL) exposed to continuous ultrasound ($f = 205$ kHz; $P = 27$ W; $t_{\text{sonolysis}} = 10$ min) The weighted formation rate constant, $k_{\text{weighted}} = 0.713$ mM min⁻¹; adjusted correlation coefficient $R^2_{\text{Adj}} = 0.9994$; were determined using the JMP program for this set ($N_{\text{TOT}} = 12$).

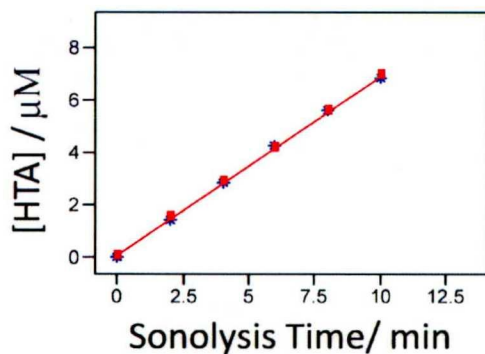


Figure 3.13 Zero order ultrasonic formation of HTA (run in duplicate) in aqueous solution (1mM, 300ml) exposed to pulsed wave (100ms lengths and 100ms intervals) ultrasound ($f = 205$ kHz; $P = 27$ W; $t_{\text{sonolysis}} = 10$ min) The weighted formation rate constant $k_{\text{weighted}} = 0.686$ mM min⁻¹; adjusted correlation coefficient $R^2_{\text{Adj}} = 0.9994$; were determined using the JMP program for this set ($N_{\text{TOT}} = 12$).

CONTINUOUS	PULSING	Pulse Interval/ ms				
		Pulse Length/ ms	30	60	100	160
Initial OBS Degradation Rate Constant $\{k \pm \text{std error (min}^{-1})\} \times 10^3$						
5.7±0.05	30	6.2±0.2	5.5±0.3	5.4±0.2	4.8±0.3	3.3±0.3
	60	5.8±0.2	5.6±0.3	5.5±0.1	5.7±0.3	6.8±0.1
	100	5.8±0.1	5.5±0.1	6.3±0.1	5.7±0.3	5.0±0.2
	160	5.8±0.1	5.6±0.2	5.7±0.1	5.9±0.1	5.8±0.3
	320	5.3±0.1	5.7±0.1	5.6±0.1	5.2±0.2	5.7±0.1
Initial HTA Formation Rate Constant $\{k \pm \text{std error (mM min}^{-1})\} \times 10^3$						
0.695±0.007	30	0.823±0.004	0.803±0.005	0.776±0.004	0.747±0.006	0.729±0.004
	60	0.780±0.007	0.783±0.007	0.770±0.005	0.762±0.008	0.726±0.010
	100	0.786±0.008	0.790±0.007	0.759±0.006	0.765±0.006	0.722±0.007
	160	0.779±0.007	0.774±0.005	0.776±0.008	0.767±0.009	0.762±0.007
	320	0.781±0.007	0.780±0.007	0.794±0.009	0.781±0.007	0.770±0.006

Table 3.1 616 kHz OBS and HTA k_{weighted} values at each pulsed setting are shown. The reported 95% confidence intervals associated with each rate constant are also reported.

CONTINUOUS	PULSING	Pulse Interval/ ms					
		Pulse Length/ ms	30	60	100	160	320
Initial OBS Degradation Rate Constants $\{k \pm \text{std error (min}^{-1})\} \times 10^3$							
5.3±0.11		30	5.3±0.1	6.2±0.2	5.8±0.4	6.1±0.1	4.7±0.8
		60	6.0±0.1	4.8±0.2	5.6±0.2	6.5±0.3	6.5±0.2
		100	6.1±0.2	5.5±0.2	7.2±0.3	5.4±0.3	5.9±0.1
		160	5.9±0.2	5.5±0.1	5.2±0.2	5.7±0.1	6.3±0.3
		320	5.3±0.3	5.8±0.3	5.7±0.1	5.2±0.1	4.7±0.2
Initial HTA Formation Rate Constants $\{k \pm \text{std error (mM min}^{-1})\} \times 10^3$							
0.713±0.005		30	0.708±0.008	0.726±0.007	0.746±0.008	0.712±0.008	0.759±0.007
		60	0.737±0.008	0.722±0.003	0.672±0.007	0.735±0.009	0.695±0.004
		100	0.711±0.004	0.699±0.005	0.686±0.005	0.711±0.008	0.68±0.02
		160	0.71±0.02	0.655±0.005	0.697±0.004	0.720±0.006	0.704±0.006
		320	0.722±0.003	0.701±0.004	0.677±0.004	0.695±0.008	0.710±0.005

Table 3.2 205 kHz OBS and HTA k_{weighted} values at each pulsed setting are shown. The reported 95% confidence intervals associated with each rate constant are also reported.

CONTINUOUS	PULSING	Pulse Interval/ ms					
		Pulse Length/ ms	30	60	100	160	320
		Initial OBS Degradation Rate Constant {k± std error (min ⁻¹)}×10 ³					
0.49±0.029		30	0.57±0.04	0.49±0.06	0.41±0.02	0.72±0.09	0.50±0.05
		60	0.41±0.05	0.62±0.05	0.45±0.06	0.41±0.02	0.58±0.06
		100	0.59±0.07	0.53±0.07	0.43±0.03	0.30±0.04	0.46±0.06
		160	0.59±0.07	0.57±0.06	0.31±0.03	0.38±0.03	0.31±0.03
		320	0.32±0.02	0.54±0.05	0.32±0.03	0.49±0.04	0.57±0.05

Table 3.3 69 kHz OBS and HTA k_{weighted} values at each pulsed setting are shown. The reported 95% confidence intervals associated with each rate constant are also reported.

CHAPTER 4

DISCUSSION

In Tables 3.1 to 3.3 documenting rate constants for sonolysis of separate aqueous solutions of OBS and TA at 616, 205 and 69 kHz, I observed that pulsed ultrasound can statistically increase or decrease both the rate of degradation of OBS and the rate of formation of HTA. From the data in Tables 3.1 to 3.3, however, it is apparent that not all pulsing conditions statistically change the rate of these sonochemical reactions compared to continuous wave ultrasound. Also, the effect of pulsed ultrasound on sonochemical rates depended on the frequency of sonolysis. Therefore, these results confirm that the experimental design used in the current study, was a useful technique to help understand the effect of pulsing on the sonochemical degradation of surface active solutes.

Yang et al. (2008) completed a comparative study on the sonochemical degradation of OBS and have explained a number of observations of the effects of pulsed ultrasound on the sonochemical degradation of OBS, in relation to the effect of pulsed ultrasound on the sonochemical yields observed in their system. Although the authors made a number of interesting observations and conclusions from their work (Yang et al., 2008), their study only considered two pulsed conditions at each of the frequencies investigated. The current work, however, considers the effect of a total of twenty-five pulsing conditions at each frequency and therefore enables a determination of whether any specific trends in the sonochemical rate of OBS degradation are observed under various pulsing

conditions and ultrasound frequencies. In Section 4.1 below, a discussion of the sonochemical rates of OBS degradation was developed to draw appropriate comparisons with the sonochemical activity in the system (i.e., HTA formation rates) under various pulsed modes and frequencies. This comparison under different conditions facilitates identification of the mechanism(s) by which pulsing enhances or also limits the rate of sonochemical degradation of OBS. Identification of mechanisms involved is necessary to determine the most efficient conditions for removal of surface active contaminants from polluted water. Further optimization investigations focused on long sonolysis times under pulsed and continuous conditions are discussed in Section 4.2, which represents a step closer to a more realistic situation, for application in environmental engineering processes.

The rate data shown in Tables 3.1 to 3.3 provides a summary of all of the data collected during this study under continuous and pulsed ultrasound conditions. However, to gain an appreciation for the effect of pulsing at different frequencies on OBS degradation rates compared to the HTA formation rates, the data was converted to a “pulse enhancement” value at each frequency, following the work of Weavers and co-workers (Yang et al., 2005, 2006, 2008) and as described in the following Section.

4.1 HTA and OBS PULSED ENHANCEMENTS

In order to understand the effect of pulsed ultrasound on the rate of degradation of OBS and how this relates to sonochemical activity in the system (i.e., determined from the rate of HTA formation), the pulsed degradation rate constants were compared to the continuous rate constants for each experiment at all frequencies (i.e., 616, 205 and 69 kHz). Specifically, pulse enhancement values, which give a measure of the effect of pulsed ultrasound relative to the sonochemical rate observed under continuous mode exposure, were determined for OBS degradation and HTA

formation. Calculation of the pulsed enhancement is shown in Equation 4.1 (Yang et al., 2005, 2006, 2008):

$$\text{Pulsed Enhancement}(\%) = \frac{C_0 k_{\text{pulsed}} - C_0 k_{\text{CW}}}{C_0 k_{\text{CW}}} \times 100 \quad (4.1)$$

where C_0 is the initial concentration ($C_0 = 1$ mM for both OBS and HTA); k_{pulsed} is the sonochemical rate observed under pulsed sonolysis and k_{CW} is that observed during continuous wave ultrasound exposure. If the pulsed enhancement is positive, then the rate of reaction was faster under the specific pulsed sonication mode than that observed during continuous mode ultrasound exposure. Alternatively, if the pulsed enhancement is negative, then the rate of reaction observed under the continuous mode was faster than that observed during pulsed sonolysis.

Figure 4.1 shows calculated pulsed enhancements for (a) OBS and (b) TA sonolysis at a frequency of 616 kHz as a function of the pulsing conditions. The 95% confidence intervals of the pulsed enhancements were calculated using the standard statistical method for propagation of the standard errors for each data point shown in Table 3.1. The line going through 0% pulsed enhancements is, by definition (i.e., Equation 4.1), the pulse enhancement value for the continuous wave experiments, to which all pulsed mode enhancements in the sonochemical reaction rates are compared. In addition, a pulsed enhancement is only considered to be either positive or negative if the 95% confidence interval for a data point is clearly above or below the 0% line. Otherwise the sonochemical rate of reaction under pulsed mode sonolysis is considered to be similar to that observed during continuous wave ultrasound (i.e. 0%). As an example, the data points at a pulse length of 30 ms and pulse intervals of 100, 160 or 320 ms during pulsed OBS sonolysis (Figure 4.1a) indicate that pulsing for these conditions has caused a decrease in the sonochemical rate of degradation of OBS, relative to that observed during the continuous mode. Alternatively, all of the pulsed mode conditions considered in the current study resulted in an enhancement of HTA formation at 616 kHz during pulsed mode compared to the continuous mode setting (Figure 4.1b).

Figures 4.2 and 4.3 are similar to that described above for Figure 4.1, except that the experiments were done at 205 and 69 kHz, respectively.

For 69 kHz sonolysis (Figure 4.3), no HTA data was obtained. The purpose of determining the rate of formation of HTA during various pulsed ultrasound modes and at different frequencies was to compare the sonochemical activity in the solution to the rate of degradation of OBS at these different conditions. However, it can be seen from the data in Figure 4.3 that the standard errors for all of the data points are relatively large compared to those observed in Figures 4.1 and 4.2. On closer examination of the successive sets of raw data of the first-order plots for sonochemical degradation of aqueous OBS solutions (see Appendix C, for 69 kHz sonolysis) two observations are immediately apparent. First, the correlation coefficients within a given sonochemical experiment are usually below 0.9 and therefore determination of the first order reaction rate is affected by the generally large spread of data within a given experimental run. For example, see Appendix C, Figure C1.1 and note the spread of data within each of the two experimental runs shown. Second, there is generally very poor reproducibility from one sonochemical experimental run to another, under presumably identical experimental conditions. For example, see the considerably low reproducibility between the sets of experiments shown in either of Figures C1.2, C1.4 or C1.5 in Appendix C.

The observation of relatively large scatter within a given experiment is consistent with the observation of poor reproducibility between successive runs under the same ultrasound exposure conditions, but it is not really clear why it is occurring at 69 kHz. One possibility is that the observed, relatively large amount of agitation caused in the solution at 69 kHz compared to higher frequencies of sonolysis is partly responsible. This vigorous agitation of liquid at this frequency caused a dramatic instability of the gas/solution surface of the 300 mL sample solution, as observed upon turning on the ultrasound. It is known that the sonochemical yield is affected by the presence of a standing wave in the liquid, formed following the reflection of the incident ultrasonic wave from the gas/solution surface of the sample solution. For this reason it is important to keep the solution volume relatively constant during sonolysis, especially at low ultrasonic frequencies (Sostaric et al.,

2001). The volume of solution changes the height of solution above the ultrasonic flat plate, and therefore the phase at which the incident wave is reflected back from the gas/solution interface. Therefore, as the nature of the standing wave changes the sonochemical activity observed per volume of solution will also change. It is possible that random agitation and instability of the gas/solution interface in the ultrasound unit at 69 kHz causes a similar effect.

Because of this, the data shown in Figure 4.3 should be viewed with a very low degree of statistical confidence and no reliable conclusions can, nor should be made on the pulse enhancements shown in Figure 4.3. For this reason, the data in Figure 4.3 will not be discussed in this study with respect to understanding the effect of pulsing on the sonochemical degradation rate of OBS in comparison to that of HTA formation.

As discussed by Yang et al. (2008), it was important only to make comparisons between pulse enhancements for OBS and HTA at any given pulsed mode and especially only within a particular frequency of sonolysis. The reason for this is that a change in ultrasound frequency results in a change in the cavitation bubble field in a way that cannot be understood in terms of energy input to the system and conversion of that ultrasound energy into sonochemistry by the cavitation bubbles (Petrier et al., 1992), (Riesse et al., 1996), (Sostaric and Riesz, 2002). Essentially, the ultrasound frequency will change the number of bubbles in the system, the size of these bubbles, the amount of OH radicals that can escape into the bulk solution to react with hydrophilic solutes, the temperature of bubble collapse (Beckett and Hua, 2001) and the ability of OBS to adsorb dynamically at the gas/solution interface of cavitation bubbles (Sostaric and Riesz, 2001, 2002). Therefore, it is almost impossible to understand what aspect of the cavitation bubbles changed to create an observed change in sonochemical rate of reaction if, for example, pulse enhancement of OBS at one frequency was compared to that at another frequency.

Following this method of comparative sonochemistry, Yang et al. (2008) only made comparisons of OBS degradation rates to HTA formation rates within a given frequency and at a particular pulsed ultrasound mode. This way, it was possible to gain insight into how an observed

change in the rate of OBS degradation during pulsed ultrasound occurred with respect to the sonochemical activity in the system, under identical exposure conditions. This comparative method is extremely important in that once such a comparison is made, it is then possible to interpret how the “comparison” is affected by a change in ultrasound frequency or pulsing conditions. The hypothesis is that the majority of variables that affect sonochemical rates of reaction when the frequency or pulsed mode is changed, do not affect the comparison, since the effect of most of these variables are essentially “cancelled out” in making the comparison, as described in detail by Sostaric and Riesz (2002).

Yang et al. (2008) identified three specific “sets” of OBS/HTA pulse enhancement comparisons within any given frequency and pulsed mode of sonolysis. The three sets of comparative data are also identifiable from the collective data presented in Figures 4.1 and 4.2 of the current study. Therefore, for clarity, these data sets are described and adhered to in the current work.

Data Set 1 was defined as all comparative data sets in which the pulse enhancement for OBS degradation at the particular ultrasound exposure condition was positive, while no pulse enhancement was observed for HTA formation, within the error of the experiment. Comparative data in Set 2 were defined as data sets in which no pulse enhancements were observed for either OBS degradation rates or HTA formation rates. Comparative data in Set 3 were described as data sets where continuous wave exposure was more effective for both OBS degradation and HTA formation, i.e., both had a negative pulse enhancement value.

However, it is immediately clear from the data shown in Figure 4.1 (616 kHz) that none of the data fit into any one of the above described sets of comparative data. A pulse enhancement was always observed for HTA; unlike the work of Yang et al. (2008) at 616 kHz; Yang et al. (2008) did not observe any HTA pulse enhancements¹. Therefore, this result provides a new set of comparative data

¹ Worthy of note is that there was one apparent HTA enhancement observed during pulsed sonolysis (100 ms:100 ms) at 206 kHz, however at the same exposure conditions an OBS pulse enhancement was observed that was an order of magnitude greater than the HTA pulse enhancement, leading to Yang et al. (2008) to conclude that this particular data set belonged to Set I(a), Table 4.1.

that had not been considered in the previous study. To clarify, all of the possible sets of data are tabulated, in Table 4.1.

Yang et al. (2008) observed comparative data Set 2 (Table 4.1), i.e., no pulse enhancement for either OBS degradation or HTA formation rates at frequencies of 620 and 803 kHz at both of the pulsed modes that they considered (i.e., pulse lengths : pulse intervals of 100 ms : 100 ms and (3540 acoustic cycles/f) ms : 100 ms). The observation was explained in terms of pulsing at these two particular frequencies having no effect on the sonochemically active bubble population. They proposed that the bubbles were of a particular size at these frequencies where neither dissolution effects (due to the Laplace pressure) or coalescence had any effect on the active bubble population.

However, it is clear that this is not the case for 616 kHz sonolysis in the current study, since all of the HTA formation rates were pulse enhanced under all pulse modes. There are a number of possible explanations for observed pulse-enhancements for HTA in the current study, including the phenomena of declustering (Sostaric thesis, 1999) and coalescence (Sunartio et al., 2007). During continuous wave ultrasound, it was proposed that bubble clusters can form (Leighton, 1994). These clusters prevent bubbles on the inside of the cluster from adsorbing enough energy to become sonochemically active cavitation bubbles. The other possibility is that the relatively close vicinity of bubbles to one another can result in an increase of bubble coalescence (Sunartio et al., 2007). This results in the formation of bubbles that are larger than the resonance radius and therefore these bubbles cannot experience inertial collapse and simply float out of the solution (Sunartio et al., 2007). The clusters can be dispersed by pulsing the ultrasound wave, thereby allowing a greater population of bubbles to become sonochemically active (Leighton, 1994).

Pulse enhancements for HTA formation rates at 620 kHz were essentially not observed in the study by Yang et al. (2008), possibly because that study was conducted using 500 mL solutions and at a higher calorimetrically determined ultrasonic power of 33 W. Since the effects of ultrasonic power and solution volume on pulse enhancement comparisons has not been studied, direct comparisons to the data of Yang et al. (2008) are tenuous at best.

Within the pulsed enhancement data at 616 kHz exposure, and pulse lengths of 30 ms (Figure 4.1a and b, data within the green oval). An apparent decrease in the pulse enhancement data for both OBS degradation rates and HTA formation rates occurs as the pulse interval is increased. However, further experimentation would be valuable to confirm this trend. A possibility to explain this trend is the effect of longer pulse intervals on the bubble population. It is known that for relatively short pulse lengths, extended pulse intervals cause a loss of the active bubble population through dissolution due to the Laplace pressure effect (Henglein, 1993; 1995). Therefore, although there is enough time for bubbles to nucleate in solution during a 30 ms pulse length, not all bubbles have enough time to grow to their resonance size and collapse, before starting to dissolve away during the pulse interval (Henglein, 1993; 1995). An even greater proportion of these bubbles dissolve away as the pulse interval is increased, thereby explaining the observed decreasing trend as the pulse interval is increased at the 30 ms pulse lengths (Figure 4.1a and b, green oval).

However, although the above discussion seems to explain the observed decreasing pulse enhancement trends at longer pulse intervals, it is not consistent with the observation that all HTA pulse enhancements are always greater than those observed under continuous wave ultrasound. That is, all HTA data points are above the 0% line (Figure 4.1b, green oval). On the other hand, it is clear that the majority of the pulsed conditions with 30 ms pulse lengths resulted in 0% or a negative pulse enhancement for OBS degradation rates. Therefore, this particular data set corresponds to set 5a and b, in Table 4.1. This observation is difficult to explain by just thinking about the possible effects that OBS has on cavitation bubbles during pulse intervals.

During pulse intervals, it is expected that OBS will more readily adsorb to the gas/solution interface of cavitation bubbles compared to that during continuous wave ultrasound. This is because pulse intervals allow the surfactant slightly more time to dynamically adsorb at the surface of these cavitation bubbles. This being the case, a greater surface excess of OBS at the bubble surface leads to a number of effects. First, it may result in enhanced declustering, due to a larger electrostatic repulsion between like charged bubbles in a cluster (Sostaric thesis, 1999). In addition, it will hinder

bubble coalescence to a greater degree than during continuous wave ultrasound (Lee, et al., 2005; Sunartio, et al., 2007), where surfactants cannot adsorb as dynamically to the gas/solution interface (Sostaric and Riesz, 2001; 2002). Finally, the lower surface tension produced when more surfactant is adsorbed to bubbles results in a decrease in the Laplace pressure inside the bubble and therefore increases the bubble lifetime during the pulse interval (Yang et al., 2008). Therefore, compared to the pulse enhancements for HTA formation rates, OBS degradation rate should have resulted in a greater pulsed enhancement, yet essentially the opposite was observed.

The result may, however be described on further consideration of the types of cavitation bubbles that are formed in a cavitation bubble field, a point that was not considered by Yang et al. in their study because the observation of pulse enhanced HTA formation was not observed (Yang et al., 2008). At 616 kHz, there will be a mixed population of transient and stable cavitation bubbles that can produce sonochemistry (Leighton, 1994). As described in detail by Sostaric and Riesz (2002) and confirmed by Sunartio et al. (2007), surfactants will not adsorb to the gas/solution interface of transient cavitation bubbles, since their lifetime is too short, i.e., only a few cycles of the ultrasonic wave. Therefore, Sostaric and Riesz (2002) concluded that all of the surfactants in their system dynamically adsorbed at rapidly vibrating surfaces of HES cavitation bubbles over hundreds of cycles of the ultrasonic wave (i.e., “high energy stable” bubbles that can produce sonochemistry). The surfactants used in their study were straight chained, sodium dodecyl sulfate (SDS) and sodium pentane sulfonate (SPSo), so it is probable that the above discussion is true for OBS too; probably more so because of the larger head group of OBS and the expected decrease in dynamic adsorption properties compared to straight chain surfactants like SDS and SPSo (Ferri and Stebe, 2000).

From the discussion above, the following interpretation is proposed for the data at 30 ms pulse lengths (Figures 4.1a and b, green oval). OBS, which only adsorbed at a positive surface excess at the surface of HES bubbles, only decomposes by thermal decomposition at the surface of these bubbles. HTA, however, is formed by reaction of TA with OH radicals that are formed and ejected into the bulk solution from both transient and stable cavitation bubbles. If this is true, then the

observation that HTA formation rates are always enhanced may be explained on the basis of pulsing preventing clustering of relatively stable bubbles. The clustering of relatively stable bubbles not only leads to a lower adsorption of ultrasound energy by bubbles in the cluster center, but will also have a negative effect on the formation of transient cavitation bubbles in the continuous ultrasound situation. When pulsed, these clusters are broken, allowing more transient bubbles to form in solution during the successive 30 ms pulse lengths.

For the case of stable bubbles, these bubbles are severely affected by longer pulse intervals. This is apparent from the negative pulse enhancements that are eventually observed for OBS degradation rates at pulse intervals of 100 ms, 160 ms and 320 ms at pulse lengths of 30 ms (Figure 4.1a), because OBS adsorbs to and decomposes only at the interface of stable bubbles (Price et al., 2004; Sostaric and Riesz, 2002)

Finally, HTA formation rates are similarly affected by the diminishing population of stable cavitation bubbles as the pulse intervals are increased at the 30 ms pulse length at 616 kHz (Figure 4.1b, green oval). However because of the contribution of OH radicals that can react with TA in the bulk solution from transient cavitation bubbles, HTA formation rates are always pulse enhanced, i.e., because of enhanced transient bubble populations due to declustering effects at all pulsing conditions.

The proposed transient and stable bubble mechanisms to describe pulsed enhancements observed at 30 ms pulse lengths (Figure 4.1b, green oval) are also valid at the longer pulse lengths considered in the current study at 616 kHz (Figure 4.1b, all pulsed modes). The point that OBS can only adsorb to the interface of stable cavitation bubbles has been proposed previously (Sostaric and Riesz, 2002; Sunartio et al., 2007). This is a point that had not been considered previously with respect to the effects of pulsed ultrasound on sonochemical degradation of surfactants (Yang, 2005, 2007, 2008), although it is possible that it is an important point, as described above.

Another noteworthy observation from the data of 616 kHz sonolysis is illustrated at the pulsed ultrasound condition of 60 ms pulse length and 320 ms pulsed interval, labeled with the

purple box in Figure 4.1. This data set is an example of where both the pulse enhancements for OBS degradation rates and HTA formation rates are positive. This particular data set fits into the comparative data Set 4, described in Table 4.1. It is difficult to explain the occurrence of this particular pulse enhancement for OBS degradation rate compared to the relatively small enhancement of HTA formation rate at this pulsed condition. It is possible to conclude that the enhanced OBS degradation rate was due to either more adsorption of OBS to the bubble surface during the pulse interval, leading to greater bubble stability through declustering or lowering of the Laplace pressure. However, it is difficult to understand why such an effect would only arise at such a relatively long pulse interval of 320 ms. This condition also occurs at pulsed length : interval times of 100 ms : 100 ms and 30 ms : 30 ms.

The results of Figure 4.2 at a sonolysis frequency of 205 kHz are interesting compared to those observed at 616 kHz from the perspective of the larger spread of comparative data sets observed. Given this spread in the data and a lack of any obvious trends with the pulsing conditions considered, it has to be concluded that the pulse enhancement data at 205 kHz shows that the sonochemical yield, accumulation of OBS on stable bubble surfaces and the relative activity of stable and transient cavitation bubbles all play an important role in determining the outcome of the pulsed enhancement value for either HTA formation rates or OBS degradation rates. Essentially, at this particular frequency of sonolysis, given the lack of trends observed in the data it is difficult to draw any conclusions on which of these variables is causing an effect from one pulsing condition to another.

With this in mind, representative data sets from Table 4.1 have been labeled on Figure 4.2 to aid in the discussion of particular comparative data sets, as described earlier. The blue box is representative of data Set 5b. This data set is interesting because it shows that although pulsing has resulted in an enhanced sonochemical yield (Figure 4.2b, blue box), this pulsed condition has clearly resulted in a decrease in the sonochemical degradation rate of OBS. In essence, the data set tells us

that we cannot use the HTA formation rates (i.e. $\text{OH}\cdot$ yield) as a measure of the efficiency of ultrasound to degrade surface active pollutants at all pulsing conditions.

The orange box (Figure 4.2) is representative of data Set 4 (Table 4.1). For this pulsing condition, pulsed enhancements were observed for both the rate of degradation of OBS and the rate of formation of HTA. The result does not help to determine any mechanistic aspects for enhanced OBS degradation, which may be due to an enhanced population of sonochemically active cavitation bubbles or due to enhanced adsorption of OBS to stable bubble interfaces during pulse intervals.

As was described in the study by Yang et al. (2008), the data Set 1 (i.e., the red box in Figure 4.2) is of great practical interest since it is a case where there was a slight decrease in the sonochemical activity in the system due to pulsing, yet the sonochemical degradation of OBS was substantially enhanced. This indicates that the surfactant properties had played a role in creating this effect. As described in Yang et al. (2008), the most probable reasons for this relatively large pulse enhancement for OBS degradation rates are related to enhanced adsorption of OBS to the surface of cavitation bubbles, since it cannot be related to an enhanced sonochemical yield during pulsing (Yang et al., 2008). During the pulse interval, more time is available for OBS to adsorb to the gas/solution interface and therefore the active bubble population will have a greater surface concentration of OBS during a pulsing condition with a pulsed length and width of 100ms each (Figure 4.2a, red box). Again, this will lead to enhanced stabilization of active bubbles due to a reduction in the Laplace pressure (Yang et al., 2008; Sostaric et al., 2002) and prevention of dissolution during pulse intervals. This can also enhanced declustering effects leading to more active bubbles through better adsorption of the ultrasound energy (Sostaric, thesis, 1999) and prevention of coalescence (Sunartio et al., 2007). The enhanced adsorption process only affects stable cavitation bubbles, for the reasons discussed above; therefore, in this case, there is at least one probable reason for the decrease in the pulse enhancements of HTA at this pulsed condition (Figure 4.2b, red box). That is, HTA is hydrophilic and cannot stabilize stable bubbles in the way that OBS can, therefore there is a loss in $\text{OH}\cdot$ radical formation due to the rapid dissolution or coalescence of stable bubbles.

The green box represents data set 3 in Table 4.1. In this case the pulse enhancements were negative for both the sonochemical activity in the solution as determined by HTA formation rates and also for the degradation rate of OBS. Using the comparative method in the current study, little information is gained regarding the effect of pulsed ultrasound on this particular comparative data set, since the negative enhancement in OBS degradation could again be due to a number of variables, namely a decrease in the active cavitation bubble population during pulsing. It is interesting just to note that of all of the pulsing conditions considered in the current study, data set 3 is a very rare occurrence and has only occurred for the particular pulsing condition shown in the green box (Figure 4.2).

Finally, data Set 2 from Table 4.1 has not been labeled on the 205 kHz graph (Figure 4.2) but represents the case where no pulse enhancement was observed for either OBS degradation rates or HTA formation rates (i.e., Figure 4.2, length : interval times of 100 ms : 160 ms and 160 ms : 160 ms). It is again difficult to understand why such a situation would arise, especially given that there should at least have been an observed effect on the degradation rate of OBS during pulsing due to an enhancement of OBS adsorption to stable bubble interfaces during pulse intervals. However, such a result simply confirms the limitations of this particular comparative method to the current system, where conclusions on the nature of the cavitation bubble field can only be made in a very specific set of circumstances. For example, when the types of trends arise that were observed for the 616 kHz study shown in Figure 4.1 (green oval).

Although the 69 kHz OBS degradation rate data is not used in the HTA formation rate comparative studies, there is still useful information that can be taken from the rate constants shown in Table 3.3. Notice how the degradation rate of OBS is much slower than that of the two higher frequencies. As the frequency of a system is decreased to 69 kHz, it is known that there will be a greater population of transient bubbles present. (Leighton, 1994). Therefore, the OBS cannot effectively adsorb to the bubbles in comparison to HES bubbles which would result in a decreased

rate of degradation. This idea fits with the above discussions to reinforce the effects of stable versus transient bubbles to explain what mechanisms of degradation are occurring.

4.2 OBS DEGRADATION AT EXTENDED SONOLYSIS TIMES

Although the data in the comparative study is useful to understand how the cavitation field is being effected by pulsing in frequency it doesn't give a full picture of how the compound is being degraded over the long term. Therefore additional experiments were conducted to gain a clearer picture of how OBS degrades over the longer experimental times. Those settings of pulsed enhancement were chosen where there was a pulsed enhancement seeing that these would be most applicable to future use of this technology.

An inflection in the pseudo first-order degradation pattern occurred at longer sonication times in the absence of pulsing as shown in Figures 4.4(616 kHz), Figure 4.7 (205 kHz), and Figure 4.9 (69 kHz). The degradation of OBS will depend on many aspects of the sonication process, including power, solution volume, frequency, temperature but as Abu-Hassan et al. (2006) (also DeVisscher et al., 1996) observed, it also depends on the sonication time.

Figure 4.1 shows a deviation in the pseudo first-order degradation rate of OBS (1 mM, 300 mL) under continuous wave ultrasound after 20 minutes. The most probable reason for this observed decrease in the rate is due to a buildup of shorter chain surface active compounds as described in Chapter 3. At a high enough concentration it is possible that these byproducts compete with the parent compound (OBS) for space at the air-water interface. If this occurs, then the degradation of the initial OBS compound decreases as a direct result. Even though these byproducts are shorter in chain length than the parent compound and are therefore less surface active than the parent compound, they are more dynamic. Less time is needed for shorter chain surface active

compounds to adsorb and orient at an interface than the longer and more bulky parent compound (Sostaric et al. 2001; 2002). A decrease in the degradation rate in Figure 4.4 after 20 minutes is consistent with a shorter chain byproduct interfering with OBS degradation. Similarly, Figure 4.7 shows the degradation of OBS at 205 kHz; after 15 minutes the initial pseudo first-order degradation rate slows as well. Additionally, this same effect is observed in Figure 4.9 at 69 kHz under continuous wave ultrasound where initial degradation rate loses its linearity after 150 minutes.

In contrast, over 60 minutes, Figure 4.5 shows good linearity in the degradation of OBS under pulsed conditions with a 100 ms pulse length and a 100 ms pulse interval at a frequency of 616 kHz. Perhaps a pulse interval allows the thermodynamically more surface active compound (i.e., OBS) to adsorb to the bubble surface compared to the shorter chain byproducts, when more time is available for adsorption. During the pulse interval the less surface active but more dynamic shorter chain byproduct moves into the bulk solution and allows the more surface active parent OBS compound to adsorb to the interface. Therefore, the compound is more effectively degraded during pulsed ultrasound where it competes more successfully against shorter chain byproducts for the bubble surface, compared to sonolysis during continuous wave ultrasound. To add, it is likely that the byproducts that are formed stay at or close to the bubble interface, as the HES bubbles collapse and reform. If this were to occur the initial adsorption of the byproducts to the bubble would not be as much of a factor. When the mode of ultrasound is pulsed the byproduct will equilibrate with the bulk (move out from the bubble interface) during the off times allow the OBS to adsorb.

To determine if this occurs at other pulsing conditions and frequencies, extended experiments were run under pulsing conditions where pulsed enhancements under these conditions were observed. Figure 4.6 shows the extended degradation of OBS at 616 kHz, where the pulsed mode was set to a length of 60 ms, and a pulsed interval of 320 ms. At 205 kHz there was a pulsed enhancement at 100 ms pulsed length and 100 ms pulsed interval, and an extended experiment at this setting is shown in Figure 4.8. Also at 69 kHz, extended experiments were run under pulsed conditions were both had a pulse length of 60 ms and pulse interval of 30 ms, (Figure 4.10) and a

pulse interval of 60 ms, (Figure 4.11). Both conditions show a pulse enhancement in the degradation of OBS compared to continuous. Notice the linearity of each figure as plotted over pseudo first order degradation. The change observed in the degradation rate under the continuous conditions at each frequency observed in Figures 4.4, 4.7 and 4.9 is not present in any of the extended pulsed mode experiments. In fact, the average correlation coefficient for the extended pulsing experiments is 0.99.

Another possibility is that as time increases a small amount of gaseous hydrocarbon ends up in the bubble core upon hot spot formation. Ashokkumar et al. (2005) reported that the ionization of hydrocarbons requires 1000kJ / mol of energy. Therefore, if OBS byproducts are present in the bubble core they have the potential to lower the temperature of the hot spot considerably. Therefore, the temperature available to degrade OBS is lowered and would explain why after a certain amount of time (of gaseous hydrocarbon build up) the degradation rate under continuous wave ultrasound changes more dramatically as shown in Figures 4.4, 4.7, and 4.9 in comparison to that resulting from selected pulsed modes as shown in Figures 4.5, 4.8 and 4.10. It is hypothesized that during the pulsed interval of the pulse setting more gaseous product can escape into the bulk of the solution and therefore over time in comparison to continuous there will be less of this gaseous byproduct built up in the bubble core. Therefore, upon bubble collapse the temperature of collapse will be less cushioned when the mode of ultrasound is pulsed in comparison to continuous. Under this possibility the greater linearity to the correlation of the extended pulsed mode experiments may also be expected.

Set Category	Pulsed Enhancement	
	OBS Degradation	HTA Formation
1a	+	0
1b	+	-
1c	0	-
2	0	0
3	-	-
4	+	+
5a	0	+
5b	-	+
5c	-	0

Table 4.1. Description of possible comparative data sets, following the definitions of Yang et al. (2008) for Sets 1(a), 2 and 3. Additional sets shown are described for the first time in the current work. "+" refers to a pulse enhancement. "-" indicates a negative pulse enhancement value (i.e., data points that lie below the 0% line in Figures 4.1 and 4.2. "0" indicates that no pulse enhancement was observed.

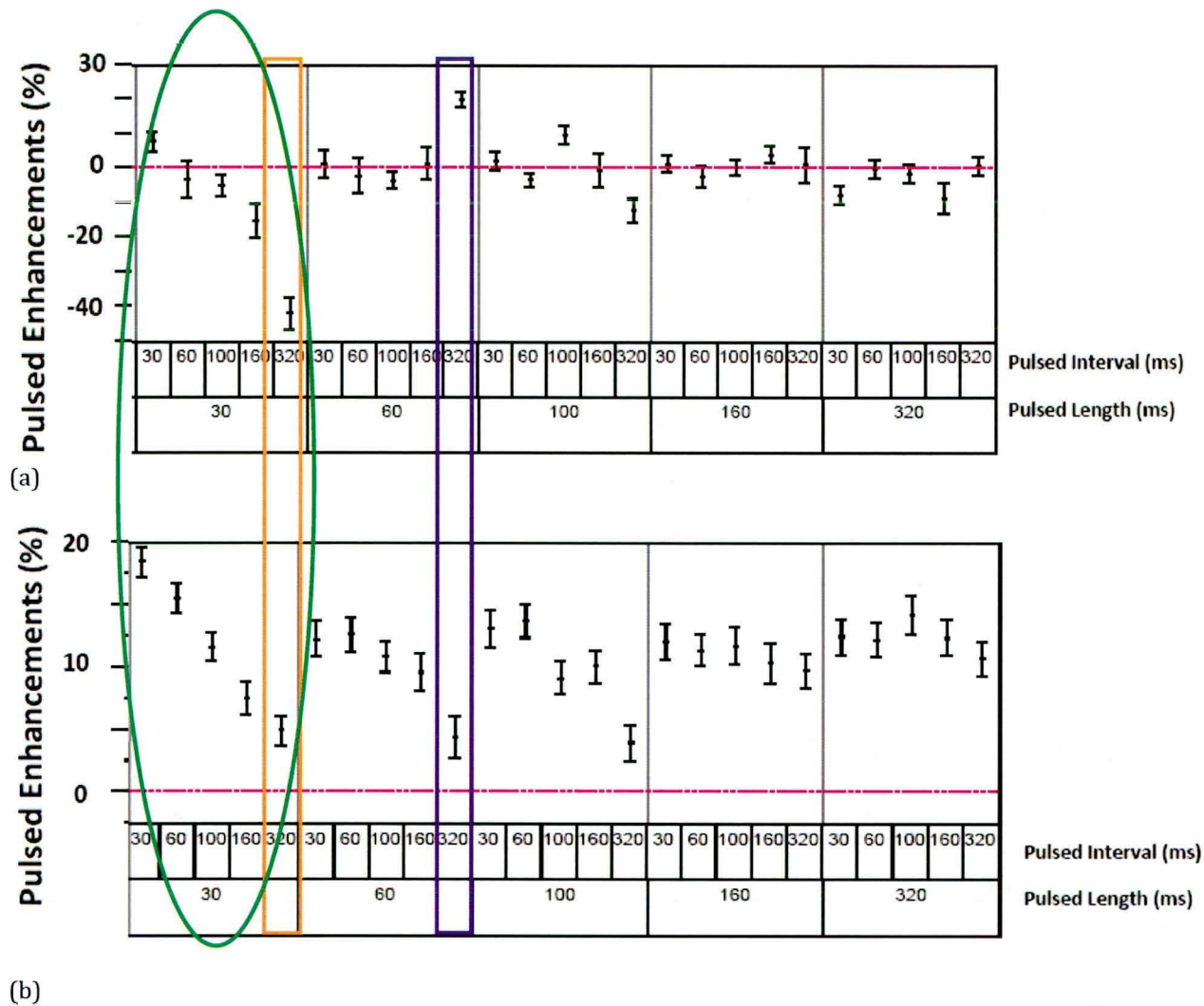
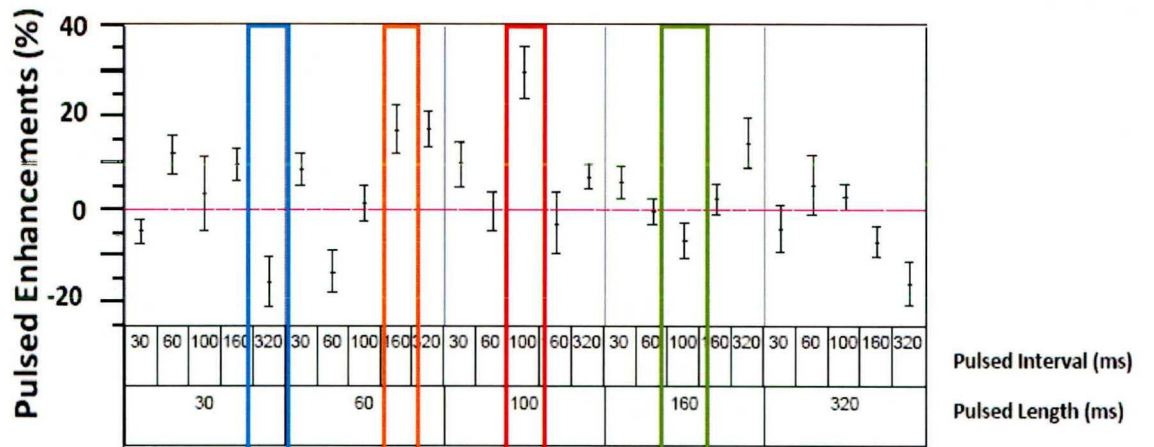
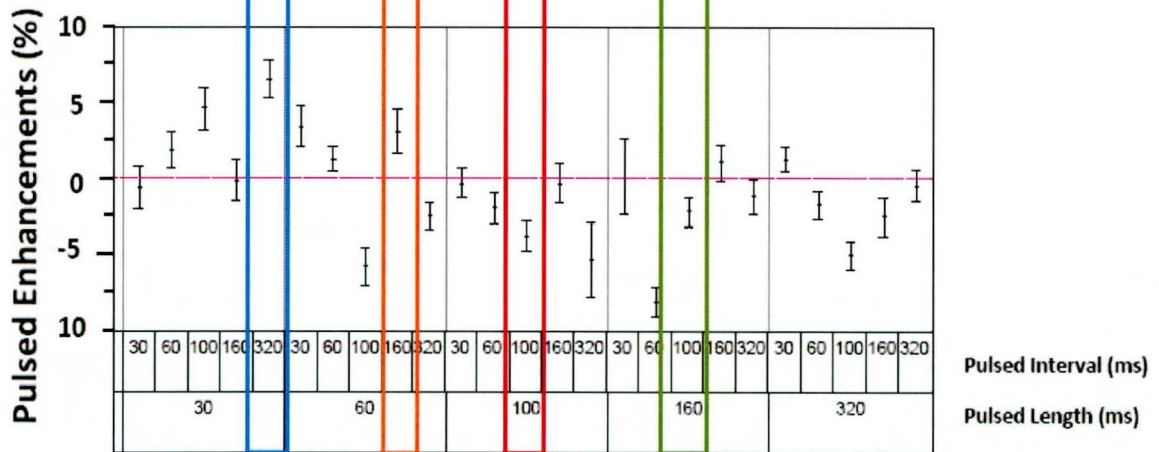


Figure 4.1 Pulsed enhancement values for, degradation of OBS (a) and formation of HTA (b) under various pulsed ultrasound ($f= 616$ kHz, $P= 27W$) conditions (data points), relative to continuous wave ultrasound (i.e., the dashed line). The 95% confidence interval for all observations within each pulsed setting is marked with the upper and lower bound bars.



(a)



(b)

Figure 4.2 Pulsed enhancement values for degradation of OBS (a) and formation of HTA (b) under various pulsed ultrasound ($f= 205$ kHz, $P= 27W$) conditions (data points), relative to continuous wave ultrasound (i.e., the dashed line). The 95% confidence interval for all observations within each pulsed setting is marked with the upper and lower bound bars.

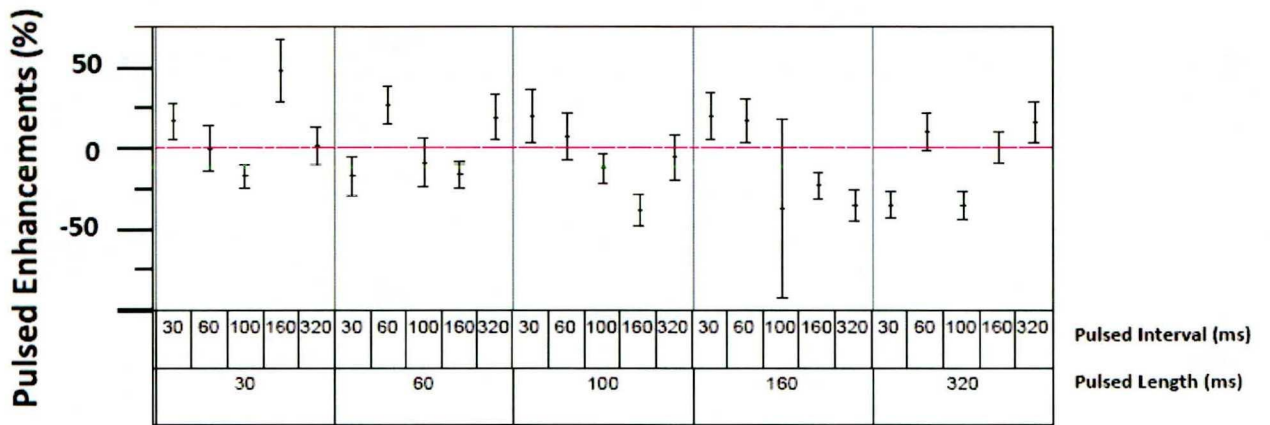


Figure 4.3 Pulsed enhancement values for degradation of OBS under various pulsed ultrasound ($f=69$ kHz; $P = 27W$) conditions (data points), relative to continuous wave ultrasound (i.e., the dashed line). The 95% confidence interval for all observations within each pulsed setting is marked with the upper and lower bound bars.

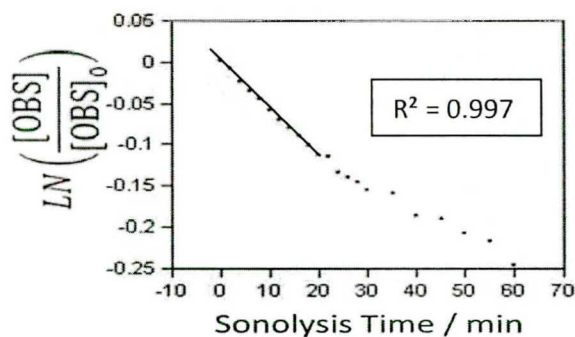


Figure 4.4 OBS first order degradation rates were determined in aqueous solutions (1mM, 300mL) exposed to continuous ultrasound ($f = 616$ kHz, $20 \pm 0.5^\circ\text{C}$). Notice that the correlation between OBS degradation and sonolysis time is highly linear up to the sonolysis time of 20 minutes. After this time the rate of reaction slows and the correlation decreases. To investigate the initial degradation rate, a total sonolysis time of 20 minutes was chosen for all 616 kHz OBS degradation experiments.

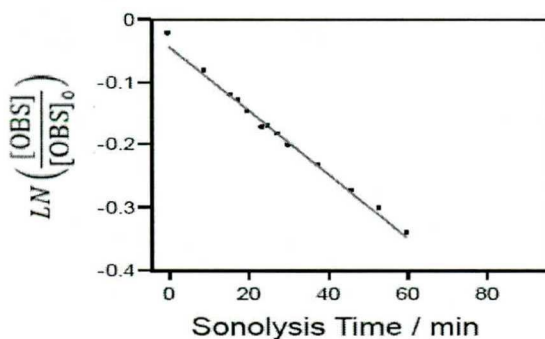


Figure 4.5 First order ultrasonic degradation of OBS in aqueous solution (1mM, 300ml) exposed to pulsed wave (length = 100ms; interval = 100ms) ultrasound ($f = 616$ kHz; $P = 27\text{W}$; $t_{\text{sonolysis}} = 60$ min) The weighted degradation rate constant, $k = 5.103 \times 10^{-3}$; adjusted correlation coefficient, $R^2 = 0.9995$; were determined using the JMP program for this set ($N_{\text{TOT}} = 13$).

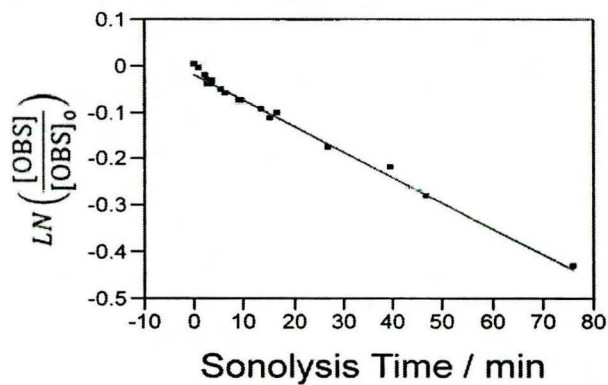


Figure 4.6 First order ultrasonic degradation of OBS in aqueous solution (1mM, 300ml) exposed to pulsed wave (length = 60ms; interval = 320ms) ultrasound (f = 616 kHz; P = 27W; $t_{\text{sonolysis}} = 78$ min) The degradation rate constant, $k = 5.521 \times 10^{-3}$; adjusted correlation coefficient, $R^2 = 0.991$; were determined using the JMP program for this set ($N_{\text{TOT}} = 15$).

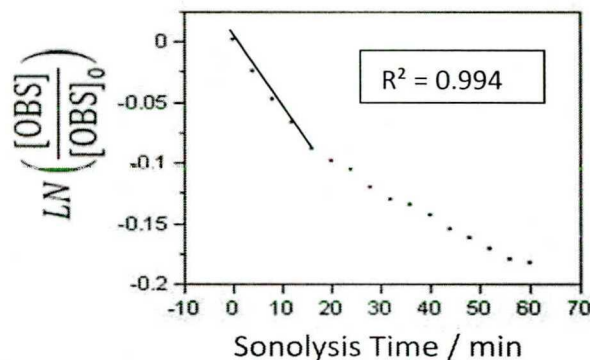


Figure 4.7 OBS first order degradation rates were determined in aqueous solutions (1mM, 300mL) exposed to continuous ultrasound ($f = 205$ kHz, $20 \pm 0.5^\circ\text{C}$). Notice that the correlation between OBS degradation and sonolysis time is highly linear up to the sonolysis time of 15 minutes. After this time the rate of reaction slows and the correlation decreases. To investigate the initial degradation rate, a total sonolysis time of 15 minutes was chosen for all 205 kHz OBS degradation experiments.

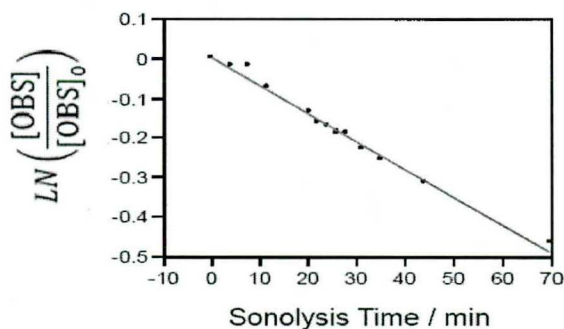


Figure 4.8 First order ultrasonic degradation of OBS in aqueous solution (1mM, 300ml) exposed to pulsed wave (length = 100ms; interval = 100ms) ultrasound ($f = 205$ kHz; $P = 27\text{W}$; $t_{\text{sonolysis}} = 70$ min). The degradation rate constant $k = 7.015 \times 10^{-3}$; adjusted correlation coefficient, $R^2 = 0.989$; were determined using the JMP program for this set ($N_{\text{TOT}} = 13$).

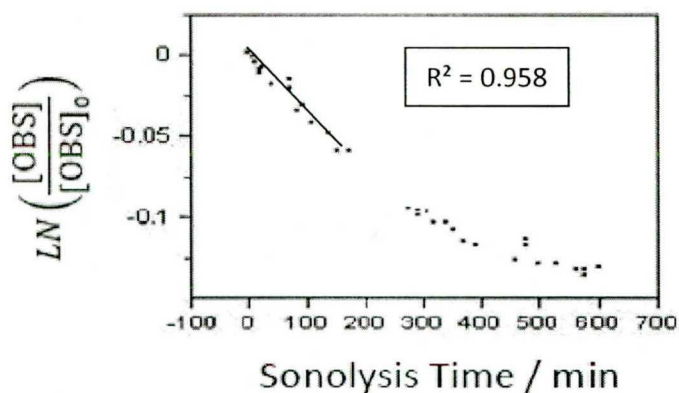


Figure 4.9 OBS first order degradation rates were determined in aqueous solutions (1mM, 300mL) exposed to continuous ultrasound ($f = 69 \text{ kHz}$, $20 \pm ^\circ\text{C}$). Notice that the correlation between OBS degradation and sonolysis time is linear up to the sonolysis time of 150 minutes at least. After this time the rate of reaction slows and the correlation decreases. To investigate the initial degradation rate, a total sonolysis time of 60 minutes was chosen for all 69 kHz OBS experiments.

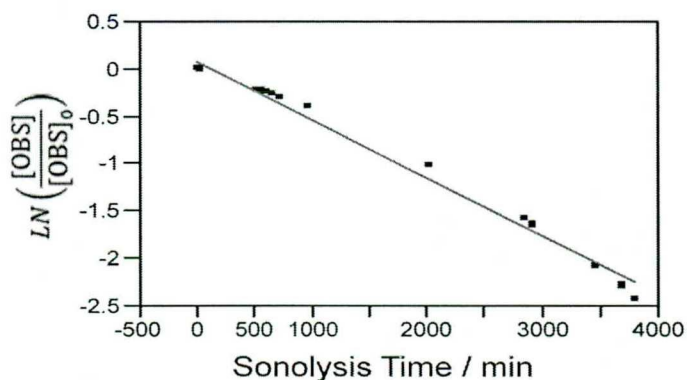


Figure 4.10 First order ultrasonic degradation of OBS in aqueous solution (1mM, 300ml) exposed to pulsed wave (length = 60ms; interval = 30ms) ultrasound ($f = 69 \text{ kHz}$; $P = 27\text{W}$; $t_{\text{sonolysis}} = 3885 \text{ min}$) The degradation rate constant, $k_{\text{weighted}} = 6.130 \times 10^{-4}$; adjusted correlation coefficient, $R^2_{\text{Adj}} = 0.989$; were determined using the JMP program for this set ($N_{\text{TOT}} = 25$).

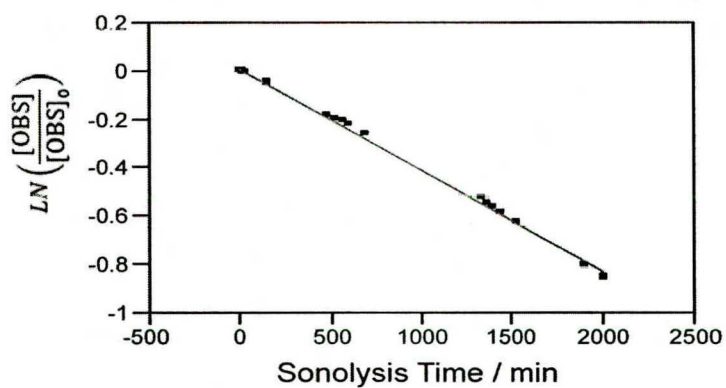


Figure 4.11 First order ultrasonic degradation of OBS in aqueous solution (1mM, 300ml) exposed to pulsed wave (length = 60ms; interval = 60ms) ultrasound (f = 69 kHz; P = 27W; $t_{\text{sonolysis}} = 2000$ min) The degradation rate constant, $k_{\text{weighted}} = 4.019 \times 10^{-4}$; adjusted correlation coefficient, $R^2_{\text{Adj}} = 0.998$; were determined using the JMP program for this set ($N_{\text{TOT}} = 26$).

CHAPTER 5

CONCLUSIONS

A very careful understanding of the type of comparative study used in the current study as well as that used by Yang et al. (2008) needs to be firmly established. The data are of value from the perspective of understanding fundamental aspects of how pulsing and frequency affects acoustic cavitation and the resulting sonochemical degradation of OBS. However, it was difficult to understand some of the observed data as a result of the chosen comparative method. As a result of the broad range of empirical conditions considered in this study, additional observations and hypotheses to those made by Yang et al. (2008) are presented.

The first was the hypothesis that the different types of bubbles present in a system (transient or stable) will effect OBS degradation in a different manner to HTA formation. This effect was observed throughout each frequency to different degrees. At 616 kHz the observation that HTA

formation rates are always enhanced during pulsing, amongst other observations, can be understood in relation to the effect of the different bubbles on HTA formation rates and OBS degradation rates. It is predicted that transient and high energy stable (HES) bubbles create the chemical reactivity (i.e., OH radical yield) of the system, but only HES bubbles result in the degradation of OBS that has accumulated at the interface of these bubbles. Because transient bubbles are of a very short lifetime, it is predicted that an insignificant amount of OBS can adsorb to and decompose at the surface of these bubbles. HTA formation rates however, will be affected by both bubble types. This hypothesis readily explains the results observed at 616 kHz. The above hypothesis is further supported by the observation that at an ultrasound frequency of 69 kHz, the degradation rate of OBS is greatly decreased relative to that observed at the two higher frequencies used in the present study. As a result it was concluded that under 69 kHz, there is a greater population of transient bubbles present in solution. Therefore, the OBS cannot effectively adsorb to the bubbles in comparison to HES bubbles. It is therefore concluded that OBS degradation and HTA formation are being affected differently under the same sonochemical environments. Although the comparative study with HTA formation rates gives some valuable insights into how OBS is adsorbing to and degrading at cavitation bubble surfaces under different modes and frequencies of sonolysis, a comparative study that uses two similar surfactants with slightly different n-alkyl chain lengths may provide further information of the effect of dynamic adsorption properties of surfactants on degradation rates during pulsed mode sonolysis.

The experimental time of OBS degradation was extended relative to the shorter sonolysis times used in section 4.1 for select conditions of pulsed mode ultrasound where an enhancement in OBS degradation occurred. It was observed that OBS degradation under continuous mode sonolysis at relatively long sonolysis times was marked by an inflection point where its degradation slowed greatly in comparison to the initial rate of degradation. This inflection point was not observed under any of the pulsed mode conditions at extended sonolysis times. This observation was attributed to two possibilities. The first, was that as sonolysis time increased the parent OBS compound was

degrading to shorter chain surface active byproducts, which after a certain amount of time built up to a concentration where they were adsorbing and competing with the parent OBS compound for space at the bubble interface. During continuous mode sonolysis, it was proposed that dynamic adsorption was the main mechanism of adsorption of all surface active compounds to the bubble. During pulsed ultrasound, the bubble surface is less dynamic in nature and the better thermodynamic adsorption properties of OBS results in its adsorption to cavitation bubbles in preference to the byproducts that possess a shorter n-alkyl chain. Therefore, the rate of OBS degradation occurs at a similar rate to the initial rates of degradation under pulsed mode at long sonication times.

The second possibility for the differences observed between continuous and pulsed modes at longer sonication times was attributed to the buildup of volatile hydrocarbons entering the stable cavitation bubbles at longer sonication times due to the effects of rectified diffusion. This buildup would act to cushion the elevated temperature upon hot spot formation, effectively resulting in a decrease in the degradation rate of OBS observed at the longer sonication times under the continuous mode. The observation that pulsing the ultrasound relieved this effect was attributed to the alleviation in the buildup of the gaseous products during the pulsed intervals. This would allow diffusion of these gaseous products out of the bubble as the bubble acted to diffuse inwards during the pulsed intervals. (Leighton, 1994)

Some valuable observations could be made using the techniques used in the current study. It has been shown that any type of sonochemical reaction cannot be relied upon to understand the way a pollutant surfactant will decompose during a comparative sonochemical reaction. It is difficult to use an OBS/HTA type comparison in order to gain clarity about what is happening to the cavitation bubble field when you pulse, because too many variables are present as a result. Instead, it might be more valuable to compare two sonochemical reactions which are very similar in most respects in order to remove as many variables from the system as possible, when the comparison is made, for

example, comparing the rate of degradation of two surfactants from a homologous series of surfactants (Sostaric and Riesz, 2002; Yang, et al., 2007).

LIST OF REFERENCES

- Abu-Hassan, M.A; Kim, J.K; Metcalfe, I.S; Mantzavinos, D. Kinetics of low frequency sonodegradation of linear alkylbenzene sulfonate solutions. *Chemosphere*, 2006, 62, 749-755.
- Adamson, A.W; Gast, A.P. *Physical Chemistry of Surfaces*. John Wiley and Sons, Inc., New York, 1997.
- Alvarez-Munoz, D; Saez, M; Gomez-Parra, A; Gonzalez-Mazo, E. Experimental Determination of Biotransformation, and Elimination of Linear Alkylbenzene Sulfonates in Solea Senegalensis. *Environmental Toxicology and Chemistry*, 2007, 26, 2597-2586.
- Ashokkumar, M.; Grieser, F. A Comparison Between Multibubble Sonoluminescence Intensity and the Temperature within Cavitation Bubbles. *J. Am. Chem. Soc.* 2005, 127, 5326-5327.
- Ashokkumar, M; Hodnett, M; Zeqiri, B; Grieser, F; Price, G.J; Acoustic Emission Spectra from 515 kHz Cavitation in Aqueous Solutions Containing Surface-Active Solutes. *J. Am. Chem. Soc.* 2007, 129, 2250-2258.
- Ashokkumar, M; Hall, R; Mulvaney, P; Grieser, F. Sonoluminescence from Aqueous Alcohol and Surfactant Solutions. *J. Phys. Chem. B.*, 1997. 101, 10845-10850.
- Ashokkumar, M.; Grieser, F. The Effects of Surface Active Solutes on Bubbles in an Acoustic Field. *Phys. Chem. Chem. Phys.*, 2007, 9, 5631-5643.
- Atchley, A; Frizzell, L; Apfel, R; Holland, C; Madanshetty, S; Roy, R. Threshold for Cavitation produced in water by Pulsed Ultrasound. *Ultrasonics Sonochemistry*, 1988, 26, 280-5
- Bakirel, T; Keles, O; Karatas, S; Ozcan, M; Turkmen, G; Candan, A. Effect of Linear Alkylbenzene Sulfonate (LAS) on Non-Specific Defense Mechanisms in Rainbow Trout. *Aquatic Toxicology*, 2005, 71, 175-181.
- Beckett, M.A; Hua, I. Impact of Ultrasonic Frequency on Aqueous Sonoluminescence and Sonochemistry. *J. Phys. Chem.* 2001, 105, 3796-3802.
- Brotchie, A; Ashokkumar, M; Grieser, F. Effects of Water-Soluble Solutes on Sonoluminescence under Dual-Frequency Sonication. *J. Phys. Chem. C.* 2007, 111, 3066-3070.
- Ciaravino, V; Flynn, H.G.; Miller, M.W. Pulsed Enhancement of Acoustic Cavitation: A Postulated Model. *Ultrasound in Med & Biol.*, 1981, 7, 159-166.
- Crum, L.A; Mason, T.J; Reisse, J.L; Suslick, K.S. *Sonochemistry and Sonoluminescence. Series C: Mathematical and Physical Sciences*, Kluwer Academic Publishers, Vol. 524, 1999.
- Dekerckheer, C; Dahlem, O; Reisse, J. On the Frequency and Isotope Effect in Sonochemistry. *Ultrasonics Sonochemistry*, 1997, 4, 205-209.

- Destallats, H; Hung, H-M; Hoffman, M.R. Degradation of Alkylphenol Ethoxylate Surfactants in Water with Ultrasonic Irradiation. *Environ. Sci. Technol.*, 2000, 34, 311-317.
- De Visscher, A; Van Eenoo, P; Drijvers, D; Van Langenhove, H. Kinetic Model for the Sonochemical Degradation of Monocyclic Aromatic Compounds in Aqueous Solution. *J. Phys. Chem.*, 1996, 100, 11636 – 11642.
- Di Corcia, A; Casassa, F; Grescenzi, C; Marcomini, A; Samperi, R. Investigation of the Fate of Linear Alkyl Benene sulfonates and Co products in a Laboratory Biodegradation Test by Using Liquid Chromatography / Mass Spectrometry. *Environ. Sci. Technol.*, 1999, 33, 4112-4118.
- Drees, C.W. Sonochemical degradation of perfluorinated sulfonate. Thesis (M.S.)—The Ohio State University, 2005.
- Drivers D., Langenhove, H.V.; and Herrygers, V. Sonolysis of Fluoro-, Chloro-, Bromo- and Iodo-benzene: a Comparative Study. *Ultrasonics sonochemistry*, 2000, 7, 87-95.
- Epstein, P.S; Plesset, M.S. On the stability of gas bubbles in liquid-gas solutions. *J. Chem. Phys.*, 1950, 18, 1505-1509.
- Fang, X; Mark,G; Sonntag, C.V. OH Radical Formation by Ultrasound in Aqueous Solutions. Part I: The Chemistry Underlying the Terephthalate Dosimeter. *Ultrasonics Sonochemistry*, 1996, 3, 57-63.
- Ferri, J.K; Stebe, K.J; Which surfactants reduce surface tension faster? A scaling argument for diffusion-controlled adsorption. *Adv. Colloid Interface Sci.* 2000, 85, 61-97.
- Flint, E.B; Suslick, K.S. The Temperature of Cavitation. *Science*, 1991, 253, 1397-1399.
- Flynn, H.G; Church, C.C. A Mechanism for the Generation of Cavitation Maxima by Pulsed Ultrasound. *J. Acoustical Soc. Am.*, 1984, 76, 505-512.
- Flynn, H.G. Generation of transient cavities in liquids by microsecond pulses of ultrasound. *J. Acoust. Soc. Am.*, (1982) 72 (1926-1932).
- Francescutto, A; Ciuti,P; Iernetti,G; Dezhkunov,N.V. Clarification of the cavitation zone by pulsed modulation of the ultrasound field. *Europhys. Lett.*, 1999, 47, 49-55.
- Fu, H; Suri, R.P.S; Chimchirian, R.F; Helmig, E; Constable. Ultrasound-Induced Destruction of Low Levels of Estrogen Hormones in Aqueous Solutions. *Environ. Sci. Technol.* 2007, 41, 5869-5874.
- Gejlsbjerg, B; Klinge C; Samsøe-Petersen,L; Madsen, T. Toxicity of Linear Alkylbenzene Sulfonates and Nonylphenol in Sludge –Amended Soil. *Environmental Toxicology and Chemistry*, 2001, 20, 2709-2716.
- Gogate, P.R; Tatake, P.A; Kanthale, P.M; Pandit A.B. Mapping of Sonochemical Reactors: Review, Analysis, and Experimental Verification. *AIChE Journal*, 2002, 47, 1542-1560.
- Grieser, F; Ashokkumar, M. The Effect of Surface Active Solutes on Bubbles Exposed to Ultrasound. *Advances in Colloid and Interface Science*, 2001, 89-90, 423-438.

Henglein, A. Chemical effects of continuous and pulsed ultrasound in aqueous solutions. *Ultrasonics Sonochemistry*, 1995, Vol2, S115-S121.

Henglein, A. Contributions to Various Aspects of Cavitation Chemistry. *Advances in Sonochemistry*, 1993, 3, 17-83.

Henglein, A; Ulrich, R; Lilie, J. Luminescence and Chemical Action by Pulsed Ultrasound. *J. Am. Chem. Soc.* 1989, 111, 1974-1979.

Holstrump, M; Krogh, P.H. Effects and Risk Assessment of Linear Alkylbenzene Sulfonates in Agricultural Soil. 3. Sub-lethal Effects on Soil Invertebrates. *Environmental Toxicology and Chemistry*, 2001, 20, 1673-1679.

Holstrump, M; Krogh, P.H; Lokke H; de Wolf, W; Marshall, S; Fox, K; Effects and risk assessment of linear alkylbenzene sulfonates in agricultural soil. 4. The influence of salt speciation, soil type, and sewage sludge on toxicity using Collembolan *Folsomia fimetaria* and the earthworm *Aporrectodea caliginosa* as test organisms. *Environ. Toxicol. Chem.*, 2001, 20, 1680-1689.

Hunter, J.R. *Foundations of Colloid Science*. Oxford University Press, Oxford, 2002.

Kimura, T; Sakamoto, T; Leveque, J-M.; Sohmiya, H; Fujita, M; Ikeda, S; Ando, T. Standardization of Ultrasonic Power for Sonochemical Reaction. *Ultrasonics Sonochemistry*, 1996, 3, S157-S161.

Kanthale, P; Ashokkumar, M; Grieser, F. Sonoluminescence, sonochemistry (H₂O₂ yield) and bubble dynamics: Frequency and power effects. *Ultrason. Sonochem.*, 2007, In Press.

Knapikowski, R; Messow, U; Brauer, P; Quitsch, K. Adsorption of Sodium Octylbenzene-sulfonate at the liquid/air interface. *Colloid. Polym. Sci.*, 1996, 274, 461-469.

Knaebel, D.B; Federle, T.W; Vestal, J.R. Mineralization of Linear Alkylbenzene Sulfonate (LAS) and Linear Alcohol Ethoxylate (LAE) in 11 Contrasting Soils. *Environmental Toxicology and Chemistry*, 1990, 9, 981-988.

Lara-Martin, P.A; Gomez-Parra, A; Gonzalez-Mazo, E. Determination and Distribution of Alkyl Ethoxysulfates and Linear Alkylbenzene Sulfonates in Coastal Marine Sediments from the Bay of Cadiz (Southwest of Spain). *Environmental Toxicology and Chemistry*, 2005, 24, 2196-2202.

Lee, J; Ashokkumar, M; Kentish, S; Grieser, F. Determination of the Size Distribution of Sonoluminescence Bubbles in a Pulsed Acoustic Field. *J. Am. Chem. Soc.*, 2005, 127, 16810-16811.

Lee, J; Ashokkumar, M; Kentish, S; Grieser, F. Effect of Alcohols on the Initial Growth of Multibubble Sonoluminescence. *J. Phys. Chem. B*, 2006, 110, 17282-17285.

Lee, J; Kentish, S; Matula, T.J; Ashokkumar, M. Effect of Surfactants in Inertial Cavitation activity in a Pulsed Acoustic Field. *J. Phys. Chem. B.*, 2005, 109, 16860-16865.

Lee, J; Tuziuti, T; Yasui, K; Kentish, S; Grieser, F; Ashokkumar, M; Iida, Y. Influence of Surface-Active Solutes on the Coalescence, Clustering, and Fragmentation of Acoustic Bubbles Confined in a Microspace. *J. Phys. Chem. C.*, 2007, 111, 19015-19023.

- Lee, J; Kentish, S.E; Ashokkumar, M. The effect of Surface-Active Solutes on Bubble Coalescence in the Presence of Ultrasound. *J. Phys. Chem. B*, 2005, 109, 5095-5099.
- Leighton T.G; Walton, A.J; Pickworth, M.J.W. *Eur. J. Phys.* 1990, 11, 47-50.
- Leighton, T. G. *The Acoustic Bubble*; Academic Press: London, 1994.
- Lin, S. H; Lin, C.M; Leu, H.G. Operating Characteristics and Kinetic Studies of Surfactant Wastewater Treatment by Fenton Oxidation. *Wat. Res.* 1999, 33, 1735-1741.
- Mason, T.J; Lorimer, J.P; Bates, D.M; Zhao, Y. Dosimetry in Sonochemistry: The use of Aqueous Terephthalate Ion as a Fluorescence Monitor. *Ultrasonics Sonochemistry.* 1994, 1, S91-S95.
- Mason, T.J; Lorimer, J.P. *Sonochemistry: Theory, Applications and uses of Ultrasound in Chemistry*; John Wiley & Sons: New York, 1988.
- Mason, T.J; Tiehm, A. *Ultrasound in Environmental Protection: Advances in Sonochemistry*, Vol. 6, Elsevier Science, Amsterdam, 2001.
- Mantzavinos, D; Burrows, D.M.P; Willey, R; Biundo, G.L; Zhang, S.F; Livingston, A.G; Metcalfe, I.S. Chemical Treatment of An Anionic Surfactant Wastewater: Electrospray-MS Studies of Intermediates and Effect on Aerobic Biodegradability. *Wat. Res.* 2001, 35, 3337-3344.
- McAvoy, D.C; Eckhoff, W.S. Rapaport, R.A; Fate of Linear Alkylbenzene Sulfonate in the Environment, *Environmental Toxicology and Chemistry.* 1993, 12, 977-987.
- McAvoy, D.C; DeCarvalho, A.J; Nielsen, A.M; Cano, M.L. Investigation of an Onsite Wastewater Treatment System in Sandy Soil: Modeling the Fate of Surfactants. *Environmental Toxicology and Chemistry*, 2002, 21, 2623-2630.
- Morgensen, A.S; Ahring, B.K. Formation of Metabolites during Biodegradation of Linear Alkylbenzene Sulfonate in an Upflow Anaerobic Sludge Bed Reactor under Thermophilic Conditions. *Biotechnology and Bioengineering*, 2002, 77, 483-488.
- Moriwaki, H; Takagi, Y; Tanaka, M; Tsuruho, K; Okitsu, K; Maeda, Y. Sonochemical Decomposition of Perfluorooctane Sulfonate and Perfluorooctanoic Acid. *Environ. Sci. Technol.*, 2005, 39, 3388-3392.
- Pee, G-Y; Rathman, J.F; Weavers, L.K. Effects of Surface Active Properties on the Cavitation Degradation of Surfactant Contaminants. *Ind. Eng. Chem. Res.*, 2004, 43, 5049-5056.
- Petrier, C; Lamy, M-F; Francony, A; Benahcene, A; David, B. Sonochemical Degradation of Phenol in Dilute Aqueous Solutions: Comparison of the Reaction Rates at 20 and 487 kHz. *J. Phys. Chem.*, 1994, 98, 10514-10520.
- Petrier, C; Francony, A; Ultrasonic waste-water Treatment: Incidence of Ultrasonic Frequency on the Rate of Phenol and Carbon Tetrachloride Degradation. *Ultrasonics sonochemistry.* 1997, 4, 295-300.
- Petrier, C; Jeunet, A.; Luche, J-L; Reverdy, G. Unexpected Frequency Effects on the Rate of Oxidative Processes Induced by Ultrasound. *J. Am. Chem. Soc.*, 1992, 114, 3148-3150.

Price, P.J; Ashokkumar, M; Hodnett, M; Zequiri, B; Grieser, F. Acoustic Emission from Cavitating Solutions: Implications for the Mechanisms of Sonochemical Reactions. *J. Phys. Chem.B*, 2005, 109, 17799-17801.

Price,G.J. Current trends in sonochemistry. Royal Society of Chemistry, School of Chemistry, University of Bath, 1992.

Price, G.J; Ashokkumar, M; Grieser,F. Sonoluminescence Emission from Aqueous Solutions of Organic Monomers. *J. Phys. Chem. B.*, 2003, 107, 14124-14129.

Price, G.J; Ashokkumar, M; Grieser, F. Sonoluminescence Quenching of Organic Compounds in Aqueous Solution: Frequency Effects and Implications for Sonochemistry. *J. Am. Chem. Soc.* 2004, 126, 2755-2762.

Price, G.J; Lenz, E.J. The Use of Dosimeters to Measure Radical Production in Aqueous Sonochemical Systems. *Ultrasonics*. 1993, 31, 451-456.

Ramsey, F; Schafer, D. The Statistical Sleuth: A Course in Methods of Data Analysis. Duxbury Press, Ed. Vol 2, 2001

Reisse, J; Caulier, T; Deckerkheer, C; Fabre, O; Vandercammen, J; Delplancke, J.L; Winand, R. Quantitative Sonochemistry. *Ultrasonics Sonochemistry*, 1996, 3, S147-S151.

Schultz, M.M; Higgins, C.P; Huset, C.A; Luthy, R.G; Barofsky, D.F; Field, J.A. Fluorochemical Mass Flows in a Municipal Wastewater Treatment Facility. *Environ. Sci. Technol.*, 2006, 40, 7350-7357.

Schultz, M.M; Barofsky, D.F; Field, J.A. Quantitative Determination of fluorinated Alkyl substances by Large-Volume-Injection Liquid Chromatography Tandem Mass Spectrometry-Characterization of Municipal Wastewaters. *Environ. Sci. Technol.*, 2006, 40, 289-295.

Sharvelle, S.; Lattyak, R; Banks, K.M; Evaluation of Biodegradability and Biodegradation Kinetics for Anionic, Nonionic and Amphoteric Surfactants. *Water Air Soil Pollut.*, 2007, 183, 177-186.

Sostaric, J.Z. A Chemical Sensor that can Detect Frequency of Ultrasound. *J. Am. Chem. Soc.*, 2008, 130, 3248-3249.

Sostaric, J.Z; Riesz,P. Adsorption of Surfactants at the Gas/Solution Interface of Cavitation Bubbles: An Ultrasound Intensity-Independent Frequency Effect in Sonochemistry. *J. Phys. Chem. B.*, 2002, 106, 12537-12548.

Sostaric, J.Z. Interfacial Effects on Aqueous Sonochemistry and Sonoluminescence. PhD Thesis, School of Chemistry, The University of Melbourne, Australia, 1999, 1-249.

Sostaric, J.Z; Riesz, P. Sonochemistry of Surfactants in Aqueous Solutions: An EPR Spin-Trapping Study. *J. Am. Chem. Soc.*, 2001, 123, 11010-11019.

Sunartio, D; Ashokkumar, M; Grieser, F. Study of the Coalescence of Acoustic Bubbles as a Function of Frequency, Power, and Water-Soluble Additives. *J. Am. Chem. Soc.*, 2007, 129, 6031-6036.

- Sunartio, D; Ashokkumar, M; Grieser, F. The Influence of Acoustical Power on Multibubble Sonoluminescence in Aqueous Solution Containing Organic Solutes. *J. Phys. Chem. B*, 2005, 109, 20044-20050.
- Suslick, K.S. *Ultrasound: Its Chemical, Physical, and Biological Effects*. VCH Publishers, Inc. 1988.
- Tronson, R; Ashokkumar, M; Grieser, F. Multibubble Sonoluminescence from Aqueous Solutions Containing Mixtures of Surface Active Solutes. *J. Phys. Chem. B*, 2003, 107, 7307.
- Torslov J; Samsoe-Petersen L, Rasmussen J.O; Kristensen, P. Use of waste products in agriculture. Contamination level, environmental risk assessment and recommendations for quality criteria. Environmental Project 328, 1997, Danish Environmental Protection Agency, Copenhagen, Denmark
- Vecitis, C.D; Park, H; Cheng, J; Mader, B.T; Hoffman, M.R. Kinetics and Mechanism of the Sonolytic Conversion of the Aqueous Perfluorinated Surfactants, Perfluorooctanoate (PFOA), and Perfluorooctane Sulfonate (PFOS) into Inorganic Products. *J. Phys. Chem. A* 2008, 112, 4261-4270.
- Venhuis, S.H; Mehrvar, M; Health Effects, Environmental Impacts, and Photochemical Degradation of selected Surfactants in Water. *International Journal of Photoenergy.*, 2004, 6, 115-125.
- Vinodgpal, K. ; Ashokkumar, M; Grieser, F. Sonochemical Degradation of a Polydisperse Nonylphenol Ethoxylate in Aqueous Solution. *J. Phys. Chem. B*, 2001, 105, 3338-3342.
- Ying, G-G. Fate, Behavior and Effects of Surfactants and Their Degradation Products in the Environment. *Environmental International.*, 2006, 32, 417-431.
- Yang, L; Sostaric, J.Z; Rathman, J.F; Kuppusamy, P; Weavers, L.K. Effects of Pulsed Ultrasound on the Adsorption of n-Alkyl Anionic Surfactants at the Gas/Solution Interface of Cavitation Bubbles. *J.Phys.Chem. B*, 2007, 111, 1361-1367.
- Yang, L; Sostaric, J.Z.; Rathman, J.F; Weavers, L.K. Effect of Ultrasound Frequency on the Pulsed Sonolytic Degradation of Octylbenzene Sulfonic Acid. *J. Phys. Chem. B.*, 2008, 112, 852-858.
- Yang, L; Rathman, J.F; Weavers, L.K. Degradation of Alkylbenzene Sulfonate Surfactants by Pulsed Ultrasound. *J. Phys. Chem. B*, 2005, 109, 16203-16209.
- Yang, L; Rathman, J.F; Weavers, L.K. Sonochemical Degradation of Alkylbenzene Sulfonate Surfactants in Aqueous Mixtures. *J. Phys. Chem. B*, 2006, 110, 18385-18391.
- Yu, X; Trapp, S; Zhou, P; Peng, X; Cao, X. Response of Weeping Willows to Linear Alkylbenzene Sulfonate. *Chemosphere*, 2006, 64, 43-48.

APPENDIX A

616 kHz

OBS AND HTA KINETIC RATE PLOTS

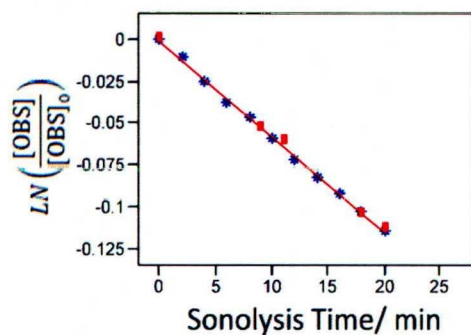


Figure A1.1 Duplicate and separate first order ultrasonic degradation of OBS in aqueous solution (1mM, 300ml) exposed to continuous ultrasound ($f = 616$ kHz; $P = 27$ W; $k_{\text{weighted}} = 5.7 \times 10^{-3} \text{ min}^{-1}$; $R^2_{\text{Adj}} = 0.998$; $N_{\text{TOT}} = 17$; $t_{\text{sonolysis}} = 20$ min).

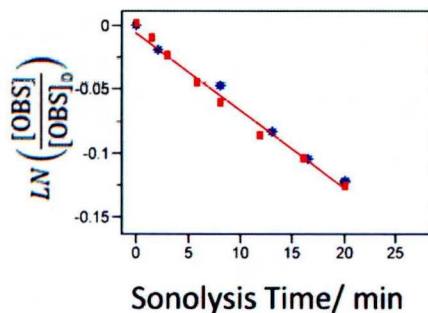


Figure A1.2 Duplicate and separate first order ultrasonic degradation of OBS in aqueous solution (1mM, 300ml) exposed to pulsed wave (30ms lengths and 30ms intervals) ultrasound ($f = 616$ kHz; $P = 27$ W; $k_{\text{weighted}} = 6.2 \times 10^{-3} \text{ min}^{-1}$; $R^2_{\text{Adj}} = 0.990$; $N_{\text{TOT}} = 16$; $t_{\text{sonolysis}} = 20$ min).

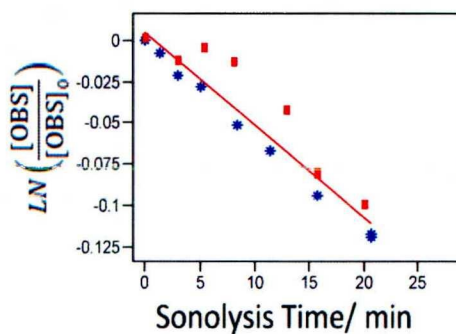


Figure A1.3 Duplicate and separate first order ultrasonic degradation of OBS in aqueous solution (1mM, 300ml) exposed to pulsed wave (30ms lengths and 60ms intervals) ultrasound ($f = 616$ kHz; $P = 27$ W; $k_{\text{weighted}} = 5.5 \times 10^{-3} \text{ min}^{-1}$; $R^2_{\text{Adj}} = 0.963$; $N_{\text{TOT}} = 16$; $t_{\text{sonolysis}} = 20$ min).

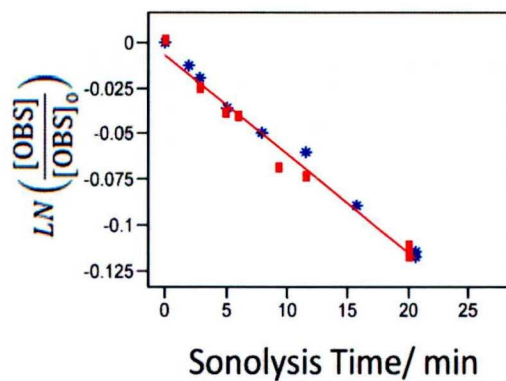


Figure A1.4 Duplicate and separate first order ultrasonic degradation of OBS in aqueous solution (1mM, 300ml) exposed to pulsed wave (30ms lengths and 100ms intervals) ultrasound ($f = 616$ kHz; $P = 27$ W; $k_{\text{weighted}} = 5.4 \times 10^{-3} \text{ min}^{-1}$; $R^2_{\text{Adj}} = 0.985$; $N_{\text{TOT}} = 17$; $t_{\text{sonolysis}} = 20$ min).

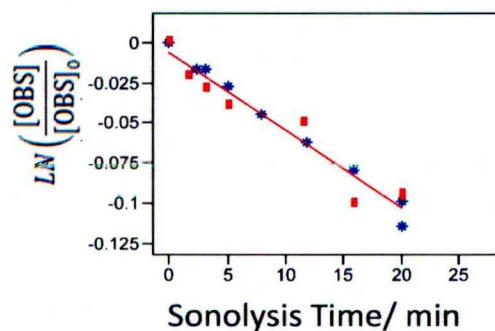


Figure A1.5 Duplicate and separate first order ultrasonic degradation of OBS in aqueous solution (1mM, 300ml) exposed to pulsed wave (30ms lengths and 160ms intervals) ultrasound ($f = 616$ kHz; $P = 27W$; $k_{\text{weighted}} = 4.8 \times 10^{-3} \text{ min}^{-1}$; $R^2_{\text{Adj}} = 0.956$; $N_{\text{TOT}} = 17$; $t_{\text{sonolysis}} = 20$ min).

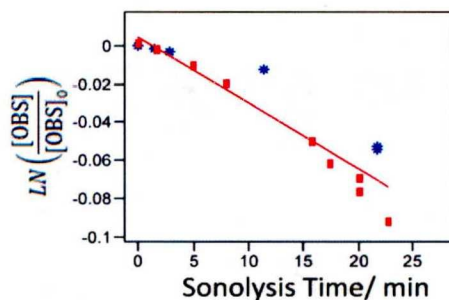


Figure A1.6 Duplicate and separate first order ultrasonic degradation of OBS in aqueous solution (1mM, 300ml) exposed to pulsed wave (30ms lengths and 320ms intervals) ultrasound ($f = 616$ kHz; $P = 27W$; $k_{\text{weighted}} = 3.3 \times 10^{-3} \text{ min}^{-1}$; $R^2_{\text{Adj}} = 0.926$; $N_{\text{TOT}} = 17$; $t_{\text{sonolysis}} = 20$ min).

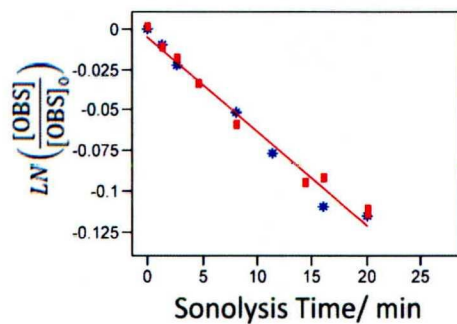


Figure A1.7 Duplicate and separate first order ultrasonic degradation of OBS in aqueous solution (1mM, 300ml) exposed to pulsed wave (60ms lengths and 30ms intervals) ultrasound ($f = 616$ kHz; $P = 27$ W; $k_{\text{weighted}} = 5.8 \times 10^{-3} \text{ min}^{-1}$; $R^2_{\text{Adj}} = 0.979$; $N_{\text{TOT}} = 16$; $t_{\text{sonolysis}} = 20$ min).

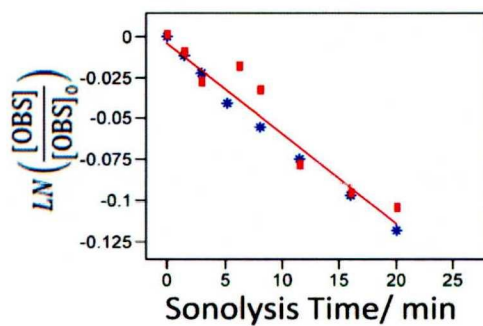


Figure A1.8 Duplicate and separate first order ultrasonic degradation of OBS in aqueous solution (1mM, 300ml) exposed to pulsed wave (60ms lengths and 60ms intervals) ultrasound ($f = 616$ kHz; $P = 27$ W; $k_{\text{weighted}} = 5.6 \times 10^{-3} \text{ min}^{-1}$; $R^2_{\text{Adj}} = 0.959$; $N_{\text{TOT}} = 17$; $t_{\text{sonolysis}} = 20$ min).

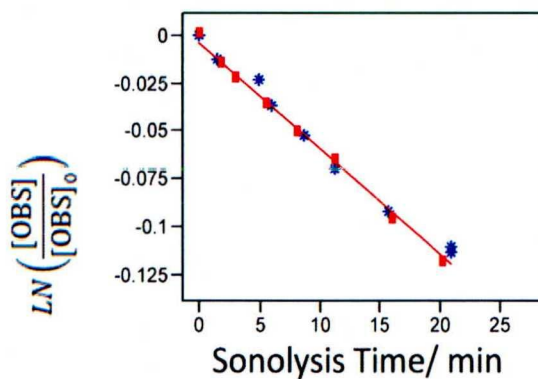


Figure A1.9 Duplicate and separate first order ultrasonic degradation of OBS in aqueous solution (1mM, 300ml) exposed to pulsed wave (60ms lengths and 100ms intervals) ultrasound ($f = 616$ kHz; $P = 27W$; $k_{\text{weighted}} = 5.5 \times 10^{-3} \text{ min}^{-1}$; $R^2_{\text{Adj}} = 0.990$; $N_{\text{TOT}} = 17$; $t_{\text{sonolysis}} = 20$ min).

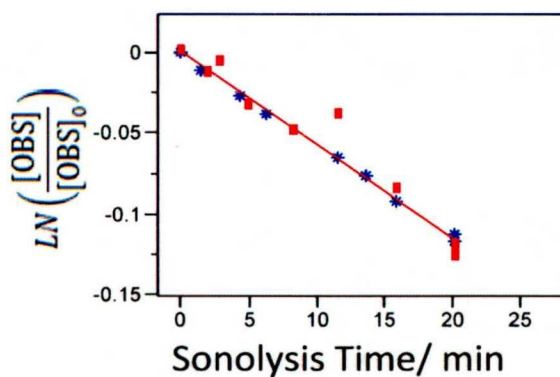


Figure A1.10 Duplicate and separate first order ultrasonic degradation of OBS in aqueous solution (1mM, 300ml) exposed to pulsed wave (60ms lengths and 160ms intervals) ultrasound ($f = 616$ kHz; $P = 27W$; $k_{\text{weighted}} = 5.8 \times 10^{-3} \text{ min}^{-1}$; $R^2_{\text{Adj}} = 0.966$; $N_{\text{TOT}} = 18$; $t_{\text{sonolysis}} = 20$ min).

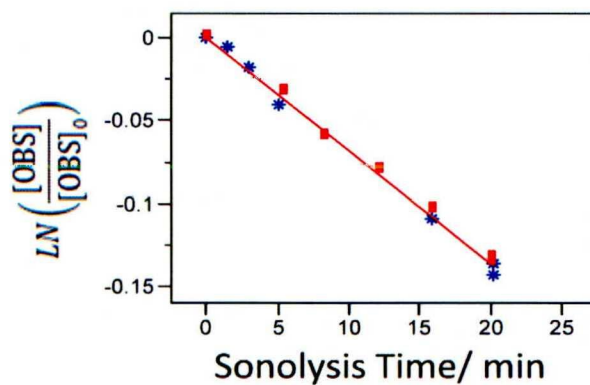


Figure A1.11 Duplicate and separate first order ultrasonic degradation of OBS in aqueous solution (1mM, 300ml) exposed to pulsed wave (60ms lengths and 320ms intervals) ultrasound ($f = 616$ kHz; $P = 27W$; $k_{\text{weighted}} = 6.8 \times 10^{-3} \text{ min}^{-1}$; $R^2_{\text{Adj}} = 0.996$; $N_{\text{TOT}} = 14$; $t_{\text{sonolysis}} = 20$ min).

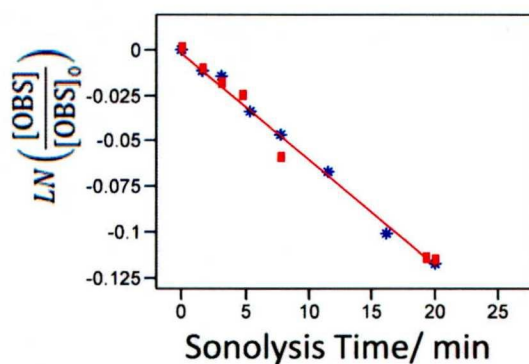


Figure A1.12 Duplicate and separate first order ultrasonic degradation of OBS in aqueous solution (1mM, 300ml) exposed to pulsed wave (100ms lengths and 30ms intervals) ultrasound ($f = 616$ kHz; $P = 27W$; $k_{\text{weighted}} = 5.8 \times 10^{-3} \text{ min}^{-1}$; $R^2_{\text{Adj}} = 0.991$; $N_{\text{TOT}} = 17$; $t_{\text{sonolysis}} = 20$ min).

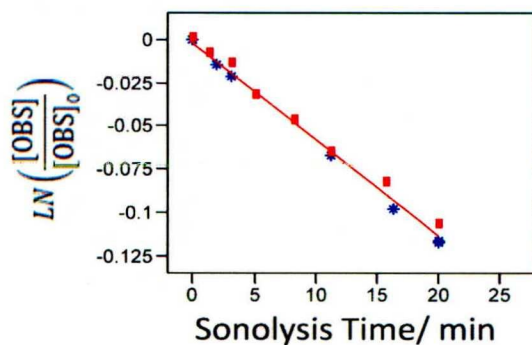


Figure A1.13 Duplicate and separate first order ultrasonic degradation of OBS in aqueous solution (1mM, 300ml) exposed to pulsed wave (100ms lengths and 60ms intervals) ultrasound ($f = 616$ kHz; $P = 27W$; $k_{\text{weighted}} = 5.5 \times 10^{-3} \text{ min}^{-1}$; $R^2_{\text{Adj}} = 0.995$; $N_{\text{TOT}} = 16$; $t_{\text{sonolysis}} = 20$ min).

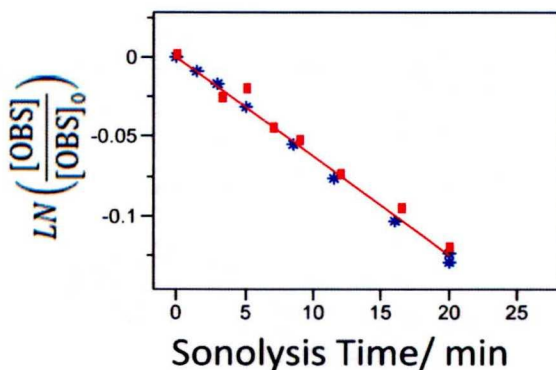


Figure A1.14 Duplicate and separate first order ultrasonic degradation of OBS in aqueous solution (1mM, 300ml) exposed to pulsed wave (100ms lengths and 100ms intervals) ultrasound ($f = 616$ kHz; $P = 27W$; $k_{\text{weighted}} = 6.3 \times 10^{-3} \text{ min}^{-1}$; $R^2_{\text{Adj}} = 0.992$; $N_{\text{TOT}} = 17$; $t_{\text{sonolysis}} = 20$ min).

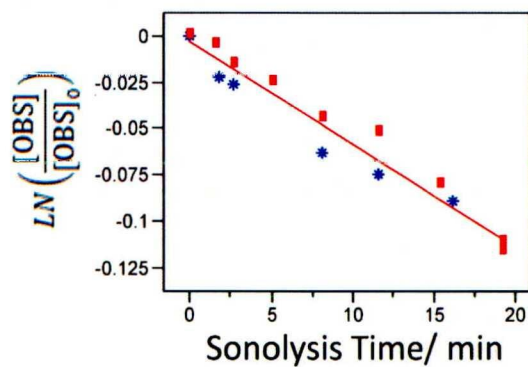


Figure A1.15 Duplicate and separate first order ultrasonic degradation of OBS in aqueous solution (1mM, 300ml) exposed to pulsed wave (100ms lengths and 160ms intervals) ultrasound ($f = 616$ kHz; $P = 27W$; $k_{\text{weighted}} = 5.7 \times 10^{-3} \text{ min}^{-1}$; $R^2_{\text{Adj}} = 0.970$; $N_{\text{TOT}} = 15$; $t_{\text{sonolysis}} = 19$ min).

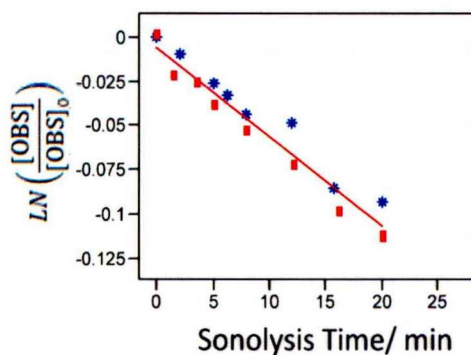


Figure A1.16 Duplicate and separate first order ultrasonic degradation of OBS in aqueous solution (1mM, 300ml) exposed to pulsed wave (100ms lengths and 320ms intervals) ultrasound ($f = 616$ kHz; $P = 27W$; $k_{\text{weighted}} = 5.0 \times 10^{-3} \text{ min}^{-1}$; $R^2_{\text{Adj}} = 0.976$; $N_{\text{TOT}} = 18$; $t_{\text{sonolysis}} = 20$ min).

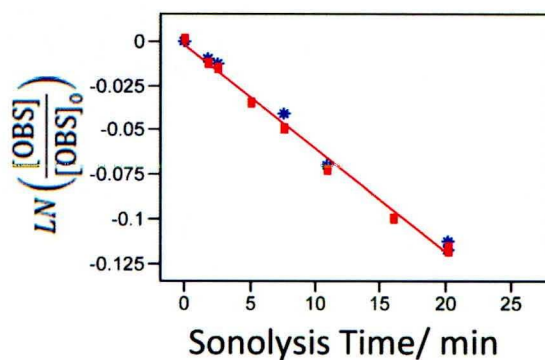


Figure A1.17 Duplicate and separate first order ultrasonic degradation of OBS in aqueous solution (1mM, 300ml) exposed to pulsed wave (160ms lengths and 30ms intervals) ultrasound ($f = 616$ kHz; $P = 27W$; $k_{\text{weighted}} = 5.8 \times 10^{-3} \text{ min}^{-1}$; $R^2_{\text{Adj}} = 0.993$; $N_{\text{TOT}} = 16$; $t_{\text{sonolysis}} = 20$ min).

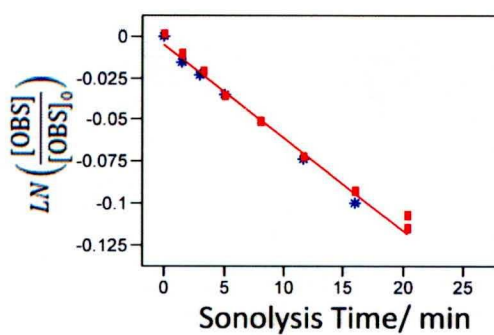


Figure A1.18 Duplicate and separate first order ultrasonic degradation of OBS in aqueous solution (1mM, 300ml) exposed to pulsed wave (160ms lengths and 60ms intervals) ultrasound ($f = 616$ kHz; $P = 27W$; $k_{\text{weighted}} = 5.6 \times 10^{-3} \text{ min}^{-1}$; $R^2_{\text{Adj}} = 0.988$; $N_{\text{TOT}} = 15$; $t_{\text{sonolysis}} = 20$ min).

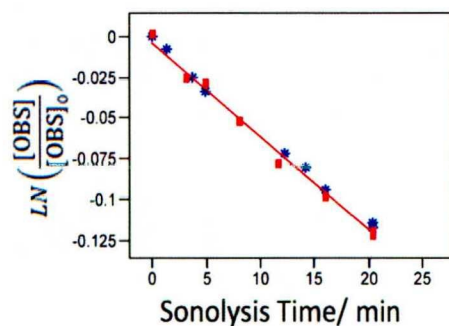


Figure A1.19 Duplicate and separate first order ultrasonic degradation of OBS in aqueous solution (1mM, 300ml) exposed to pulsed wave (160ms lengths and 100ms intervals) ultrasound ($f = 616$ kHz; $P = 27W$; $k_{\text{weighted}} = 5.7 \times 10^{-3} \text{ min}^{-1}$; $R^2_{\text{Adj}} = 0.994$; $N_{\text{TOT}} = 17$; $t_{\text{sonolysis}} = 20 \text{ min}$).

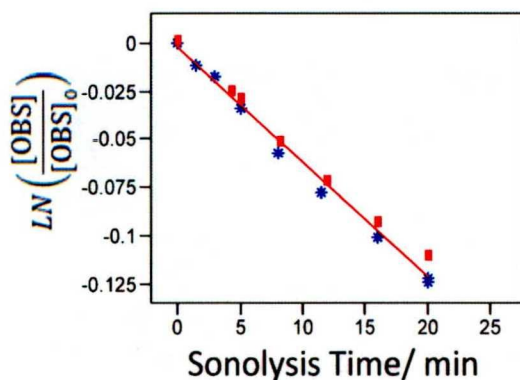


Figure A1.20 Duplicate and separate first order ultrasonic degradation of OBS in aqueous solution (1mM, 300ml) exposed to pulsed wave (160ms lengths and 160ms intervals) ultrasound ($f = 616$ kHz; $P = 27W$; $k_{\text{weighted}} = 5.9 \times 10^{-3} \text{ min}^{-1}$; $R^2_{\text{Adj}} = 0.992$; $N_{\text{TOT}} = 16$; $t_{\text{sonolysis}} = 20 \text{ min}$).

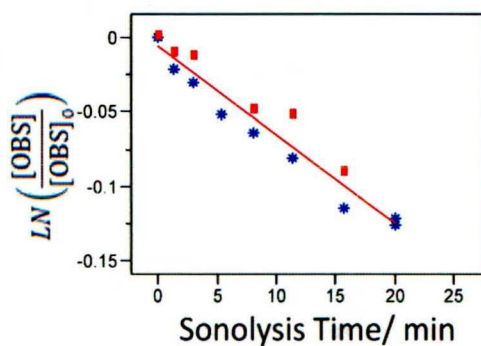


Figure A1.21 Duplicate and separate first order ultrasonic degradation of OBS in aqueous solution (1mM, 300ml) exposed to pulsed wave (160ms lengths and 320ms intervals) ultrasound ($f = 616$ kHz; $P = 27W$; $k_{\text{weighted}} = 5.8 \times 10^{-3} \text{ min}^{-1}$; $R^2_{\text{Adj}} = 0.973$; $N_{\text{TOT}} = 15$; $t_{\text{sonolysis}} = 20$ min).

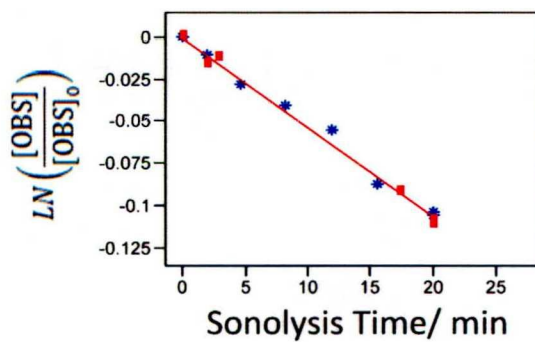


Figure A1.22 Duplicate and separate first order ultrasonic degradation of OBS in aqueous solution (1mM, 300ml) exposed to pulsed wave (320ms lengths and 30ms intervals) ultrasound ($f = 616$ kHz; $P = 27W$; $k_{\text{weighted}} = 5.3 \times 10^{-3} \text{ min}^{-1}$; $R^2_{\text{Adj}} = 0.992$; $N_{\text{TOT}} = 14$; $t_{\text{sonolysis}} = 20$ min).

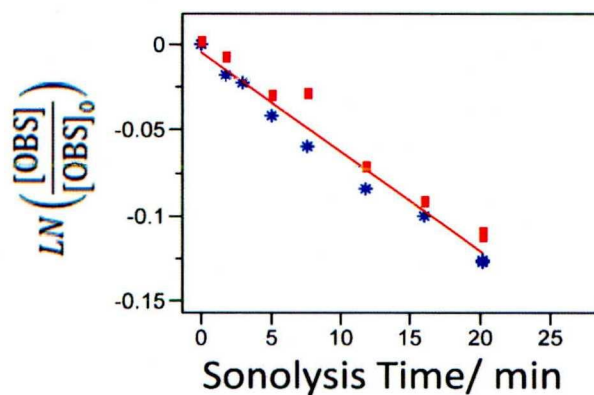


Figure A1.23 Duplicate and separate first order ultrasonic degradation of OBS in aqueous solution (1mM, 300ml) exposed to pulsed wave (320ms lengths and 60ms intervals) ultrasound ($f = 616$ kHz; $P = 27W$; $k_{\text{weighted}} = 5.9 \times 10^{-3} \text{ min}^{-1}$; $R^2_{\text{Adj}} = 0.985$; $N_{\text{TOT}} = 17$; $t_{\text{sonolysis}} = 20$ min).

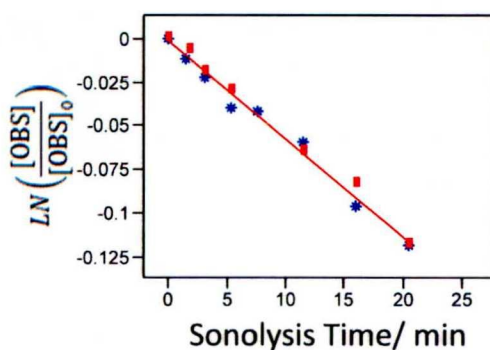


Figure A1.24 Duplicate and separate first order ultrasonic degradation of OBS in aqueous solution (1mM, 300ml) exposed to pulsed wave (320ms lengths and 100ms intervals) ultrasound ($f = 616$ kHz; $P = 27W$; $k_{\text{weighted}} = 5.6 \times 10^{-3} \text{ min}^{-1}$; $R^2_{\text{Adj}} = 0.990$; $N_{\text{TOT}} = 16$; $t_{\text{sonolysis}} = 20$ min).

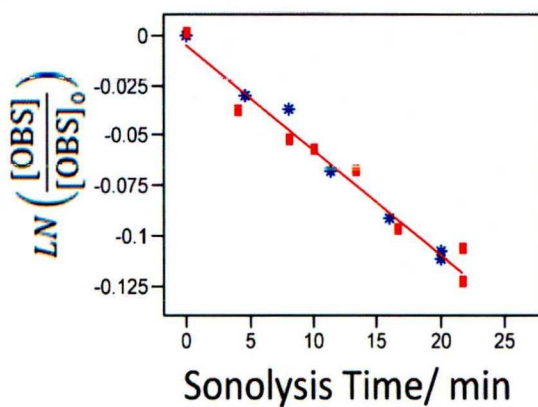


Figure A1.25 Duplicate and separate first order ultrasonic degradation of OBS in aqueous solution (1mM, 300ml) exposed to pulsed wave (320ms lengths and 160ms intervals) ultrasound ($f = 616$ kHz; $P = 27W$; $k_{\text{weighted}} = 5.2 \times 10^{-3} \text{ min}^{-1}$; $R^2_{\text{Adj}} = 0.970$; $N_{\text{TOT}} = 15$; $t_{\text{sonolysis}} = 20$ min).

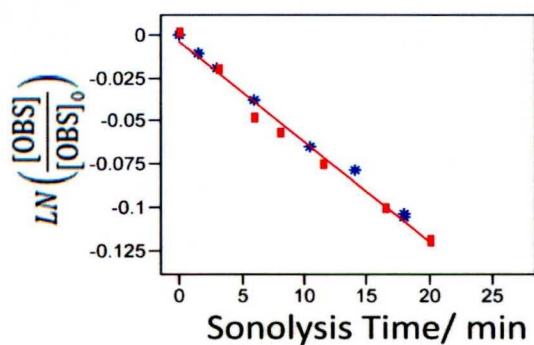


Figure A1.26 Duplicate and separate first order ultrasonic degradation of OBS in aqueous solution (1mM, 300ml) exposed to pulsed wave (320ms lengths and 320ms intervals) ultrasound ($f = 616$ kHz; $P = 27W$; $k_{\text{weighted}} = 5.7 \times 10^{-3} \text{ min}^{-1}$; $R^2_{\text{Adj}} = 0.991$; $N_{\text{TOT}} = 16$; $t_{\text{sonolysis}} = 20$ min).

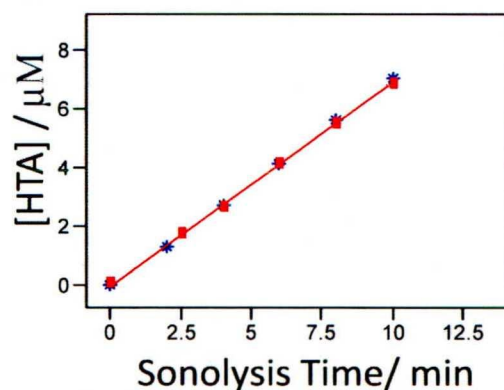


Figure A2.1 Duplicate and separate zero order ultrasonic HTA formation reactions of in aqueous solution (1mM, 300ml) exposed to continuous ultrasound ($f = 616$ kHz; $P = 27W$; $k_{\text{weighted}} = 0.695\text{mM min}^{-1}$; $R^2_{\text{Adj}} = 0.998$; $N_{\text{TOT}} = 12$; $t_{\text{sonolysis}} = 10$ min).

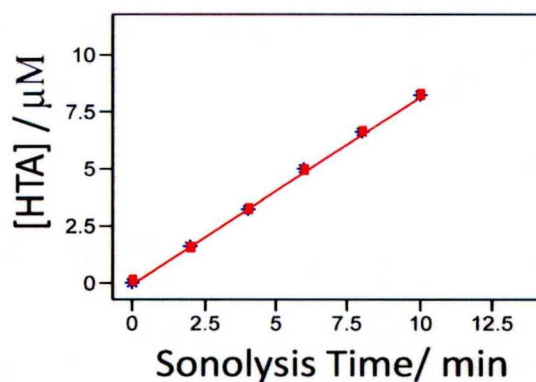


Figure A2.2 Duplicate and separate zero order ultrasonic HTA formation reactions of in aqueous solution (1mM, 300ml) exposed to pulsed wave (30ms lengths and 30ms intervals) ultrasound ($f = 616$ kHz; $P = 27W$; $k_{\text{weighted}} = 0.823$ mM min⁻¹; $R^2_{\text{Adj}} = 0.9996$; $N_{\text{TOT}} = 12$; $t_{\text{sonolysis}} = 10$ min).

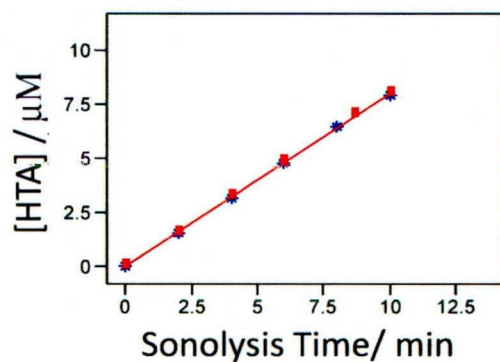


Figure A2.3 Duplicate and separate zero order ultrasonic HTA formation reactions of in aqueous solution (1mM, 300ml) exposed to pulsed wave (30ms lengths and 60ms intervals) ultrasound ($f = 616$ kHz; $P = 27W$; $k_{\text{weighted}} = 0.803$ mM min⁻¹; $R^2_{\text{Adj}} = 0.9996$; $N_{\text{TOT}} = 12$; $t_{\text{sonolysis}} = 10$ min).

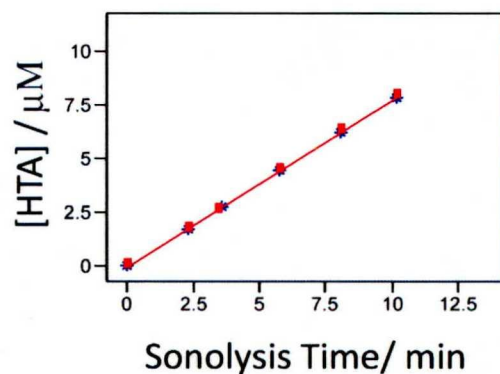


Figure A2.4 Duplicate and separate zero order ultrasonic HTA formation reactions of in aqueous solution (1mM, 300ml) exposed to pulsed wave (30ms lengths and 100ms intervals) ultrasound ($f = 616$ kHz; $P = 27W$; $k_{\text{weighted}} = 0.776$ mM min⁻¹; $R^2_{\text{Adj}} = 0.9997$; $N_{\text{TOT}} = 12$; $t_{\text{sonolysis}} = 10$ min).

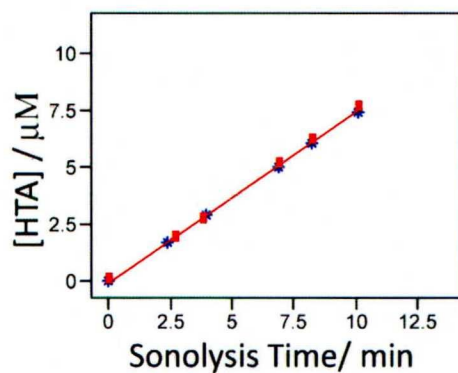


Figure A2.5 Duplicate and separate zero order ultrasonic HTA formation reactions of in aqueous solution (1mM, 300ml) exposed to pulsed wave (30ms lengths and 160ms intervals) ultrasound ($f = 616$ kHz; $P = 27W$; $k_{\text{weighted}} = 0.747$ mM min⁻¹; $R^2_{\text{Adj}} = 0.9992$; $N_{\text{TOT}} = 12$; $t_{\text{sonolysis}} = 10$ min).

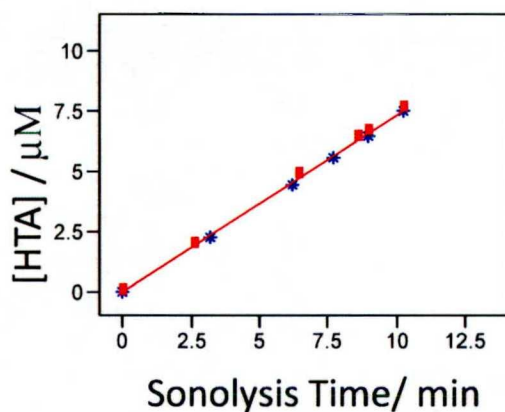


Figure A2.6 Duplicate and separate zero order ultrasonic HTA formation reactions of in aqueous solution (1mM, 300ml) exposed to pulsed wave (30ms lengths and 320ms intervals) ultrasound ($f = 616$ kHz; $P = 27W$; $k_{\text{weighted}} = 0.729$ mM min⁻¹; $R^2_{\text{Adj}} = 0.9995$; $N_{\text{TOT}} = 12$; $t_{\text{sonolysis}} = 10$ min).

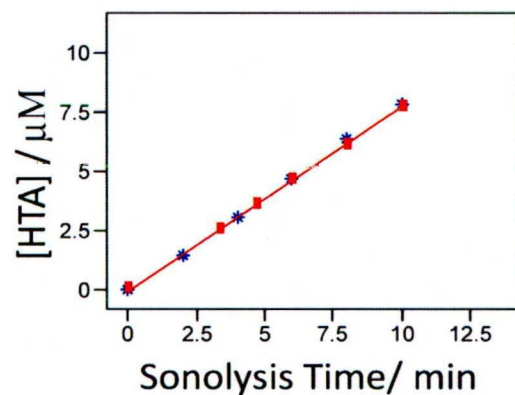


Figure A2.7 Duplicate and separate zero order ultrasonic HTA formation reactions of in aqueous solution (1mM, 300ml) exposed to pulsed wave (60ms lengths and 30ms intervals) ultrasound ($f = 616$ kHz; $P = 27W$; $k_{\text{weighted}} = 0.780$ mM min⁻¹; $R^2_{\text{Adj}} = 0.9990$; $N_{\text{TOT}} = 12$; $t_{\text{sonolysis}} = 10$ min).

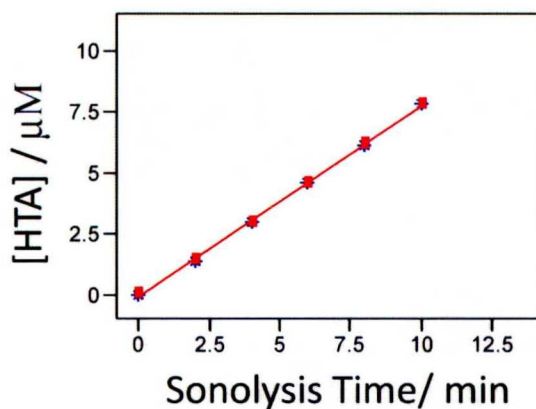


Figure A2.8 Duplicate and separate zero order ultrasonic HTA formation reactions of in aqueous solution (1mM, 300ml) exposed to pulsed wave (60ms lengths and 60ms intervals) ultrasound ($f = 616$ kHz; $P = 27W$; $k_{\text{weighted}} = 0.783$ mM min⁻¹; $R^2_{\text{Adj}} = 0.9993$; $N_{\text{TOT}} = 12$; $t_{\text{sonolysis}} = 10$ min).

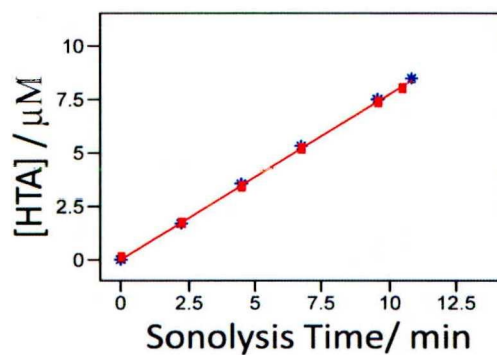


Figure A2.9 Duplicate and separate zero order ultrasonic HTA formation reactions of in aqueous solution (1mM, 300ml) exposed to pulsed wave (60ms lengths and 100ms intervals) ultrasound ($f = 616$ kHz; $P = 27W$; $k_{\text{weighted}} = 0.771$ mM min⁻¹; $R^2_{\text{Adj}} = 0.9995$; $N_{\text{TOT}} = 12$; $t_{\text{sonolysis}} = 10$ min).

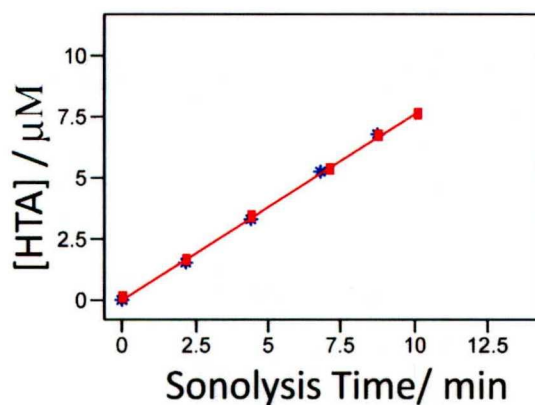


Figure A2.10 Duplicate and separate zero order ultrasonic HTA formation reactions of in aqueous solution (1mM, 300ml) exposed to pulsed wave (60ms lengths and 160ms intervals) ultrasound ($f = 616$ kHz; $P = 27W$; $k_{\text{weighted}} = 0.762$ mM min⁻¹; $R^2_{\text{Adj}} = 0.9992$; $N_{\text{TOT}} = 11$; $t_{\text{sonolysis}} = 10$ min).

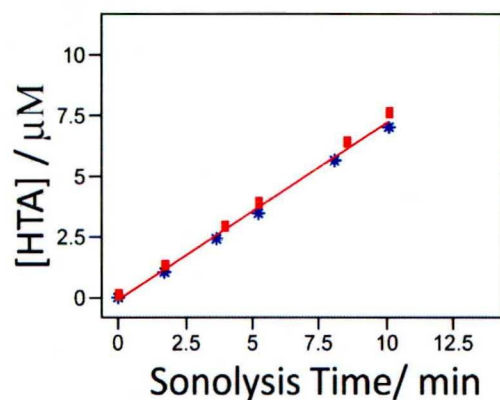


Figure A2.11 Duplicate and separate zero order ultrasonic HTA formation reactions of in aqueous solution (1mM, 300ml) exposed to pulsed wave (60ms lengths and 320ms intervals) ultrasound ($f = 616$ kHz; $P = 27W$; $k_{\text{weighted}} = 0.726$ mM min⁻¹; $R^2_{\text{Adj}} = 0.998$; $N_{\text{TOT}} = 12$; $t_{\text{sonolysis}} = 10$ min).

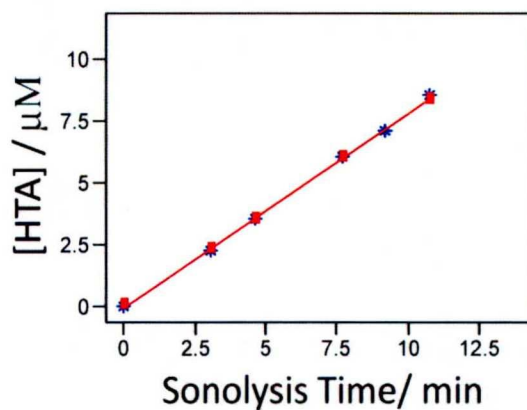


Figure A2.12 Duplicate and separate zero order ultrasonic HTA formation reactions of in aqueous solution (1mM, 300ml) exposed to pulsed wave (100ms lengths and 30ms intervals) ultrasound ($f = 616$ kHz; $P = 27W$; $k_{\text{weighted}} = 0.786$ mM min⁻¹; $R^2_{\text{Adj}} = 0.9990$; $N_{\text{TOT}} = 11$; $t_{\text{sonolysis}} = 10$ min).

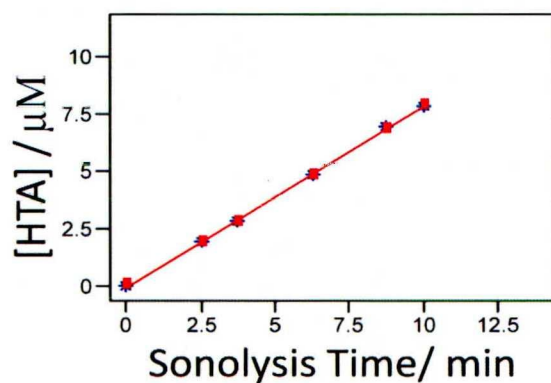


Figure A2.13 Duplicate and separate zero order ultrasonic HTA formation reactions of in aqueous solution (1mM, 300ml) exposed to pulsed wave (100ms lengths and 60ms intervals) ultrasound ($f = 616$ kHz; $P = 27$ W; $k_{\text{weighted}} = 0.790$ mM min⁻¹; $R^2_{\text{Adj}} = 0.9992$; $N_{\text{TOT}} = 12$; $t_{\text{sonolysis}} = 10$ min).

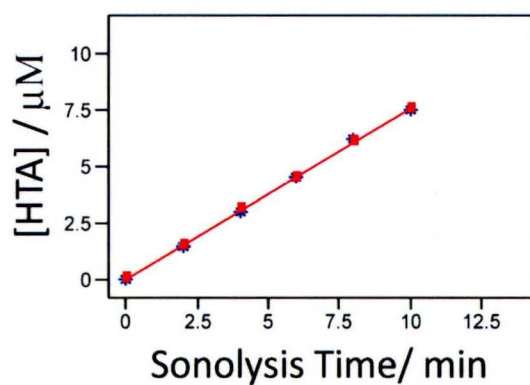


Figure A2.14 Duplicate and separate zero order ultrasonic HTA formation reactions of in aqueous solution (1mM, 300ml) exposed to pulsed wave (100ms lengths and 100ms intervals) ultrasound ($f = 616$ kHz; $P = 27$ W; $k_{\text{weighted}} = 0.759$ mM min⁻¹; $R^2_{\text{Adj}} = 0.9993$; $N_{\text{TOT}} = 12$; $t_{\text{sonolysis}} = 10$ min).

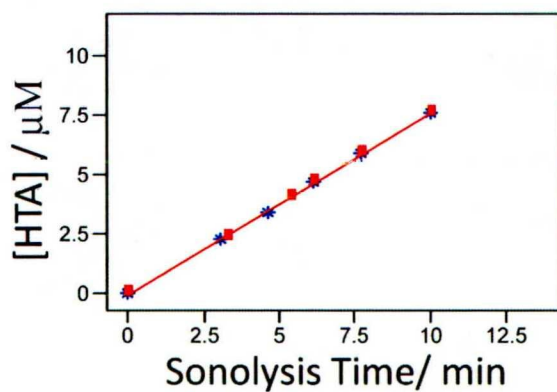


Figure A2.15 Duplicate and separate zero order ultrasonic HTA formation reactions of in aqueous solution (1mM, 300ml) exposed to pulsed wave (100ms lengths and 160ms intervals) ultrasound ($f = 616$ kHz; $P = 27$ W; $k_{\text{weighted}} = 0.765$ mM min⁻¹; $R^2_{\text{Adj}} = 0.9993$; $N_{\text{TOT}} = 12$; $t_{\text{sonolysis}} = 10$ min).

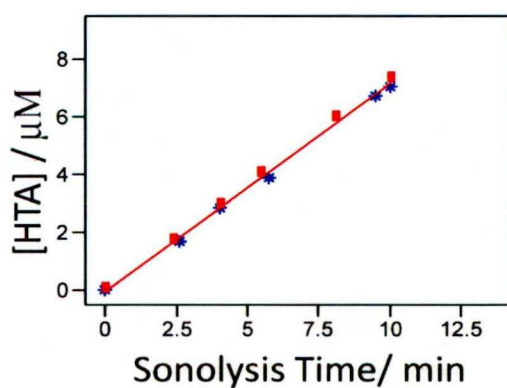


Figure A2.16 Duplicate and separate zero order ultrasonic HTA formation reactions of in aqueous solution (1mM, 300ml) exposed to pulsed wave (100ms lengths and 320ms intervals) ultrasound ($f = 616$ kHz; $P = 27$ W; $k_{\text{weighted}} = 0.722$ mM min⁻¹; $R^2_{\text{Adj}} = 0.9991$; $N_{\text{TOT}} = 12$; $t_{\text{sonolysis}} = 10$ min).

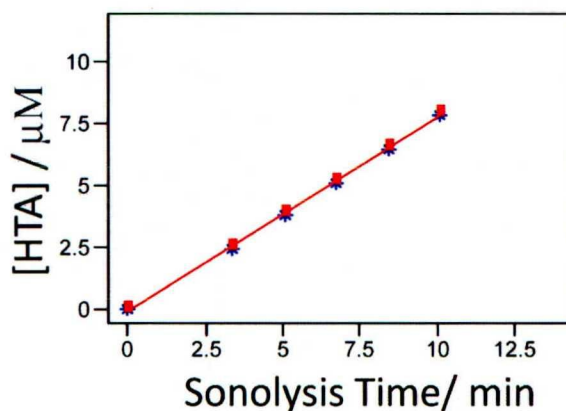


Figure A2.17 Duplicate and separate zero order ultrasonic HTA formation reactions of in aqueous solution (1mM, 300ml) exposed to pulsed wave (160ms lengths and 30ms intervals) ultrasound ($f = 616$ kHz; $P = 27W$; $k_{\text{weighted}} = 0.779$ mM min⁻¹; $R^2_{\text{Adj}} = 0.9992$; $N_{\text{TOT}} = 12$; $t_{\text{sonolysis}} = 10$ min).

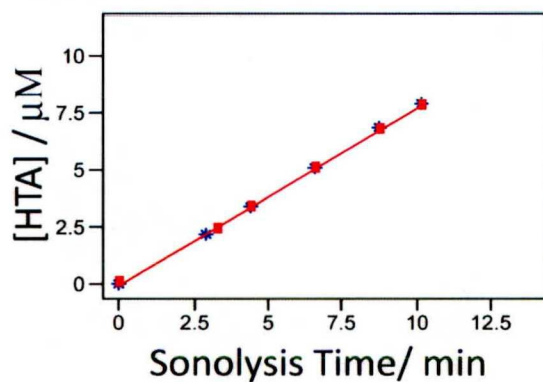


Figure A2.18 Duplicate and separate zero order ultrasonic HTA formation reactions of in aqueous solution (1mM, 300ml) exposed to pulsed wave (160ms lengths and 60ms intervals) ultrasound ($f = 616$ kHz; $P = 27W$; $k_{\text{weighted}} = 0.774$ mM min⁻¹; $R^2_{\text{Adj}} = 0.9994$; $N_{\text{TOT}} = 12$; $t_{\text{sonolysis}} = 10$ min).

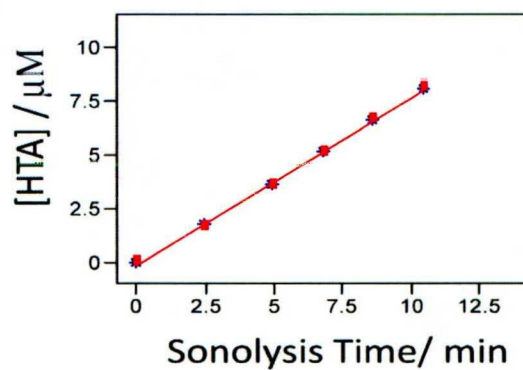


Figure A2.19 Duplicate and separate zero order ultrasonic HTA formation reactions of in aqueous solution (1mM, 300ml) exposed to pulsed wave (160ms lengths and 100ms intervals) ultrasound ($f = 616$ kHz; $P = 27$ W; $k_{\text{weighted}} = 0.776$ mM min⁻¹; $R^2_{\text{Adj}} = 0.998$; $N_{\text{TOT}} = 12$; $t_{\text{sonolysis}} = 10$ min).

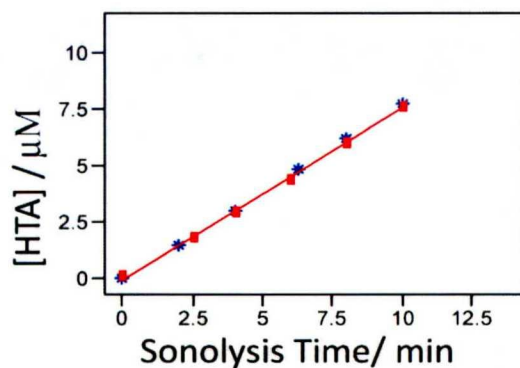


Figure A2.20 Duplicate and separate zero order ultrasonic HTA formation reactions of in aqueous solution (1mM, 300ml) exposed to pulsed wave (160ms lengths and 160ms intervals) ultrasound ($f = 616$ kHz; $P = 27$ W; $k_{\text{weighted}} = 0.767$ mM min⁻¹; $R^2_{\text{Adj}} = 0.998$; $N_{\text{TOT}} = 12$; $t_{\text{sonolysis}} = 10$ min).

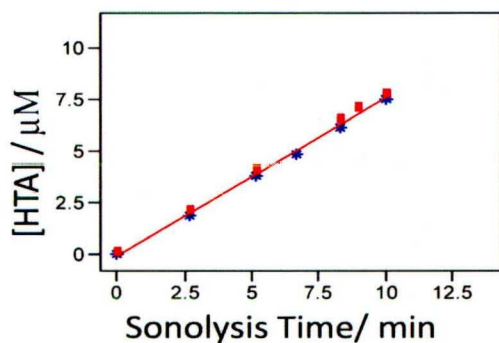


Figure A2.21 Duplicate and separate zero order ultrasonic HTA formation reactions of in aqueous solution (1mM, 300ml) exposed to pulsed wave (160ms lengths and 320ms intervals) ultrasound ($f = 616$ kHz; $P = 27W$; $k_{\text{weighted}} = 0.763$ mM min⁻¹; $R^2_{\text{Adj}} = 0.999$; $N_{\text{TOT}} = 12$; $t_{\text{sonolysis}} = 10$ min).

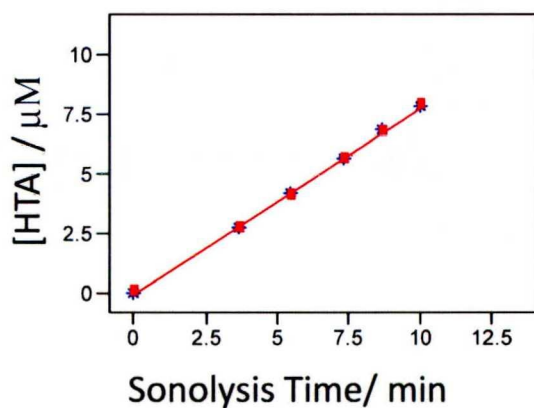


Figure A2.22 Duplicate and separate zero order ultrasonic HTA formation reactions of in aqueous solution (1mM, 300ml) exposed to pulsed wave (320ms lengths and 30ms intervals) ultrasound ($f = 616$ kHz; $P = 27W$; $k_{\text{weighted}} = 0.781$ mM min⁻¹; $R^2_{\text{Adj}} = 0.9990$; $N_{\text{TOT}} = 12$; $t_{\text{sonolysis}} = 10$ min).

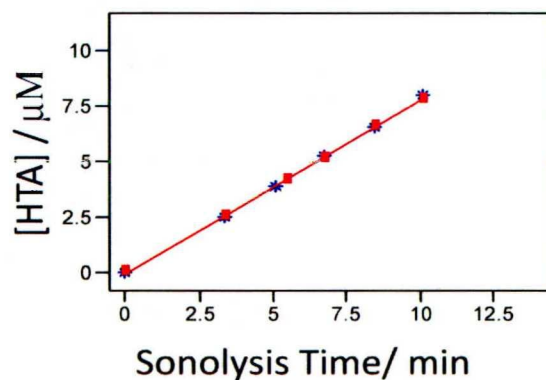


Figure A2.23 Duplicate and separate zero order ultrasonic HTA formation reactions of in aqueous solution (1mM, 300ml) exposed to pulsed wave (320ms lengths and 60ms intervals) ultrasound ($f = 616$ kHz; $P = 27W$; $k_{\text{weighted}} = 0.780$ mM min⁻¹; $R^2_{\text{Adj}} = 0.9992$; $N_{\text{TOT}} = 12$; $t_{\text{sonolysis}} = 10$ min).

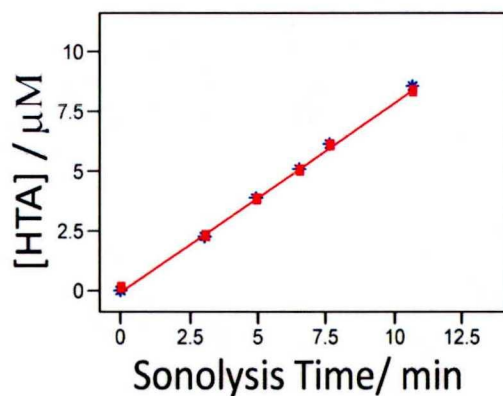


Figure A2.24 Duplicate and separate zero order ultrasonic HTA formation reactions of in aqueous solution (1mM, 300ml) exposed to pulsed wave (320ms lengths and 100ms intervals) ultrasound ($f = 616$ kHz; $P = 27W$; $k_{\text{weighted}} = 0.794$ mM min⁻¹; $R^2_{\text{Adj}} = 0.998$; $N_{\text{TOT}} = 12$; $t_{\text{sonolysis}} = 10$ min).

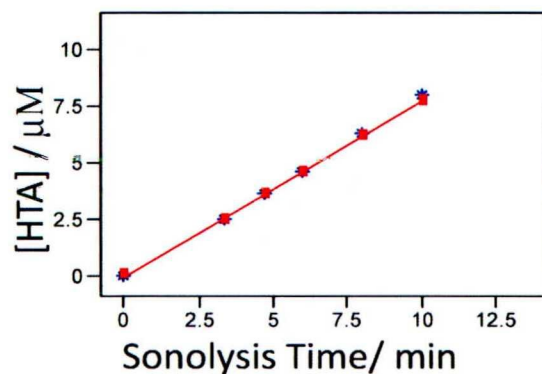


Figure A2.25 Duplicate and separate zero order ultrasonic HTA formation reactions of in aqueous solution (1mM, 300ml) exposed to pulsed wave (320ms lengths and 160ms intervals) ultrasound ($f = 616$ kHz; $P = 27$ W; $k_{\text{weighted}} = 0.781$ mM min⁻¹; $R^2_{\text{Adj}} = 0.998$; $N_{\text{TOT}} = 12$; $t_{\text{sonolysis}} = 10$ min).

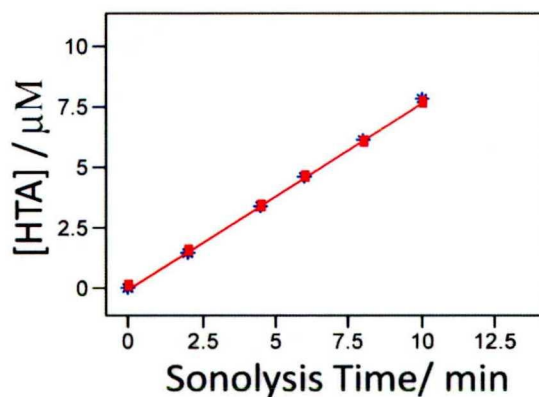


Figure A2.26 Duplicate and separate zero order ultrasonic HTA formation reactions of in aqueous solution (1mM, 300ml) exposed to pulsed wave (320ms lengths and 320ms intervals) ultrasound ($f = 616$ kHz; $P = 27$ W; $k_{\text{weighted}} = 0.770$ mM min⁻¹; $R^2_{\text{Adj}} = 0.9992$; $N_{\text{TOT}} = 12$; $t_{\text{sonolysis}} = 10$ min).

APPENDIX B

205 kHz

OBS AND HTA KINETIC RATE PLOTS

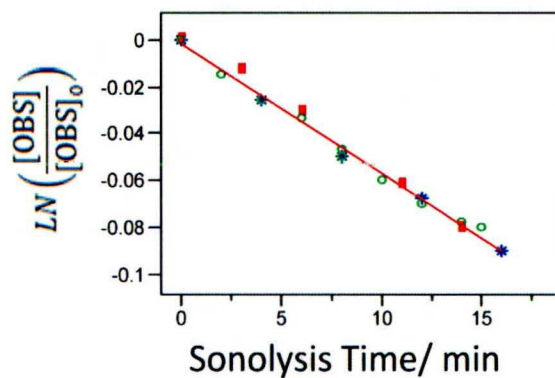


Figure B1.1 Duplicate and separate first order ultrasonic degradation of OBS in aqueous solution (1mM, 300ml) exposed to continuous ultrasound ($f = 205$ kHz; $P = 27W$; $k_{\text{weighted}} = 5.5 \times 10^{-3} \text{ min}^{-1}$; $R^2_{\text{Adj}} = 0.992$; $N_{\text{TOT}} = 20$; $t_{\text{sonolysis}} = 16$ min).

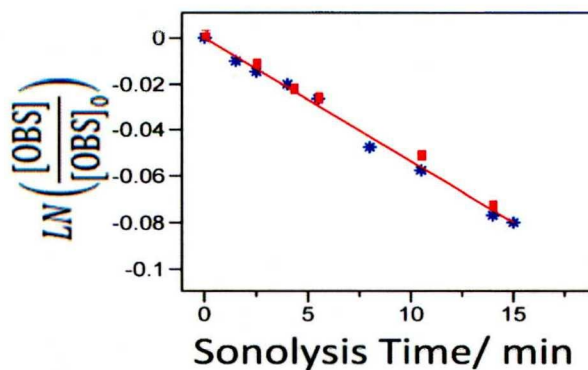


Figure B1.2 Duplicate and separate first order ultrasonic degradation of OBS in aqueous solution (1mM, 300ml) exposed to pulsed wave (30ms lengths and 30ms intervals) ultrasound ($f = 205$ kHz; $P = 27W$; $k_{\text{weighted}} = 5.3 \times 10^{-3} \text{ min}^{-1}$; $R^2_{\text{Adj}} = 0.994$; $N_{\text{TOT}} = 15$; $t_{\text{sonolysis}} = 15$ min).

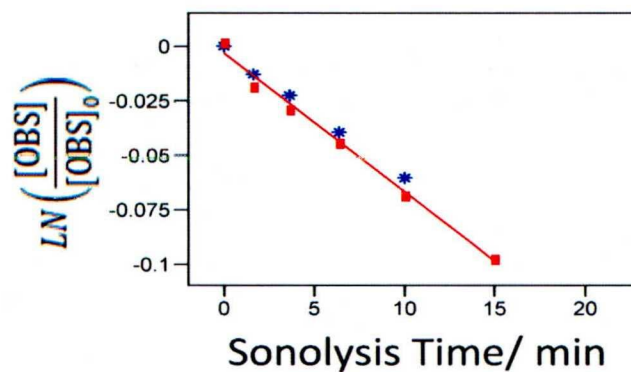


Figure B1.3 Duplicate and separate first order ultrasonic degradation of OBS in aqueous solution (1mM, 300ml) exposed to pulsed wave (30ms lengths and 60ms intervals) ultrasound ($f = 205$ kHz; $P = 27$ W; $k_{\text{weighted}} = 6.2 \times 10^{-3} \text{ min}^{-1}$; $R^2_{\text{Adj}} = 0.991$; $N_{\text{TOT}} = 11$; $t_{\text{sonolysis}} = 15$ min).

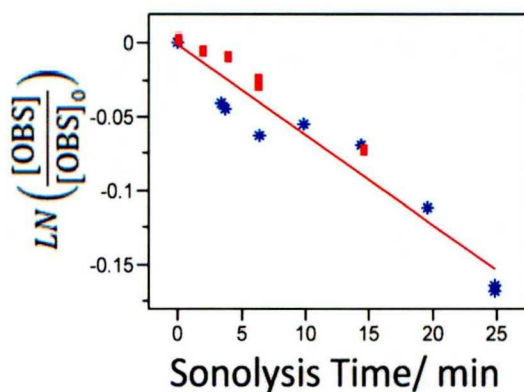


Figure B1.4 Duplicate and separate first order ultrasonic degradation of OBS in aqueous solution (1mM, 300ml) exposed to pulsed wave (30ms lengths and 100ms intervals) ultrasound ($f = 205$ kHz; $P = 27$ W; $k_{\text{weighted}} = 5.7 \times 10^{-3} \text{ min}^{-1}$; $R^2_{\text{Adj}} = 0.945$; $N_{\text{TOT}} = 15$; $t_{\text{sonolysis}} = 25$ min).

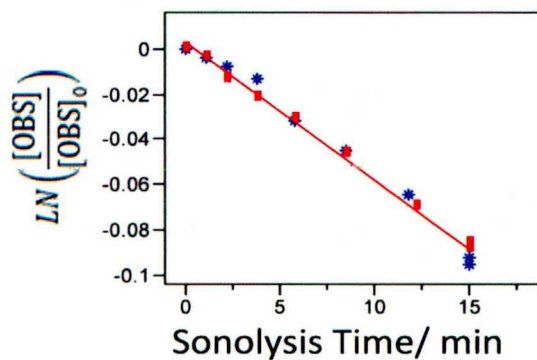


Figure B1.5 Duplicate and separate first order ultrasonic degradation of OBS in aqueous solution (1mM, 300ml) exposed to pulsed wave (30ms lengths and 160ms intervals) ultrasound ($f = 205$ kHz; $P = 27W$; $k_{\text{weighted}} = 6.1 \times 10^{-3} \text{ min}^{-1}$; $R^2_{\text{Adj}} = 0.989$; $N_{\text{TOT}} = 18$; $t_{\text{sonolysis}} = 15$ min).

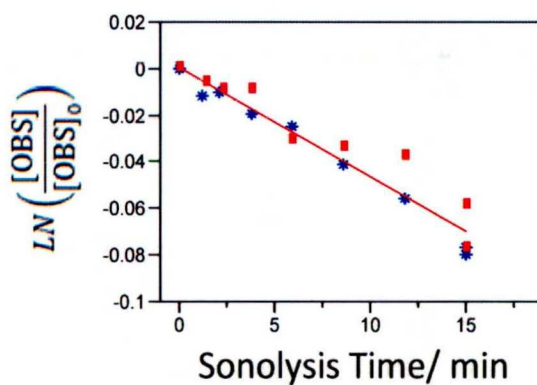


Figure B1.6 Duplicate and separate first order ultrasonic degradation of OBS in aqueous solution (1mM, 300ml) exposed to pulsed wave (30ms lengths and 320ms intervals) ultrasound ($f = 205$ kHz; $P = 27W$; $k_{\text{weighted}} = 4.7 \times 10^{-3} \text{ min}^{-1}$; $R^2_{\text{Adj}} = 0.946$; $N_{\text{TOT}} = 18$; $t_{\text{sonolysis}} = 15$ min).

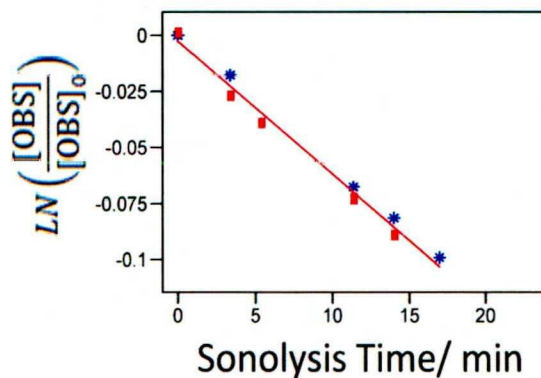


Figure B1.7 Duplicate and separate first order ultrasonic degradation of OBS in aqueous solution (1mM, 300ml) exposed to pulsed wave (60ms lengths and 30ms intervals) ultrasound ($f = 205$ kHz; $P = 27$ W; $k_{\text{weighted}} = 6.0 \times 10^{-3} \text{ min}^{-1}$; $R^2_{\text{Adj}} = 0.994$; $N_{\text{TOT}} = 10$; $t_{\text{sonolysis}} = 17$ min).

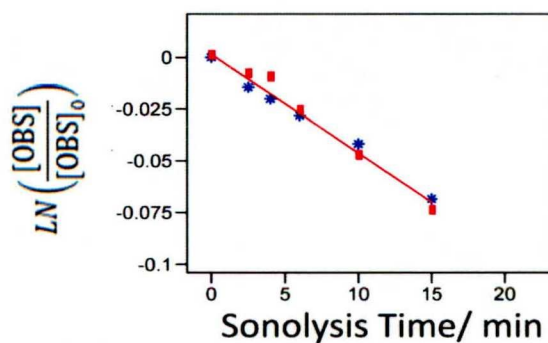


Figure B1.8 Duplicate and separate first order ultrasonic degradation of OBS in aqueous solution (1mM, 300ml) exposed to pulsed wave (60ms lengths and 60ms intervals) ultrasound ($f = 205$ kHz; $P = 27$ W; $k_{\text{weighted}} = 4.8 \times 10^{-3} \text{ min}^{-1}$; $R^2_{\text{Adj}} = 0.976$; $N_{\text{TOT}} = 12$; $t_{\text{sonolysis}} = 15$ min).

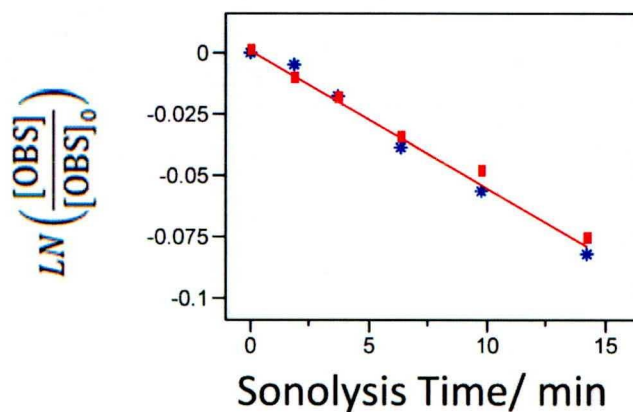


Figure B1.9 Duplicate and separate first order ultrasonic degradation of OBS in aqueous solution (1mM, 300ml) exposed to pulsed wave (60ms lengths and 100ms intervals) ultrasound ($f = 205$ kHz; $P = 27W$; $k_{\text{weighted}} = 5.6 \times 10^{-3} \text{ min}^{-1}$; $R^2_{\text{Adj}} = 0.988$; $N_{\text{TOT}} = 12$; $t_{\text{sonolysis}} = 15$ min).

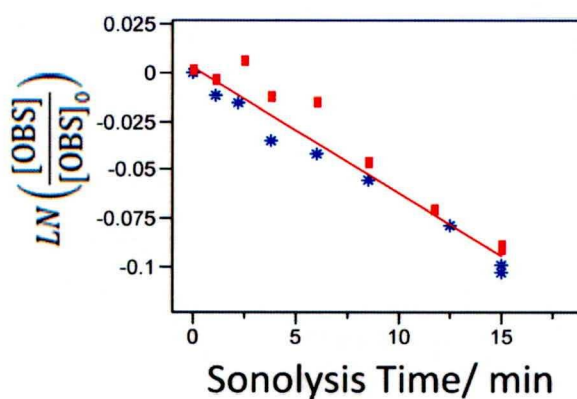


Figure B1.10 Duplicate and separate first order ultrasonic degradation of OBS in aqueous solution (1mM, 300ml) exposed to pulsed wave (60ms lengths and 160ms intervals) ultrasound ($f = 205$ kHz; $P = 27W$; $k_{\text{weighted}} = 6.5 \times 10^{-3} \text{ min}^{-1}$; $R^2_{\text{Adj}} = 0.972$; $N_{\text{TOT}} = 18$; $t_{\text{sonolysis}} = 15$ min).

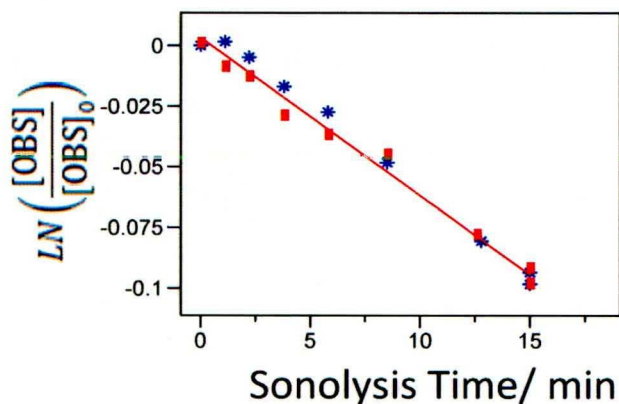


Figure B1.11 Duplicate and separate first order ultrasonic degradation of OBS in aqueous solution (1mM, 300ml) exposed to pulsed wave (60ms lengths and 320ms intervals) ultrasound ($f = 205$ kHz; $P = 27W$; $k_{\text{weighted}} = 6.5 \times 10^{-3} \text{ min}^{-1}$; $R^2_{\text{Adj}} = 0.986$; $N_{\text{TOT}} = 18$; $t_{\text{sonolysis}} = 15$ min).

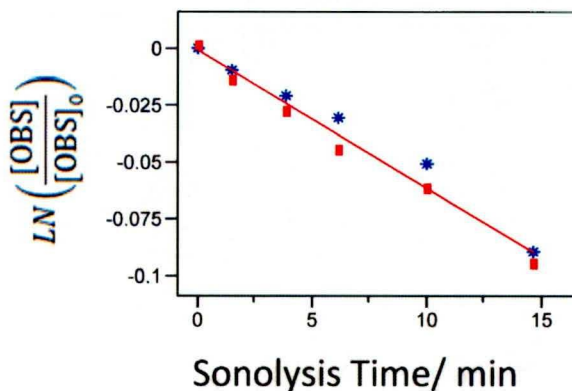


Figure B1.12 Duplicate and separate first order ultrasonic degradation of OBS in aqueous solution (1mM, 300ml) exposed to pulsed wave (100ms lengths and 30ms intervals) ultrasound ($f = 205$ kHz; $P = 27W$; $k_{\text{weighted}} = 6.1 \times 10^{-3} \text{ min}^{-1}$; $R^2_{\text{Adj}} = 0.983$; $N_{\text{TOT}} = 12$; $t_{\text{sonolysis}} = 15$ min).

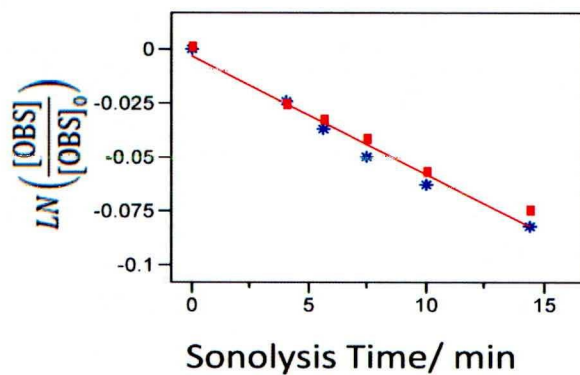


Figure B1.13 Duplicate and separate first order ultrasonic degradation of OBS in aqueous solution (1mM, 300ml) exposed to pulsed wave (100ms lengths and 60ms intervals) ultrasound ($f = 205$ kHz; $P = 27W$; $k_{\text{weighted}} = 5.5 \times 10^{-3} \text{ min}^{-1}$; $R^2_{\text{Adj}} = 0.984$; $N_{\text{TOT}} = 12$; $t_{\text{sonolysis}} = 15$ min).

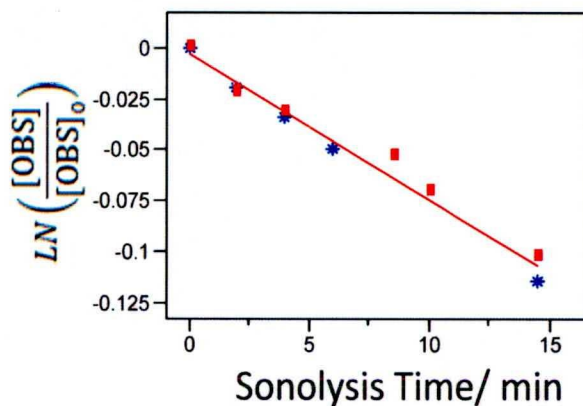


Figure B1.14 Duplicate and separate first order ultrasonic degradation of OBS in aqueous solution (1mM, 300ml) exposed to pulsed wave (100ms lengths and 100ms intervals) ultrasound ($f = 205$ kHz; $P = 27W$; $k_{\text{weighted}} = 7.2 \times 10^{-3} \text{ min}^{-1}$; $R^2_{\text{Adj}} = 0.984$; $N_{\text{TOT}} = 11$; $t_{\text{sonolysis}} = 15$ min).

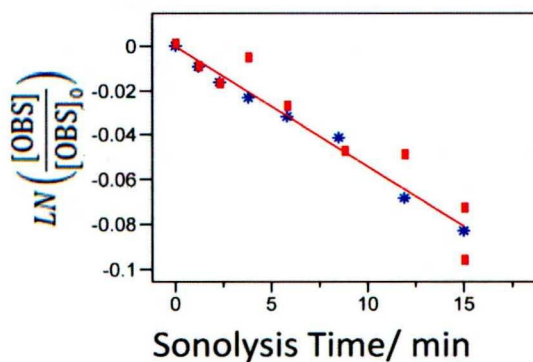


Figure B1.15 Duplicate and separate first order ultrasonic degradation of OBS in aqueous solution (1mM, 300ml) exposed to pulsed wave (100ms lengths and 160ms intervals) ultrasound ($f = 205$ kHz; $P = 27W$; $k_{\text{weighted}} = 5.4 \times 10^{-3} \text{ min}^{-1}$; $R^2_{\text{Adj}} = 0.943$; $N_{\text{TOT}} = 17$; $t_{\text{sonolysis}} = 15 \text{ min}$).

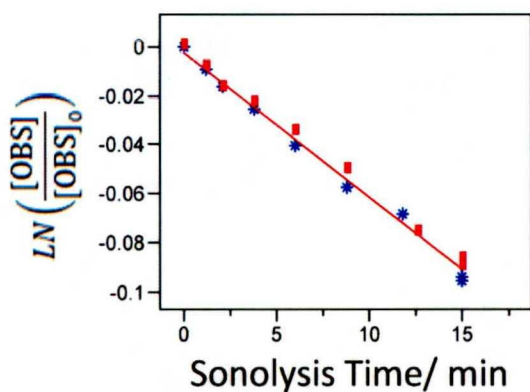


Figure B1.16 Duplicate and separate first order ultrasonic degradation of OBS in aqueous solution (1mM, 300ml) exposed to pulsed wave (100ms lengths and 320ms intervals) ultrasound ($f = 205$ kHz; $P = 27W$; $k_{\text{weighted}} = 5.9 \times 10^{-3} \text{ min}^{-1}$; $R^2_{\text{Adj}} = 0.995$; $N_{\text{TOT}} = 20$; $t_{\text{sonolysis}} = 15 \text{ min}$).

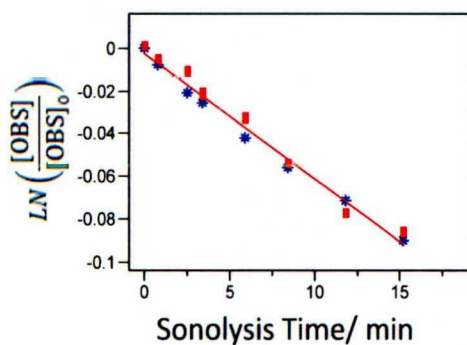


Figure B1.17 Duplicate and separate first order ultrasonic degradation of OBS in aqueous solution (1mM, 300ml) exposed to pulsed wave (160ms lengths and 30ms intervals) ultrasound ($f = 205$ kHz; $P = 27W$; $k_{\text{weighted}} = 5.9 \times 10^{-3} \text{ min}^{-1}$; $R^2_{\text{Adj}} = 0.987$; $N_{\text{TOT}} = 19$; $t_{\text{sonolysis}} = 15$ min).

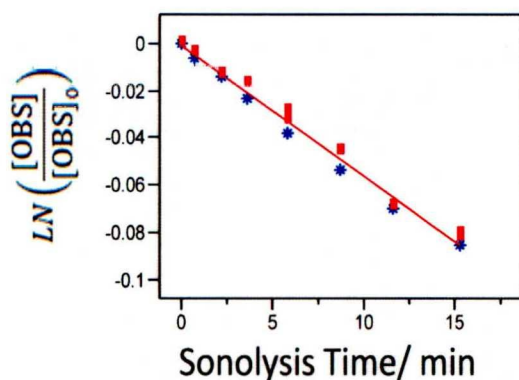


Figure B1.18 Duplicate and separate first order ultrasonic degradation of OBS in aqueous solution (1mM, 300ml) exposed to pulsed wave (160ms lengths and 60ms intervals) ultrasound ($f = 205$ kHz; $P = 27W$; $k_{\text{weighted}} = 5.5 \times 10^{-3} \text{ min}^{-1}$; $R^2_{\text{Adj}} = 0.993$; $N_{\text{TOT}} = 18$; $t_{\text{sonolysis}} = 15$ min).

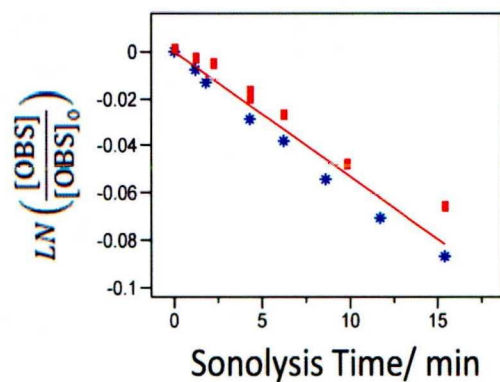


Figure B1.19 Duplicate and separate first order ultrasonic degradation of OBS in aqueous solution (1mM, 300ml) exposed to pulsed wave (160ms lengths and 100ms intervals) ultrasound ($f = 205$ kHz; $P = 27W$; $k_{\text{weighted}} = 5.2 \times 10^{-3} \text{ min}^{-1}$; $R^2_{\text{Adj}} = 0.979$; $N_{\text{TOT}} = 16$; $t_{\text{sonolysis}} = 15 \text{ min}$).

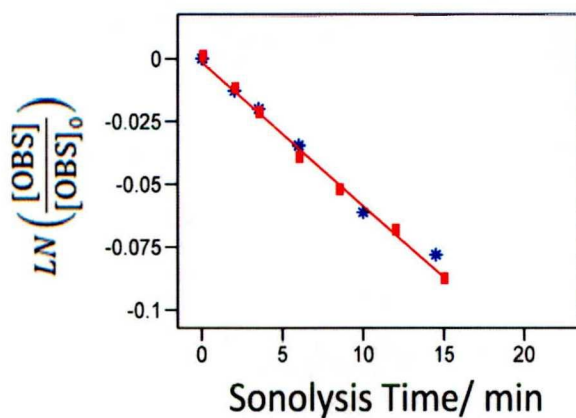


Figure B1.20 Duplicate and separate first order ultrasonic degradation of OBS in aqueous solution (1mM, 300ml) exposed to pulsed wave (160ms lengths and 160ms intervals) ultrasound ($f = 205$ kHz; $P = 27W$; $k_{\text{weighted}} = 5.7 \times 10^{-3} \text{ min}^{-1}$; $R^2_{\text{Adj}} = 0.992$; $N_{\text{TOT}} = 13$; $t_{\text{sonolysis}} = 15 \text{ min}$).

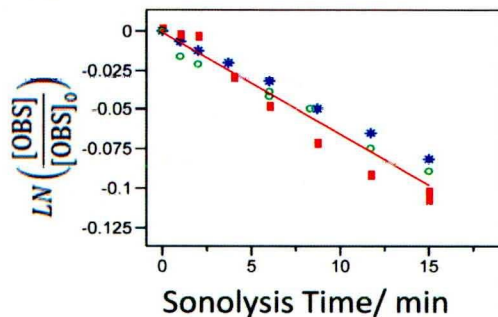


Figure B1.21 Triplicate and separate first order ultrasonic degradation of OBS in aqueous solution (1mM, 300ml) exposed to pulsed wave (160ms lengths and 320ms intervals) ultrasound ($f = 205$ kHz; $P = 27W$; $k_{\text{weighted}} = 6.3 \times 10^{-3} \text{ min}^{-1}$; $R^2_{\text{Adj}} = 0.958$; $N_{\text{TOT}} = 25$; $t_{\text{sonolysis}} = 15 \text{ min}$).

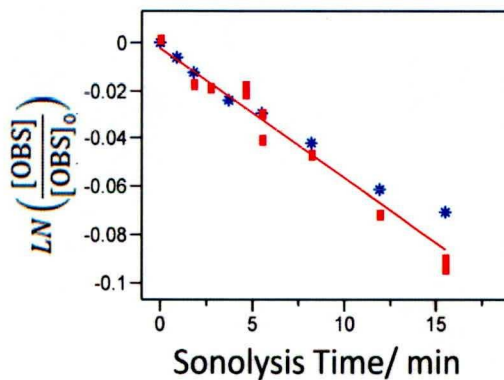


Figure B1.22 Duplicate and separate first order ultrasonic degradation of OBS in aqueous solution (1mM, 300ml) exposed to pulsed wave (320ms lengths and 30ms intervals) ultrasound ($f = 205$ kHz; $P = 27W$; $k_{\text{weighted}} = 5.3 \times 10^{-3} \text{ min}^{-1}$; $R^2_{\text{Adj}} = 0.960$; $N_{\text{TOT}} = 19$; $t_{\text{sonolysis}} = 15 \text{ min}$).

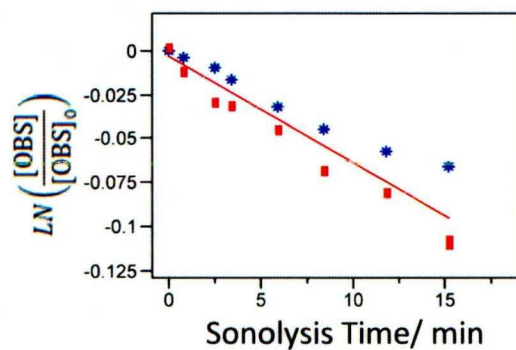


Figure B1.23 Duplicate and separate first order ultrasonic degradation of OBS in aqueous solution (1mM, 300ml) exposed to pulsed wave (320ms lengths and 60ms intervals) ultrasound ($f = 205$ kHz; $P = 27W$; $k_{\text{weighted}} = 5.8 \times 10^{-3} \text{ min}^{-1}$; $R^2_{\text{Adj}} = 0.954$; $N_{\text{TOT}} = 17$; $t_{\text{sonolysis}} = 15$ min).

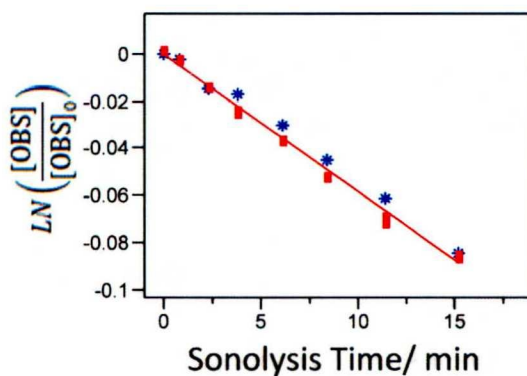


Figure B1.24 Duplicate and separate first order ultrasonic degradation of OBS in aqueous solution (1mM, 300ml) exposed to pulsed wave (320ms lengths and 100ms intervals) ultrasound ($f = 205$ kHz; $P = 27W$; $k_{\text{weighted}} = 5.7 \times 10^{-3} \text{ min}^{-1}$; $R^2_{\text{Adj}} = 0.993$; $N_{\text{TOT}} = 19$; $t_{\text{sonolysis}} = 15$ min).

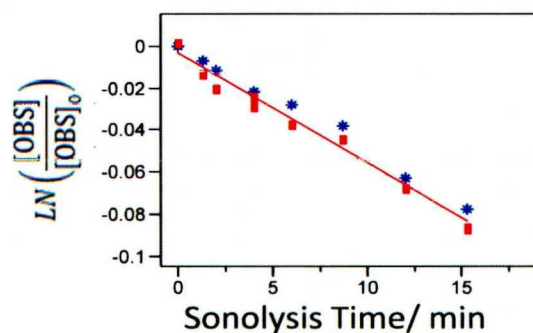


Figure B1.25 Duplicate and separate first order ultrasonic degradation of OBS in aqueous solution (1mM, 300ml) exposed to pulsed wave (320ms lengths and 160ms intervals) ultrasound ($f = 205$ kHz; $P = 27W$; $k_{\text{weighted}} = 5.2 \times 10^{-3} \text{ min}^{-1}$; $R^2_{\text{Adj}} = 0.985$; $N_{\text{TOT}} = 19$; $t_{\text{sonolysis}} = 15 \text{ min}$).

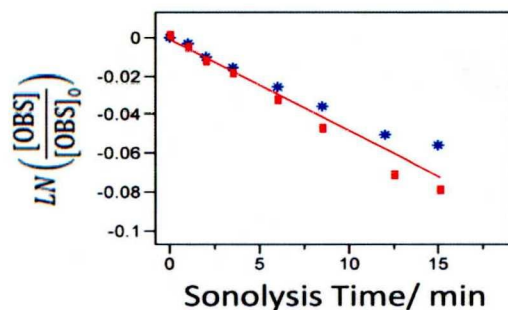


Figure B1.26 Duplicate and separate first order ultrasonic degradation of OBS in aqueous solution (1mM, 300ml) exposed to pulsed wave (320ms lengths and 320ms intervals) ultrasound ($f = 205$ kHz; $P = 27W$; $k_{\text{weighted}} = 4.6 \times 10^{-3} \text{ min}^{-1}$; $R^2_{\text{Adj}} = 0.963$; $N_{\text{TOT}} = 16$; $t_{\text{sonolysis}} = 15 \text{ min}$).

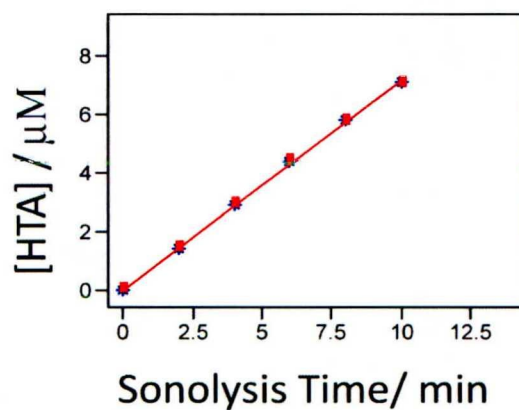


Figure B2.1 Duplicate and separate zero order ultrasonic HTA formation reactions of in aqueous solution (1mM, 300ml) exposed to continuous ultrasound ($f = 205$ kHz; $P = 27$ W; $k_{\text{weighted}} = 0.713$ mM min^{-1} ; $R^2_{\text{Adj}} = 0.9994$; $N_{\text{TOT}} = 12$; $t_{\text{sonolysis}} = 10$ min).

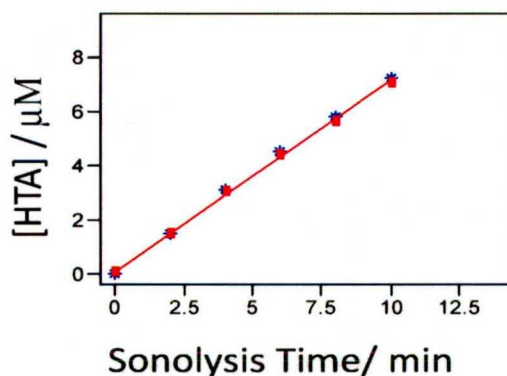


Figure B2.2 Duplicate and separate zero order ultrasonic HTA formation reactions of in aqueous solution (1mM, 300ml) exposed to pulsed wave (30ms lengths and 30ms intervals) ultrasound ($f = 205$ kHz; $P = 27$ W; $k_{\text{weighted}} = 0.709$ mM min^{-1} ; $R^2_{\text{Adj}} = 0.998$; $N_{\text{TOT}} = 12$; $t_{\text{sonolysis}} = 10$ min).

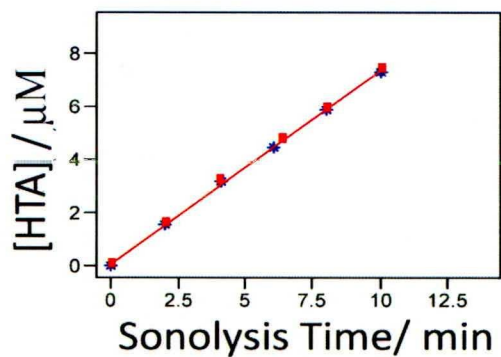


Figure B2.3 Duplicate and separate zero order ultrasonic HTA formation reactions of in aqueous solution (1mM, 300ml) exposed to pulsed wave (30ms lengths and 60ms intervals) ultrasound ($f = 205$ kHz; $P = 27\text{W}$; $k_{\text{weighted}} = 0.726 \text{ mM min}^{-1}$; $R^2_{\text{Adj}} = 0.998$; $N_{\text{TOT}} = 12$; $t_{\text{sonolysis}} = 10$ min).

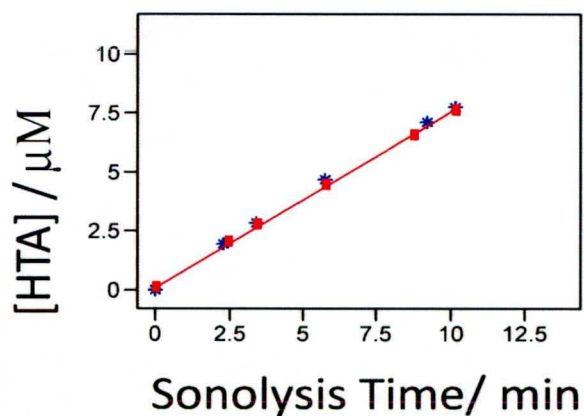


Figure B2.4 Duplicate and separate zero order ultrasonic HTA formation reactions of in aqueous solution (1mM, 300ml) exposed to pulsed wave (30ms lengths and 100ms intervals) ultrasound ($f = 205$ kHz; $P = 27\text{W}$; $k_{\text{weighted}} = 0.746 \text{ mM min}^{-1}$; $R^2_{\text{Adj}} = 0.998$; $N_{\text{TOT}} = 12$; $t_{\text{sonolysis}} = 10$ min).

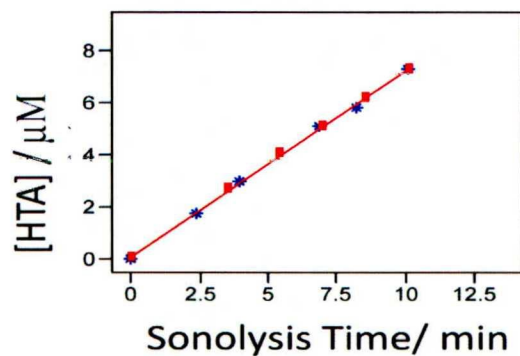


Figure B2.5 Duplicate and separate zero order ultrasonic HTA formation reactions of in aqueous solution (1mM, 300ml) exposed to pulsed wave (30ms lengths and 160ms intervals) ultrasound ($f = 205 \text{ kHz}$; $P = 27\text{W}$; $k_{\text{weighted}} = 0.712 \text{ mM min}^{-1}$; $R^2_{\text{Adj}} = 0.998$; $N_{\text{TOT}} = 12$; $t_{\text{sonolysis}} = 10 \text{ min}$).

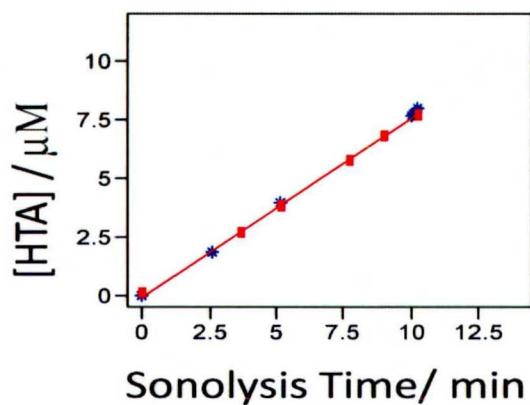


Figure B2.6 Duplicate and separate zero order ultrasonic HTA formation reactions of in aqueous solution (1mM, 300ml) exposed to pulsed wave (30ms lengths and 320ms intervals) ultrasound ($f = 205 \text{ kHz}$; $P = 27\text{W}$; $k_{\text{weighted}} = 0.759 \text{ mM min}^{-1}$; $R^2_{\text{Adj}} = 0.9990$; $N_{\text{TOT}} = 12$; $t_{\text{sonolysis}} = 10 \text{ min}$).

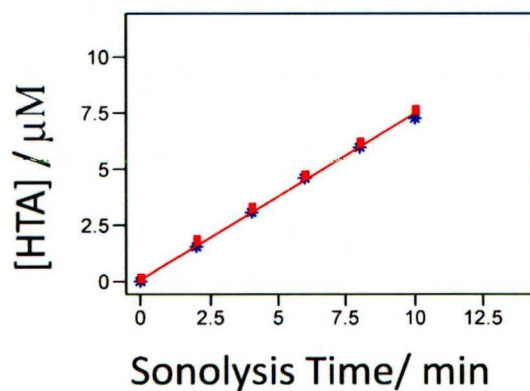


Figure B2.7 Duplicate and separate zero order ultrasonic HTA formation reactions of in aqueous solution (1mM, 300ml) exposed to pulsed wave (60ms lengths and 30ms intervals) ultrasound ($f = 205$ kHz; $P = 27$ W; $k_{\text{weighted}} = 0.737$ mM min⁻¹; $R^2_{\text{Adj}} = 0.998$; $N_{\text{TOT}} = 12$; $t_{\text{sonolysis}} = 10$ min).

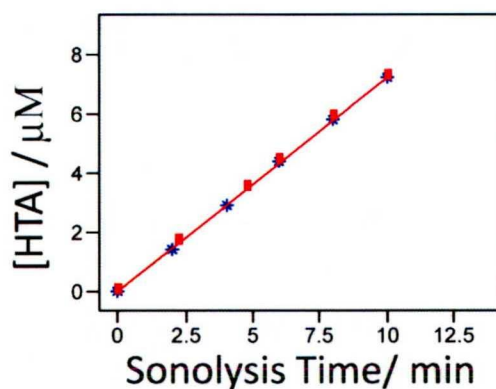


Figure B2.8 Duplicate and separate zero order ultrasonic HTA formation reactions of in aqueous solution (1mM, 300ml) exposed to pulsed wave (60ms lengths and 60ms intervals) ultrasound ($f = 205$ kHz; $P = 27$ W; $k_{\text{weighted}} = 0.722$ mM min⁻¹; $R^2_{\text{Adj}} = 0.9998$; $N_{\text{TOT}} = 12$; $t_{\text{sonolysis}} = 10$ min).

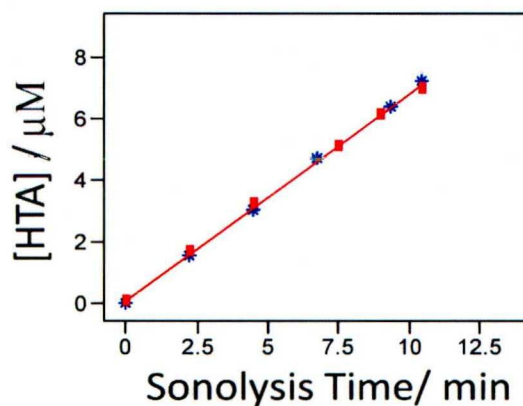


Figure B2.9 Duplicate and separate zero order ultrasonic HTA formation reactions of in aqueous solution (1mM, 300ml) exposed to pulsed wave (60ms lengths and 100ms intervals) ultrasound ($f = 205$ kHz; $P = 27W$; $k_{\text{weighted}} = 0.672$ mM min⁻¹; $R^2_{\text{Adj}} = 0.9998$; $N_{\text{TOT}} = 12$; $t_{\text{sonolysis}} = 10$ min).

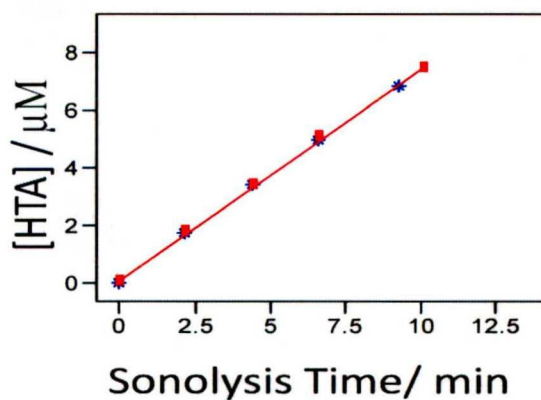


Figure B2.10 Duplicate and separate zero order ultrasonic HTA formation reactions of in aqueous solution (1mM, 300ml) exposed to pulsed wave (60ms lengths and 160ms intervals) ultrasound ($f = 205$ kHz; $P = 27W$; $k_{\text{weighted}} = 0.735$ mM min⁻¹; $R^2_{\text{Adj}} = 0.998$; $N_{\text{TOT}} = 10$; $t_{\text{sonolysis}} = 10$ min).

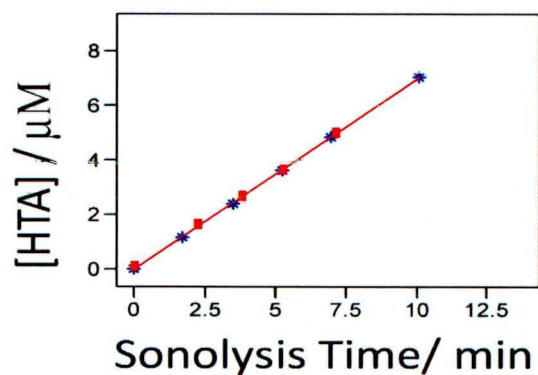


Figure B2.11 Duplicate and separate zero order ultrasonic HTA formation reactions of in aqueous solution (1mM, 300ml) exposed to pulsed wave (60ms lengths and 320ms intervals) ultrasound ($f = 205$ kHz; $P = 27$ W; $k_{\text{weighted}} = 0.695$ mM min⁻¹; $R^2_{\text{Adj}} = 0.9996$; $N_{\text{TOT}} = 11$; $t_{\text{sonolysis}} = 10$ min).

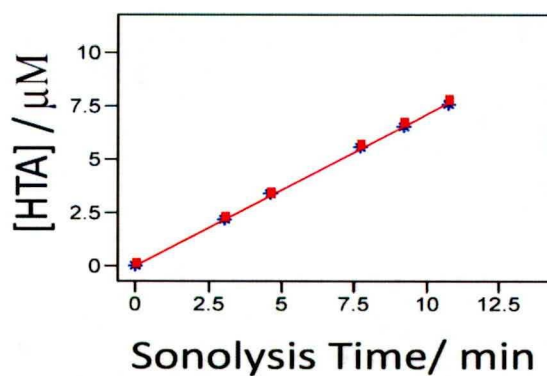


Figure B2.12 Duplicate and separate zero order ultrasonic HTA formation reactions of in aqueous solution (1mM, 300ml) exposed to pulsed wave (100ms lengths and 30ms intervals) ultrasound ($f = 205$ kHz; $P = 27$ W; $k_{\text{weighted}} = 0.711$ mM min⁻¹; $R^2_{\text{Adj}} = 0.9996$; $N_{\text{TOT}} = 12$; $t_{\text{sonolysis}} = 10$ min).

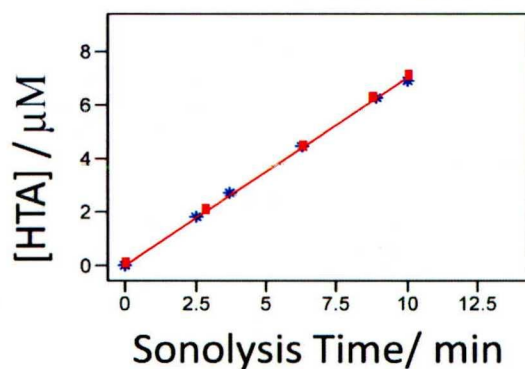


Figure B2.13 Duplicate and separate zero order ultrasonic HTA formation reactions of in aqueous solution (1mM, 300ml) exposed to pulsed wave (100ms lengths and 60ms intervals) ultrasound ($f = 205$ kHz; $P = 27$ W; $k_{\text{weighted}} = 0.699$ mM min⁻¹; $R^2_{\text{Adj}} = 0.9994$; $N_{\text{TOT}} = 11$; $t_{\text{sonolysis}} = 10$ min).

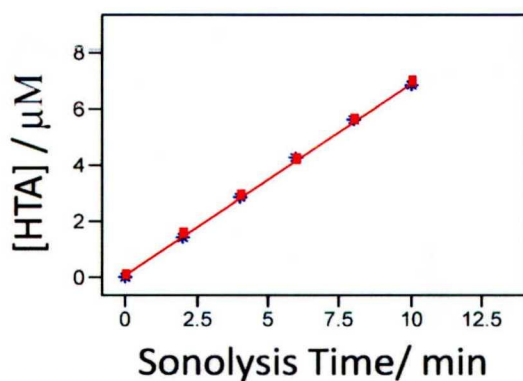


Figure B2.14 Duplicate and separate zero order ultrasonic HTA formation reactions of in aqueous solution (1mM, 300ml) exposed to pulsed wave (100ms lengths and 100ms intervals) ultrasound ($f = 205$ kHz; $P = 27$ W; $k_{\text{weighted}} = 0.6857$ mM min⁻¹; $R^2_{\text{Adj}} = 0.9994$; $N_{\text{TOT}} = 12$; $t_{\text{sonolysis}} = 10$ min).

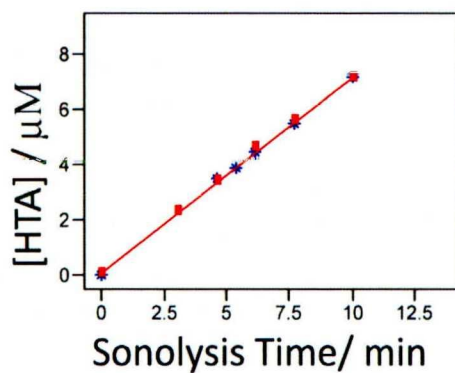


Figure B2.15 Duplicate and separate zero order ultrasonic HTA formation reactions of in aqueous solution (1mM, 300ml) exposed to pulsed wave (100ms lengths and 160ms intervals) ultrasound ($f = 205$ kHz; $P = 27W$; $k_{\text{weighted}} = 0.711 \text{ mM min}^{-1}$; $R^2_{\text{Adj}} = 0.998$; $N_{\text{TOT}} = 12$; $t_{\text{sonolysis}} = 10 \text{ min}$).

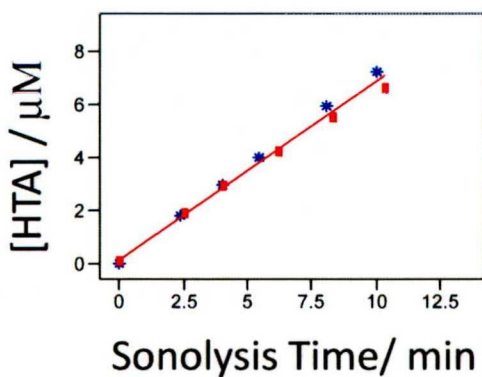


Figure B2.16 Duplicate and separate zero order ultrasonic HTA formation reactions of in aqueous solution (1mM, 300ml) exposed to pulsed wave (100ms lengths and 320ms intervals) ultrasound ($f = 205$ kHz; $P = 27W$; $k_{\text{weighted}} = 0.675 \text{ mM min}^{-1}$; $R^2_{\text{Adj}} = 0.993$; $N_{\text{TOT}} = 12$; $t_{\text{sonolysis}} = 10 \text{ min}$).

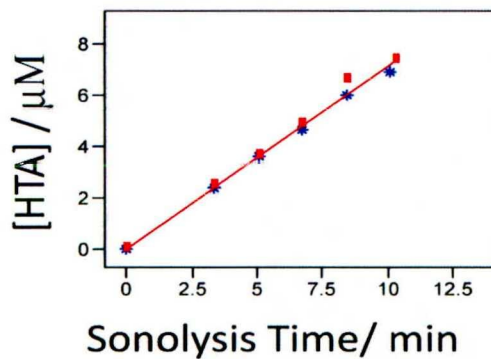


Figure B2.17 Duplicate and separate zero order ultrasonic HTA formation reactions of in aqueous solution (1mM, 300ml) exposed to pulsed wave (160ms lengths and 30ms intervals) ultrasound ($f = 205$ kHz; $P = 27W$; $k_{\text{weighted}} = 0.714$ mM min⁻¹; $R^2_{\text{Adj}} = 0.994$; $N_{\text{TOT}} = 12$; $t_{\text{sonolysis}} = 10$ min).

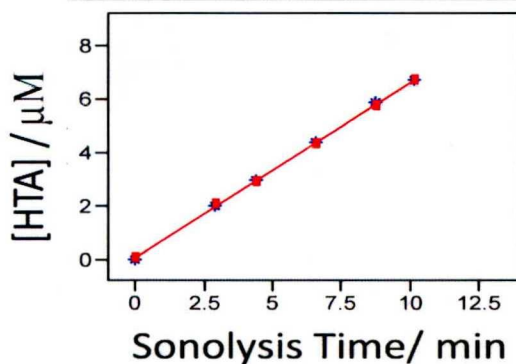


Figure B2.18 Duplicate and separate zero order ultrasonic HTA formation reactions of in aqueous solution (1mM, 300ml) exposed to pulsed wave (160ms lengths and 60ms intervals) ultrasound ($f = 205$ kHz; $P = 27W$; $k_{\text{weighted}} = 0.655$ mM min⁻¹; $R^2_{\text{Adj}} = 0.9994$; $N_{\text{TOT}} = 12$; $t_{\text{sonolysis}} = 10$ min).

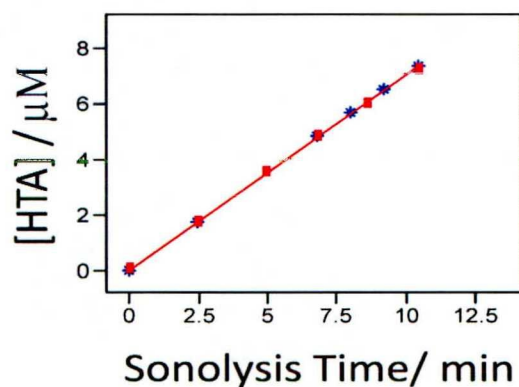


Figure B2.19 Duplicate and separate zero order ultrasonic HTA formation reactions of in aqueous solution (1mM, 300ml) exposed to pulsed wave (160ms lengths and 100ms intervals) ultrasound ($f = 205$ kHz; $P = 27W$; $k_{\text{weighted}} = 0.697$ mM min⁻¹; $R^2_{\text{Adj}} = 0.9995$; $N_{\text{TOT}} = 12$; $t_{\text{sonolysis}} = 10$ min).

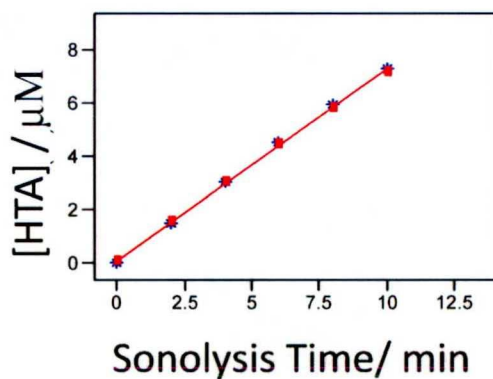


Figure B2.20 Duplicate and separate zero order ultrasonic HTA formation reactions of in aqueous solution (1mM, 300ml) exposed to pulsed wave (160ms lengths and 160ms intervals) ultrasound ($f = 205$ kHz; $P = 27W$; $k_{\text{weighted}} = 0.720$ mM min⁻¹; $R^2_{\text{Adj}} = 0.9991$; $N_{\text{TOT}} = 12$; $t_{\text{sonolysis}} = 10$ min).

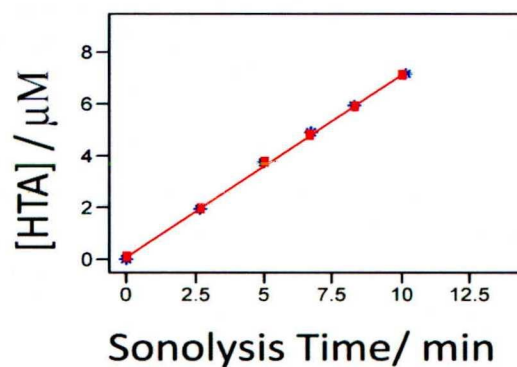


Figure B2.21 Duplicate and separate zero order ultrasonic HTA formation reactions of in aqueous solution (1mM, 300ml) exposed to pulsed wave (160ms lengths and 320ms intervals) ultrasound ($f = 205$ kHz; $P = 27W$; $k_{\text{weighted}} = 0.704$ mM min⁻¹; $R^2_{\text{Adj}} = 0.9990$; $N_{\text{TOT}} = 12$; $t_{\text{sonolysis}} = 10$ min).

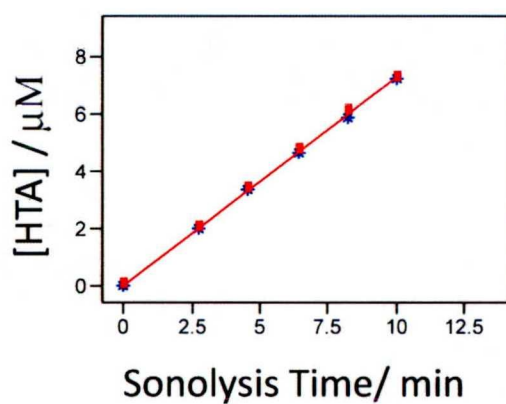


Figure B2.22 Duplicate and separate zero order ultrasonic HTA formation reactions of in aqueous solution (1mM, 300ml) exposed to pulsed wave (320ms lengths and 30ms intervals) ultrasound ($f = 205$ kHz; $P = 27W$; $k_{\text{weighted}} = 0.722$ mM min⁻¹; $R^2_{\text{Adj}} = 0.9997$; $N_{\text{TOT}} = 12$; $t_{\text{sonolysis}} = 10$ min).

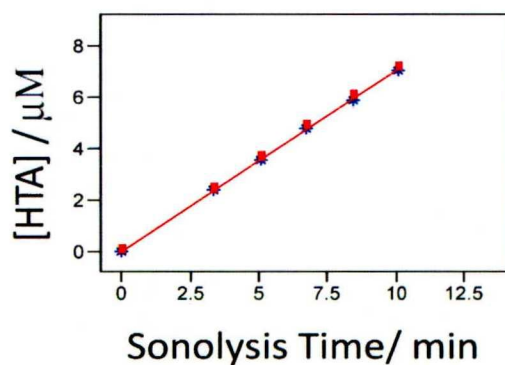


Figure B2.23 Duplicate and separate zero order ultrasonic HTA formation reactions of in aqueous solution (1mM, 300ml) exposed to pulsed wave (320ms lengths and 60ms intervals) ultrasound ($f = 205$ kHz; $P = 27$ W; $k_{\text{weighted}} = 0.701$ mM min⁻¹; $R^2_{\text{Adj}} = 0.9996$; $N_{\text{TOT}} = 12$; $t_{\text{sonolysis}} = 10$ min).

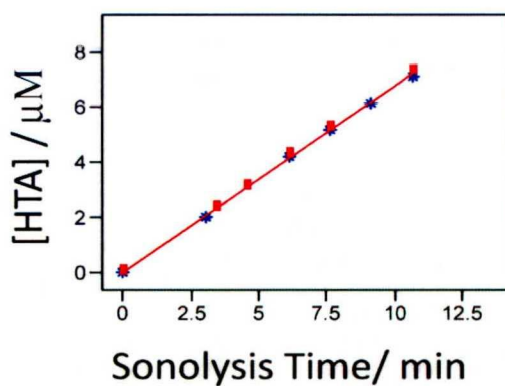


Figure B2.24 Duplicate and separate zero order ultrasonic HTA formation reactions of in aqueous solution (1mM, 300ml) exposed to pulsed wave (320ms lengths and 100ms intervals) ultrasound ($f = 205$ kHz; $P = 27$ W; $k_{\text{weighted}} = 0.677$ mM min⁻¹; $R^2_{\text{Adj}} = 0.9996$; $N_{\text{TOT}} = 12$; $t_{\text{sonolysis}} = 10$ min).

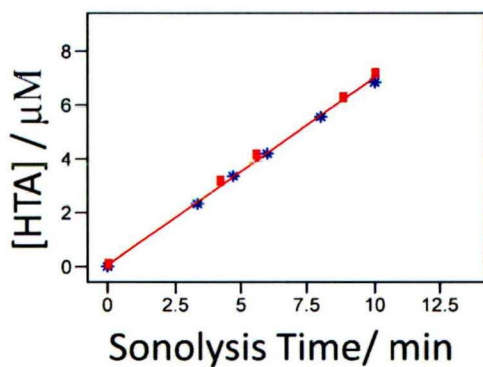


Figure B2.25 Duplicate and separate zero order ultrasonic HTA formation reactions of in aqueous solution (1mM, 300ml) exposed to pulsed wave (320ms lengths and 160ms intervals) ultrasound ($f = 205$ kHz; $P = 27$ W; $k_{\text{weighted}} = 0.695$ mM min⁻¹; $R^2_{\text{Adj}} = 0.998$; $N_{\text{TOT}} = 12$; $t_{\text{sonolysis}} = 10$ min).

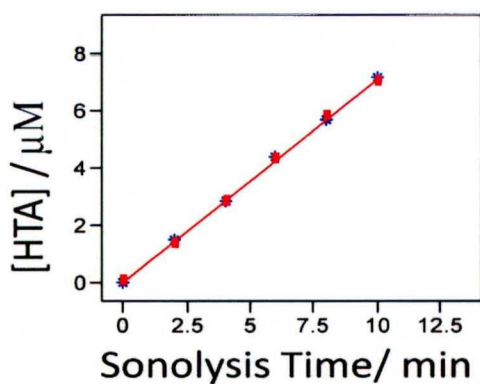


Figure B2.26 Duplicate and separate zero order ultrasonic HTA formation reactions of in aqueous solution (1mM, 300ml) exposed to pulsed wave (320ms lengths and 320ms intervals) ultrasound ($f = 205$ kHz; $P = 27$ W; $k_{\text{weighted}} = 0.710$ mM min⁻¹; $R^2_{\text{Adj}} = 0.9995$; $N_{\text{TOT}} = 12$; $t_{\text{sonolysis}} = 10$ min).

APPENDIX C

69 kHz

OBS KINETIC RATE PLOTS

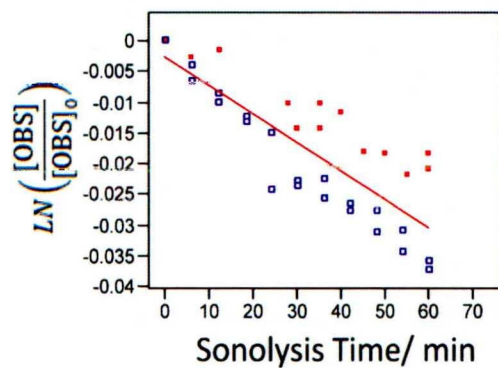


Figure C1.1 Duplicate and separate first order ultrasonic degradation of OBS in aqueous solution (1mM, 300ml) exposed to continuous ultrasound ($f = 69$ kHz; $P = 27$ W. $k_{\text{weighted}} = 4.9 \times 10^{-4} \text{ min}^{-1}$, $R^2_{\text{Adj}} = 0.908$; $N_{\text{TOT}} = 34$).

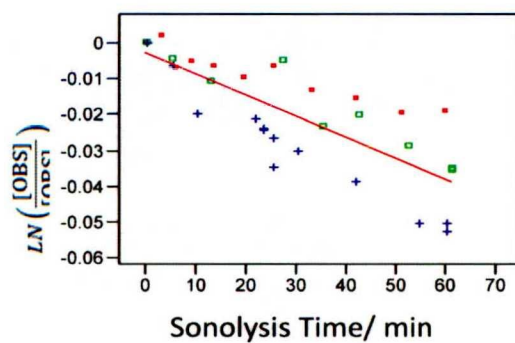


Figure C1.2 Triplicate and separate first order ultrasonic degradation of OBS in aqueous solution (1mM, 300ml) exposed to pulsed wave (30ms lengths and 30ms intervals) ultrasound ($f = 69$ kHz; $P = 27$ W; $k_{\text{weighted}} = 5.7 \times 10^{-4} \text{ min}^{-1}$; $R^2_{\text{Adj}} = 0.87$; $N_{\text{TOT}} = 33$; $t_{\text{sonolysis}} = 60$ min).

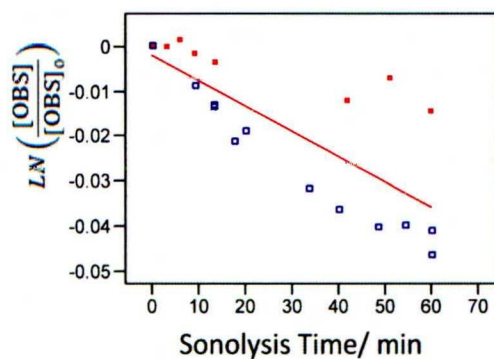


Figure C1.3 Duplicate and separate first order ultrasonic degradation of OBS in aqueous solution (1mM, 300ml) exposed to pulsed wave (30ms lengths and 60ms intervals) ultrasound ($f = 69$ kHz; $P = 27$ W; $k_{\text{weighted}} = 4.9 \times 10^{-4} \text{ min}^{-1}$; $R^2_{\text{Adj}} = 0.857$; $N_{\text{TOT}} = 20$; $t_{\text{sonolysis}} = 60$ min).

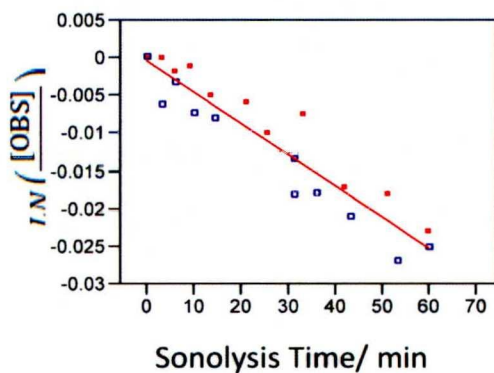


Figure C1.4 Duplicate and separate first order ultrasonic degradation of OBS in aqueous solution (1mM, 300ml) exposed to pulsed wave (30ms lengths and 100ms intervals) ultrasound ($f = 69$ kHz; $P = 27$ W; $k_{\text{weighted}} = 4.4 \times 10^{-4} \text{ min}^{-1}$; $R^2_{\text{Adj}} = 0.95$; $N_{\text{TOT}} = 22$; $t_{\text{sonolysis}} = 60$ min).

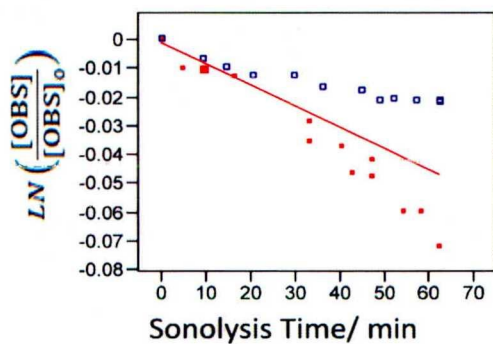


Figure C1.5 Duplicate and separate first order ultrasonic degradation of OBS in aqueous solution (1mM, 300ml) exposed to pulsed wave (30ms lengths and 160ms intervals) ultrasound ($f = 69$ kHz; $P = 27$ W; $k_{\text{weighted}} = 7.2 \times 10^{-4} \text{ min}^{-1}$; $R^2_{\text{Adj}} = 0.81$; $N_{\text{TOT}} = 26$; $t_{\text{sonolysis}} = 60$ min).

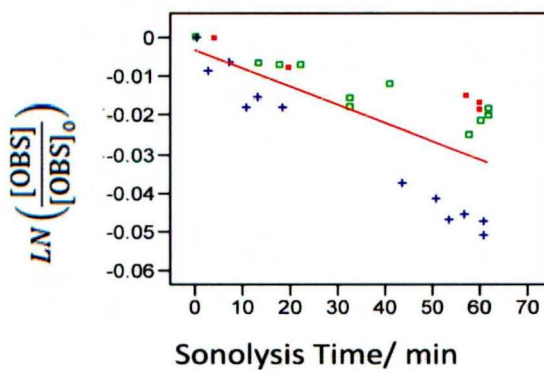


Figure C1.6 Triplicate and separate first order ultrasonic degradation of OBS in aqueous solution (1mM, 300ml) exposed to pulsed wave (30ms lengths and 320ms intervals) ultrasound ($f = 69$ kHz; $P = 27$ W; $k_{\text{weighted}} = 5.0 \times 10^{-4} \text{ min}^{-1}$; $R^2_{\text{Adj}} = 0.84$; $N_{\text{TOT}} = 29$; $t_{\text{sonolysis}} = 60$ min).

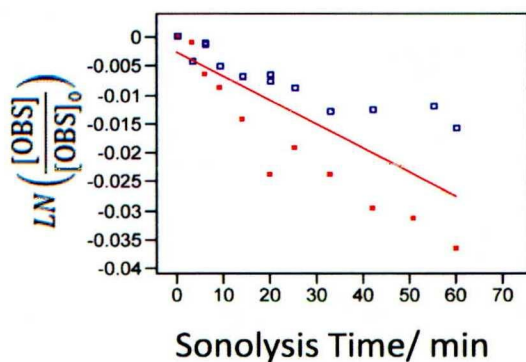


Figure C1.7 Duplicate and separate first order ultrasonic degradation of OBS in aqueous solution (1mM, 300ml) exposed to pulsed wave (60ms lengths and 30ms intervals) ultrasound ($f = 69 \text{ kHz}$; $P = 27\text{W}$; $k_{\text{weighted}} = 4.1 \times 10^{-4} \text{ min}^{-1}$; $R^2_{\text{Adj}} = 0.81$; $N_{\text{TOT}} = 24$; $t_{\text{sonolysis}} = 60 \text{ min}$).

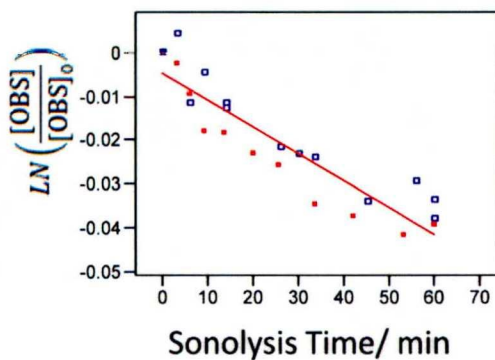


Figure C1.8 Duplicate and separate first order ultrasonic degradation of OBS in aqueous solution (1mM, 300ml) exposed to pulsed wave (60ms lengths and 60ms intervals) ultrasound ($f = 69 \text{ kHz}$; $P = 27\text{W}$; $k_{\text{weighted}} = 6.2 \times 10^{-4} \text{ min}^{-1}$; $R^2_{\text{Adj}} = 0.88$; $N_{\text{TOT}} = 24$; $t_{\text{sonolysis}} = 60 \text{ min}$).

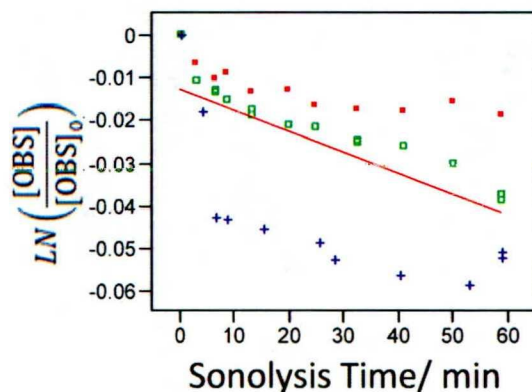


Figure C1.9 Triplicate and separate first order ultrasonic degradation of OBS in aqueous solution (1mM, 300ml) exposed to pulsed wave (60ms lengths and 100ms intervals) ultrasound ($f = 69$ kHz; $P = 27$ W; $k_{\text{weighted}} = 4.5 \times 10^{-4} \text{ min}^{-1}$; $R^2_{\text{Adj}} = 0.78$; $N_{\text{TOT}} = 37$; $t_{\text{sonolysis}} = 60$ min).

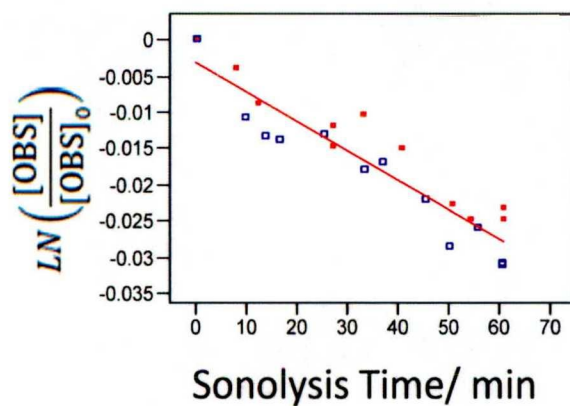


Figure C1.10 Duplicate and separate first order ultrasonic degradation of OBS in aqueous solution (1mM, 300ml) exposed to pulsed wave (60ms lengths and 160ms intervals) ultrasound ($f = 69$ kHz; $P = 27$ W; $k_{\text{weighted}} = 4.1 \times 10^{-4} \text{ min}^{-1}$; $R^2_{\text{Adj}} = 0.93$; $N_{\text{TOT}} = 24$; $t_{\text{sonolysis}} = 60$ min).

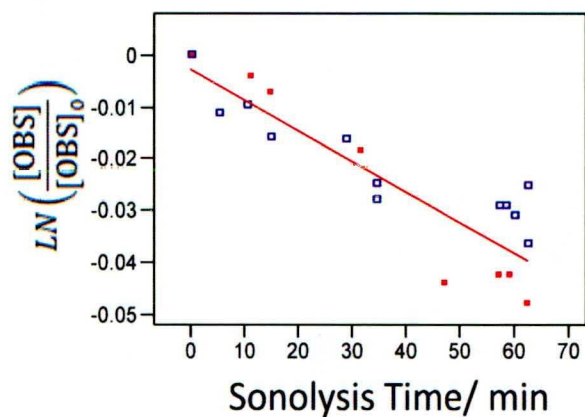


Figure C1.11 Duplicate and separate first order ultrasonic degradation of OBS in aqueous solution (1mM, 300ml) exposed to pulsed wave (60ms lengths and 320ms intervals) ultrasound ($f = 69$ kHz; $P = 27$ W; $k_{\text{weighted}} = 5.8 \times 10^{-4} \text{ min}^{-1}$; $R^2_{\text{Adj}} = 0.82$; $N_{\text{TOT}} = 21$; $t_{\text{sonolysis}} = 60$ min).

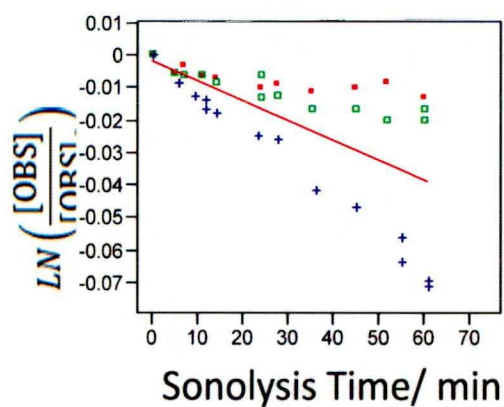


Figure C1.12 Triplicate and separate first order ultrasonic degradation of OBS in aqueous solution (1mM, 300ml) exposed to pulsed wave (100ms lengths and 30ms intervals) ultrasound ($f = 69$ kHz; $P = 27$ W; $k_{\text{weighted}} = 5.9 \times 10^{-4} \text{ min}^{-1}$; $R^2_{\text{Adj}} = 0.75$; $N_{\text{TOT}} = 21$; $t_{\text{sonolysis}} = 60$ min).

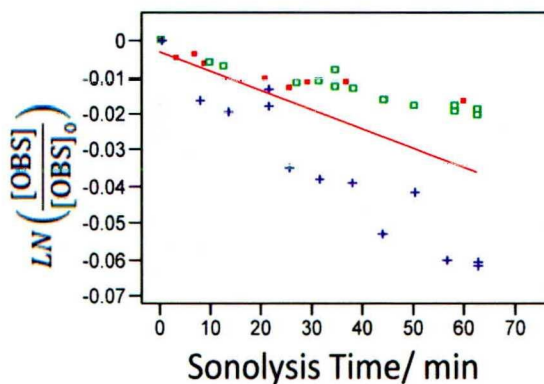


Figure C1.13 Triplicate and separate first order ultrasonic degradation of OBS in aqueous solution (1mM, 300ml) exposed to pulsed wave (100ms lengths and 60ms intervals) ultrasound ($f = 69$ kHz; $P = 27$ W; $k_{\text{weighted}} = 5.3 \times 10^{-4} \text{ min}^{-1}$; $R^2_{\text{Adj}} = 0.80$; $N_{\text{TOT}} = 36$; $t_{\text{sonolysis}} = 60$ min).

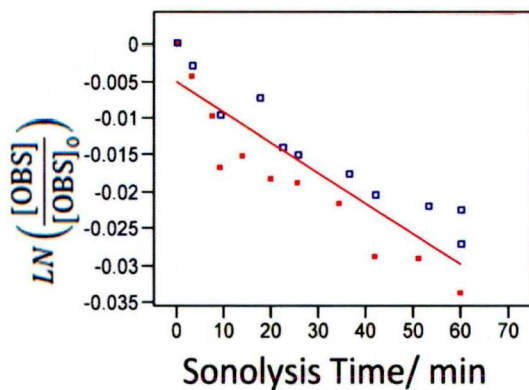


Figure C1.14 Duplicate and separate first order ultrasonic degradation of OBS in aqueous solution (1mM, 300ml) exposed to pulsed wave (100ms lengths and 100ms intervals) ultrasound ($f = 69$ kHz; $P = 27$ W; $k_{\text{weighted}} = 4.3 \times 10^{-4} \text{ min}^{-1}$; $R^2_{\text{Adj}} = 0.88$; $N_{\text{TOT}} = 22$; $t_{\text{sonolysis}} = 60$ min).

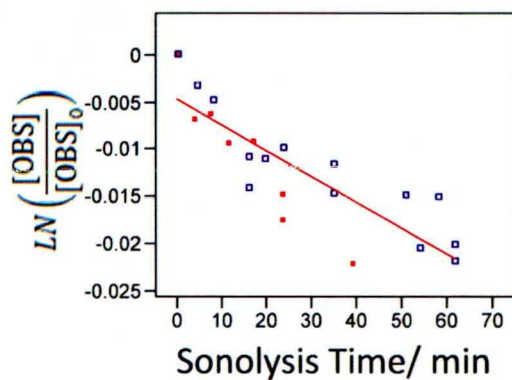


Figure C1.15 Duplicate and separate first order ultrasonic degradation of OBS in aqueous solution (1mM, 300ml) exposed to pulsed wave (100ms lengths and 160ms intervals) ultrasound ($f = 69$ kHz; $P = 27W$; $k_{\text{weighted}} = 3.0 \times 10^{-4} \text{ min}^{-1}$; $R^2_{\text{Adj}} = 0.755$; $N_{\text{TOT}} = 22$; $t_{\text{sonolysis}} = 60$ min).

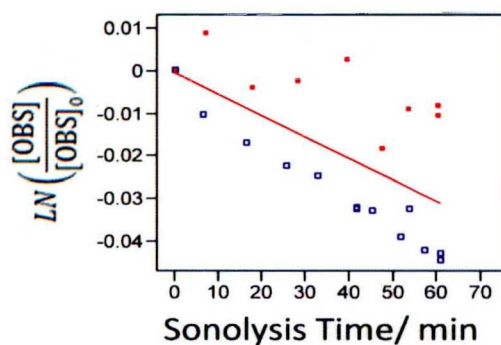


Figure C1.16 Duplicate and separate first order ultrasonic degradation of OBS in aqueous solution (1mM, 300ml) exposed to pulsed wave (100ms lengths and 320ms intervals) ultrasound ($f = 69$ kHz; $P = 27W$; $k_{\text{weighted}} = 4.6 \times 10^{-4} \text{ min}^{-1}$; $R^2_{\text{Adj}} = 0.86$; $N_{\text{TOT}} = 22$; $t_{\text{sonolysis}} = 60$ min).

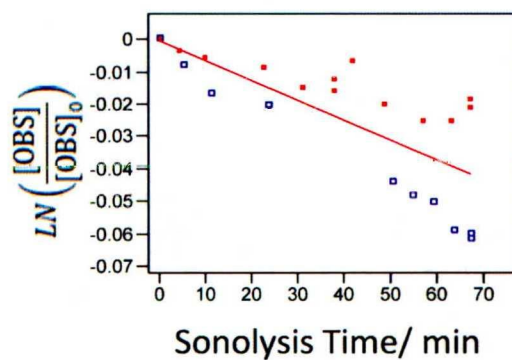


Figure C1.17 Duplicate and separate first order ultrasonic degradation of OBS in aqueous solution (1mM, 300ml) exposed to pulsed wave (160ms lengths and 30ms intervals) ultrasound ($f = 69$ kHz; $P = 27$ W; $k_{\text{weighted}} = 5.9 \times 10^{-4} \text{ min}^{-1}$; $R^2_{\text{Adj}} = 0.85$; $N_{\text{TOT}} = 23$; $t_{\text{sonolysis}} = 60$ min).

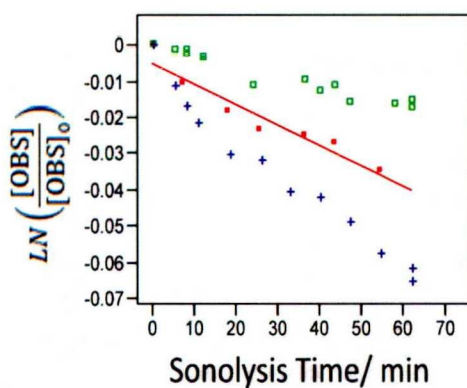


Figure C1.18 Triplicate and separate first order ultrasonic degradation of OBS in aqueous solution (1mM, 300ml) exposed to pulsed wave (160ms lengths and 60ms intervals) ultrasound ($f = 69$ kHz; $P = 27$ W; $k_{\text{weighted}} = 5.7 \times 10^{-4} \text{ min}^{-1}$; $R^2_{\text{Adj}} = 0.85$; $N_{\text{TOT}} = 33$; $t_{\text{sonolysis}} = 60$ min).

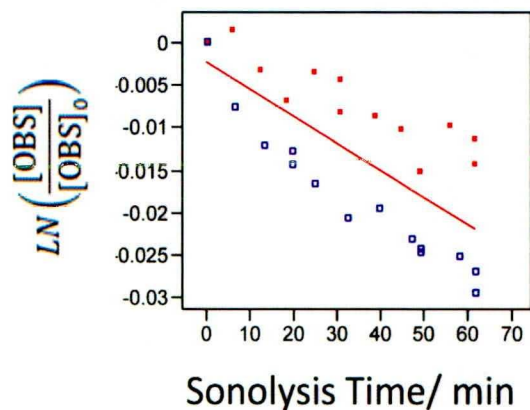


Figure C1.19 Duplicate and separate first order ultrasonic degradation of OBS in aqueous solution (1mM, 300ml) exposed to pulsed wave (160ms lengths and 100ms intervals) ultrasound ($f = 69$ kHz; $P = 27$ W; $k_{\text{weighted}} = 3.1 \times 10^{-4} \text{ min}^{-1}$; $R^2_{\text{Adj}} = 0.90$; $N_{\text{TOT}} = 27$; $t_{\text{sonolysis}} = 60$ min).

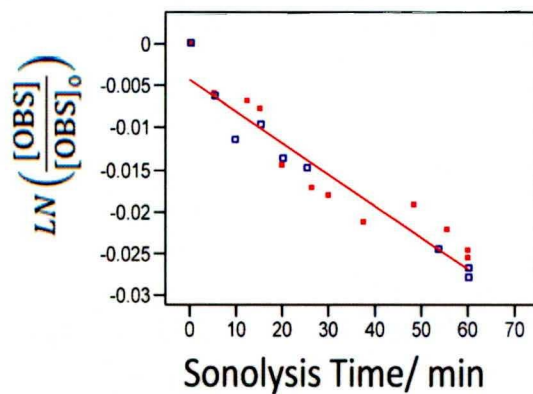


Figure C1.20 Duplicate and separate first order ultrasonic degradation of OBS in aqueous solution (1mM, 300ml) exposed to pulsed wave (160ms lengths and 160ms intervals) ultrasound ($f = 69$ kHz; $P = 27$ W; $k_{\text{weighted}} = 3.8 \times 10^{-4} \text{ min}^{-1}$; $R^2_{\text{Adj}} = 0.90$; $N_{\text{TOT}} = 22$; $t_{\text{sonolysis}} = 60$ min).

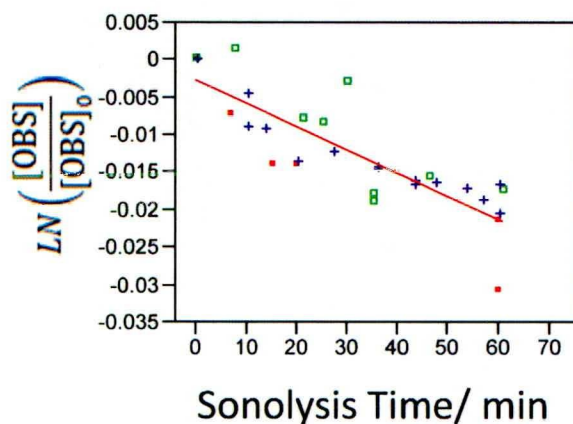


Figure C1.21 Triplicate and separate first order ultrasonic degradation of OBS in aqueous solution (1mM, 300ml) exposed to pulsed wave (160ms lengths and 320ms intervals) ultrasound ($f = 69$ kHz; $P = 27$ W; $k_{\text{weighted}} = 3.1 \times 10^{-4} \text{ min}^{-1}$; $R^2_{\text{Adj}} = 0.76$; $N_{\text{TOT}} = 29$; $t_{\text{sonolysis}} = 60$ min).

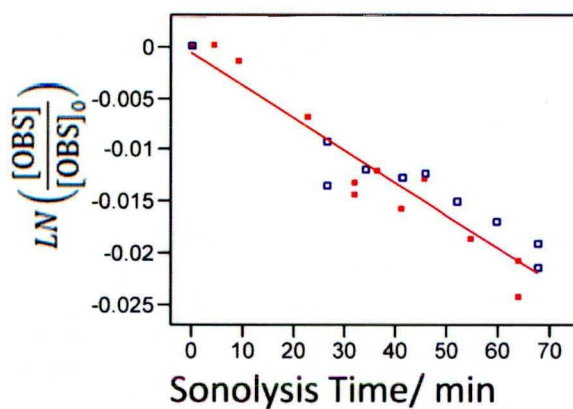


Figure C1.22 Duplicate and separate first order ultrasonic degradation of OBS in aqueous solution (1mM, 300ml) exposed to pulsed wave (320ms lengths and 30ms intervals) ultrasound ($f = 69$ kHz; $P = 27$ W; $k_{\text{weighted}} = 3.2 \times 10^{-4} \text{ min}^{-1}$; $R^2_{\text{Adj}} = 0.90$; $N_{\text{TOT}} = 22$; $t_{\text{sonolysis}} = 60$ min).

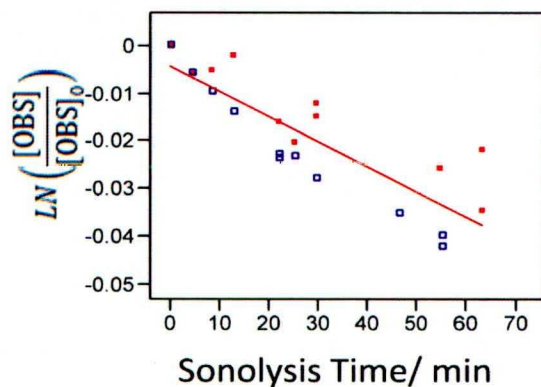


Figure C1.23 Duplicate and separate first order ultrasonic degradation of OBS in aqueous solution (1mM, 300ml) exposed to pulsed wave (320ms lengths and 60ms intervals) ultrasound ($f = 69$ kHz; $P = 27$ W; $k_{\text{weighted}} = 5.4 \times 10^{-4} \text{ min}^{-1}$; $R^2_{\text{Adj}} = 0.86$; $N_{\text{TOT}} = 22$; $t_{\text{sonolysis}} = 60$ min).

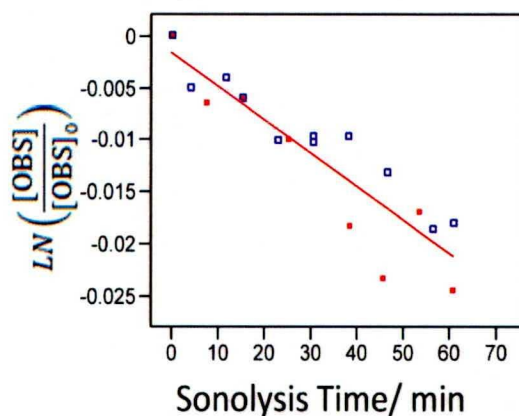


Figure C1.24 Duplicate and separate first order ultrasonic degradation of OBS in aqueous solution (1mM, 300ml) exposed to pulsed wave (320ms lengths and 100ms intervals) ultrasound ($f = 69$ kHz; $P = 27$ W; $k_{\text{weighted}} = 3.2 \times 10^{-4} \text{ min}^{-1}$; $R^2_{\text{Adj}} = 0.87$; $N_{\text{TOT}} = 19$; $t_{\text{sonolysis}} = 60$ min).

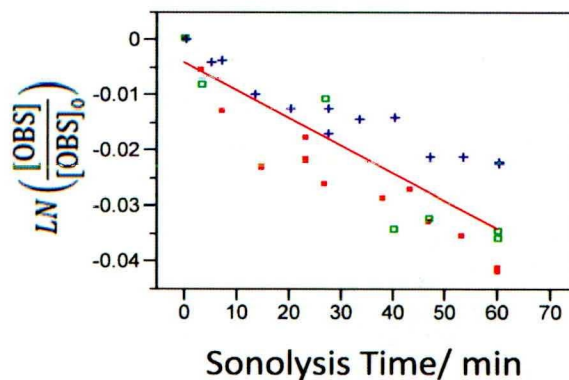


Figure C1.25 Triplicate and separate first order ultrasonic degradation of OBS in aqueous solution (1mM, 300ml) exposed to pulsed wave (320ms lengths and 160ms intervals) ultrasound ($f = 69$ kHz; $P = 27W$; $k_{\text{weighted}} = 4.9 \times 10^{-4} \text{ min}^{-1}$; $R^2_{\text{Adj}} = 0.88$; $N_{\text{TOT}} = 33$; $t_{\text{sonolysis}} = 60$ min).

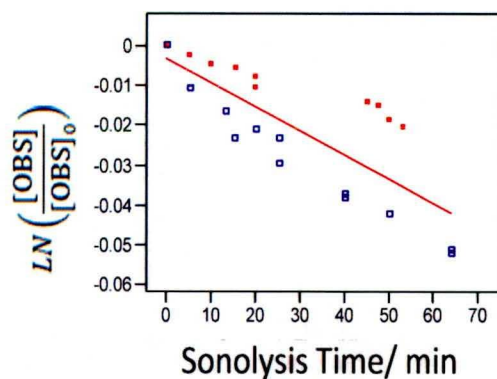


Figure C1.26 Duplicate and separate first order ultrasonic degradation of OBS in aqueous solution (1mM, 300ml) exposed to pulsed wave (320ms lengths and 320ms intervals) ultrasound ($f = 69$ kHz; $P = 27W$; $k_{\text{weighted}} = 5.7 \times 10^{-4} \text{ min}^{-1}$; $R^2_{\text{Adj}} = 0.90$; $N_{\text{TOT}} = 22$; $t_{\text{sonolysis}} = 60$ min).

APPENDIX D

IMPEDANCE GRAPHS

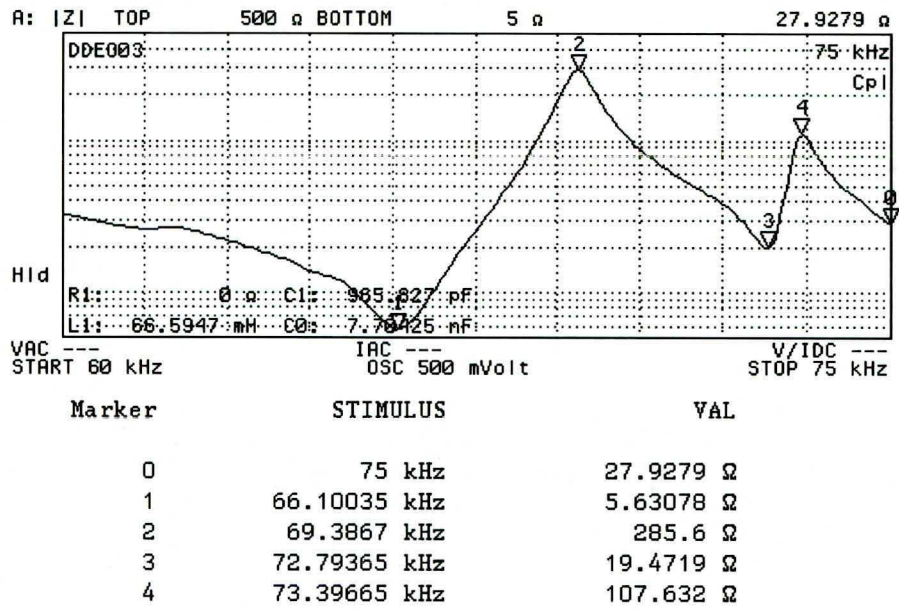


Figure D.1 Impedance test output of the 70 kHz transducer.

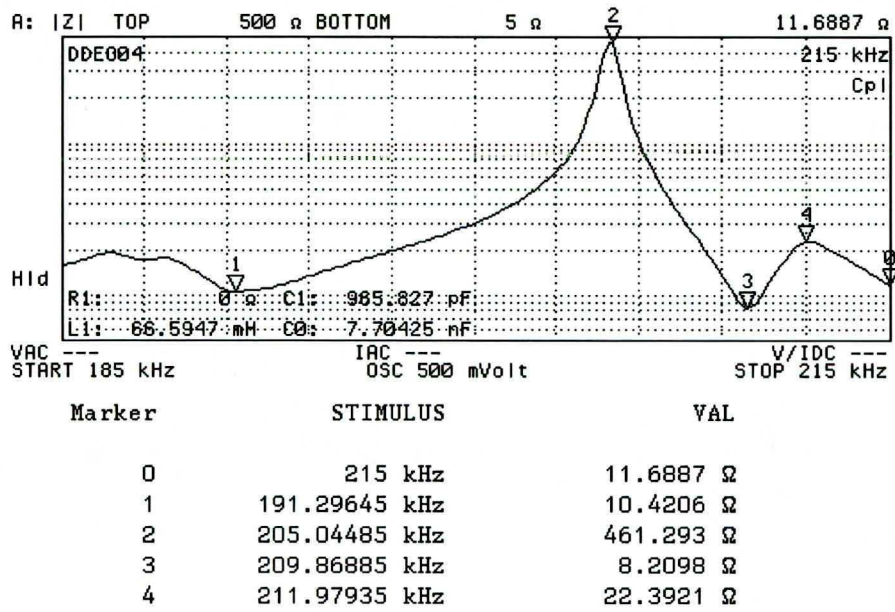


Figure D.2 Impedance test output of the 205 kHz transducer

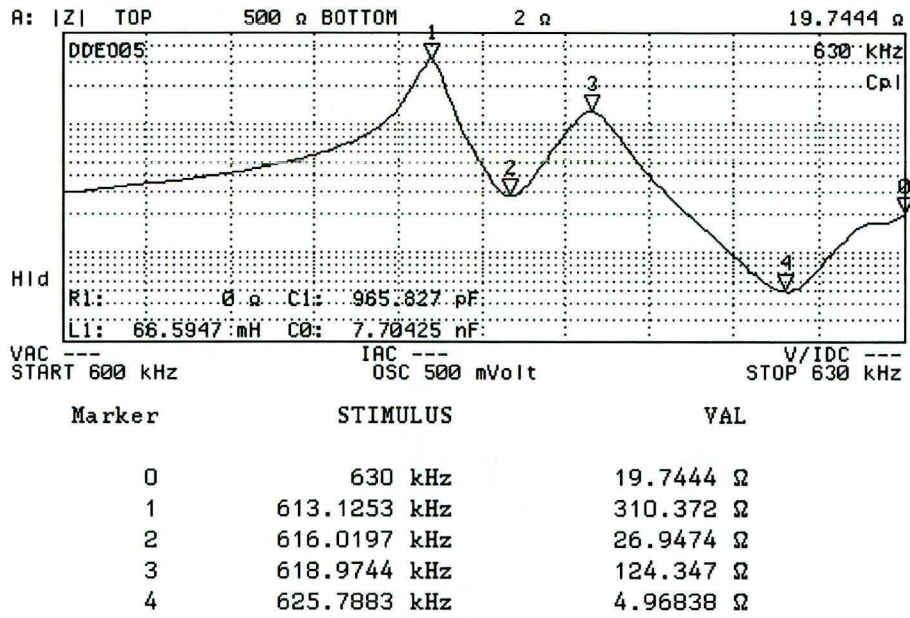


Figure D.3 Impedance test output of the 620 kHz transducer

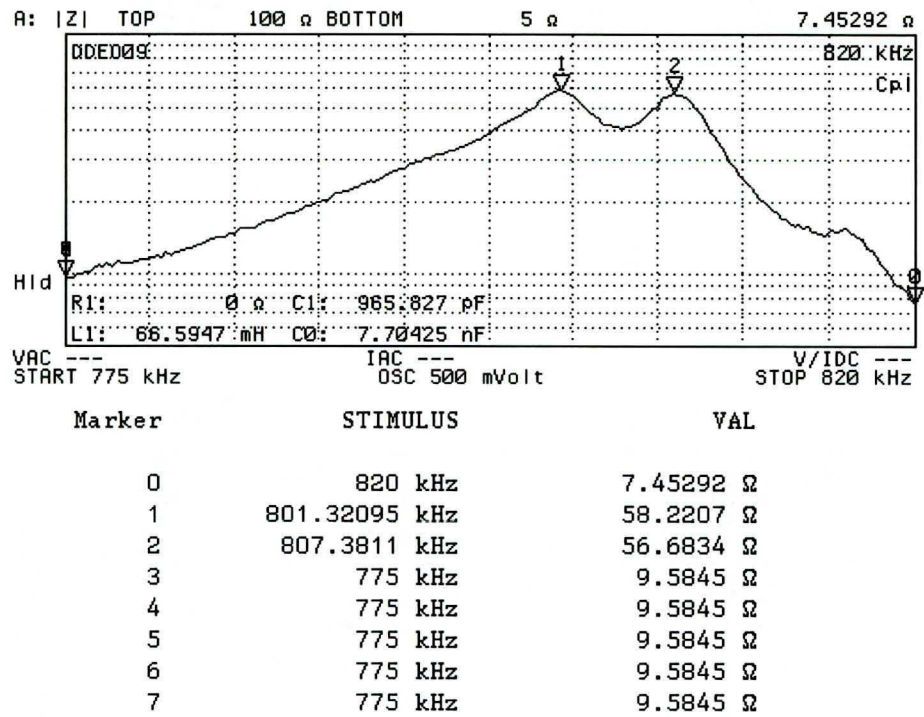


Figure D.4 Impedance test output of the 806 kHz transducer

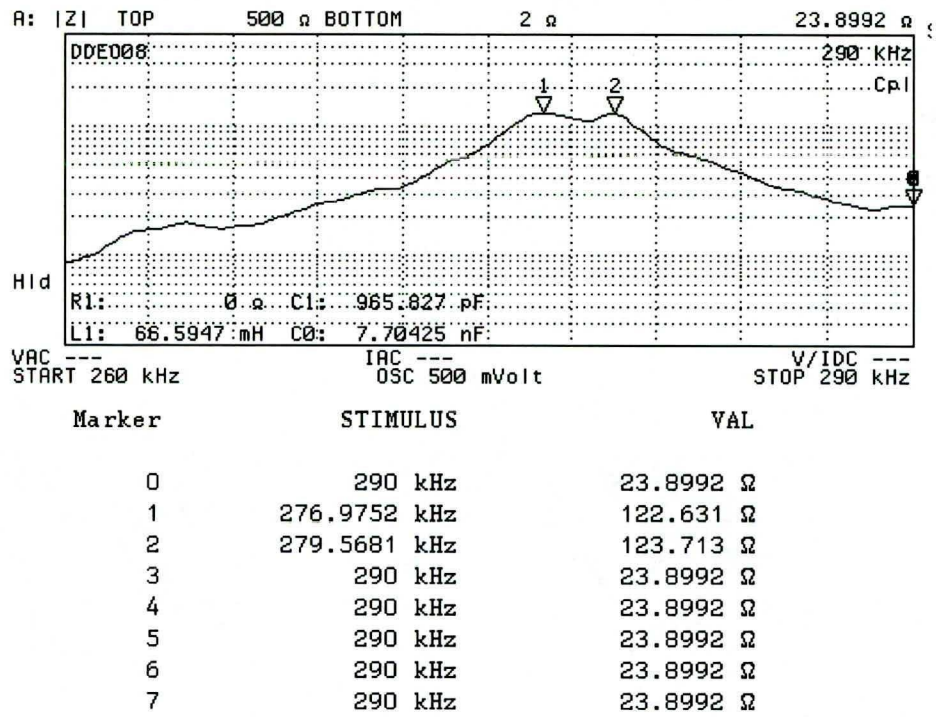


Figure D.5 Impedance test output of the 279 kHz transducer

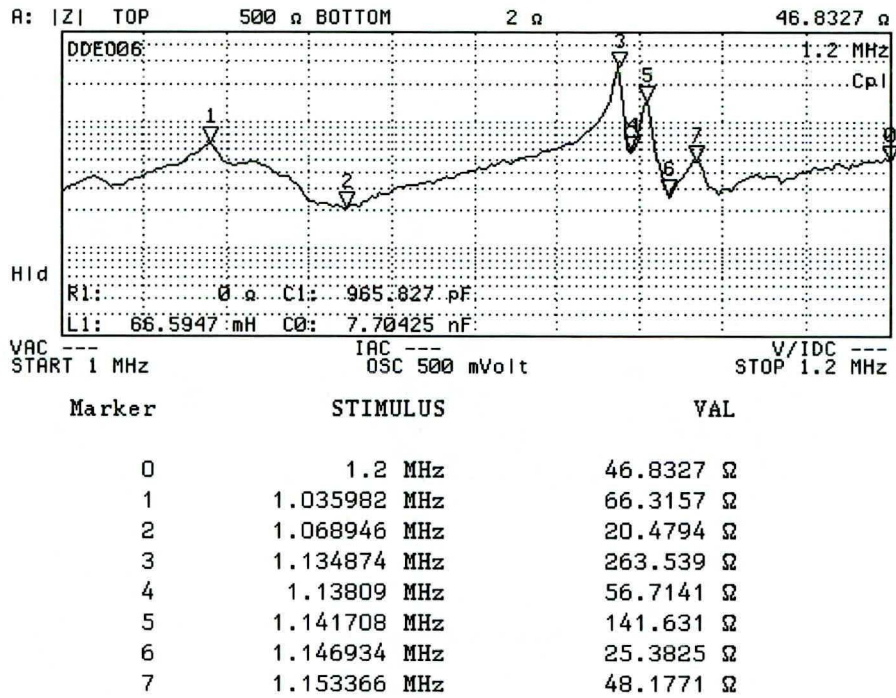


Figure D.6 Impedance test output of the 1054 kHz transducer

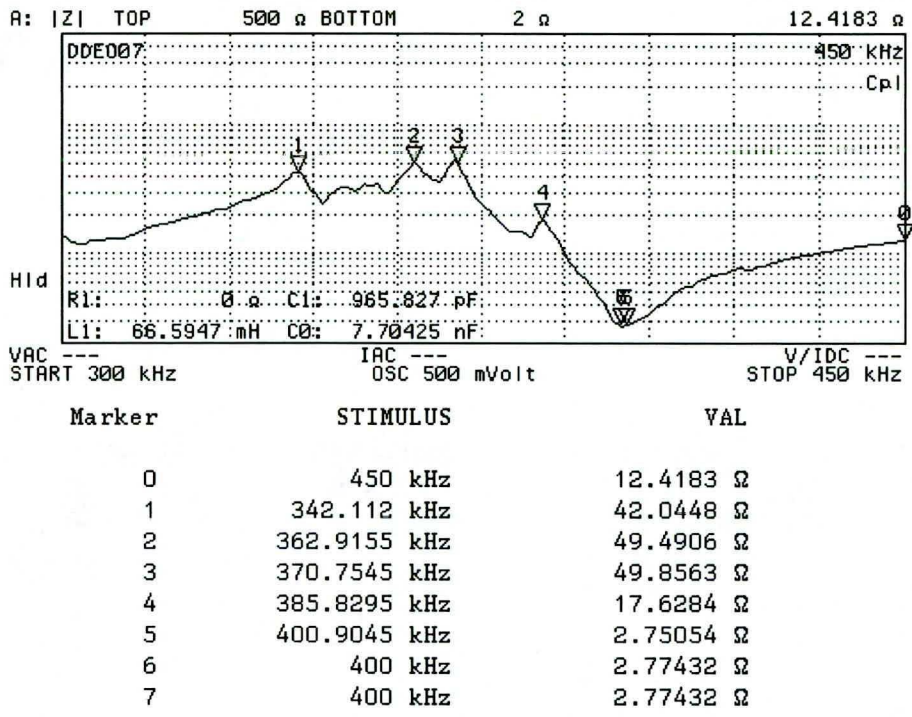


Figure D.7 Impedance test output of the 354 kHz transducer

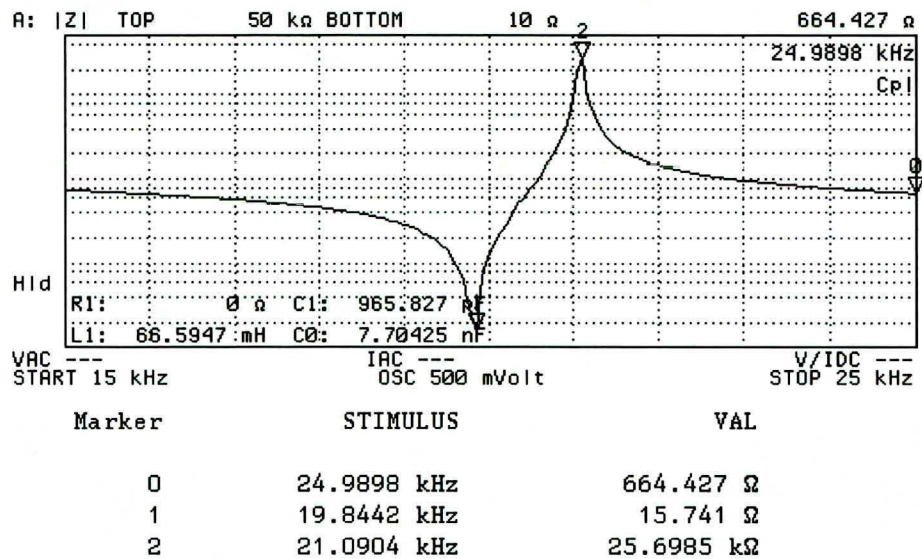


Figure D.8 Comparative Impedance test output of a standard 20 kHz transducer